USAAMRDL-TR-75-35

THE DEVELOPMENT AND APPLICATION OF AN ANALYSIS FOR THE DETERMINATION OF COUPLED TAIL ROTOR/HELICOPTER AIR RESONANCE BEHAVIOR

Rochester Applied Science Associates ~~Div.~~
~~Systems Research Laboratories, Inc.~~
Rochester, N.Y. 14618

August 1975

Final Report

Approved for public release; distribution unlimited.

Prepared for

EUSTIS DIRECTORATE
U. S. ARMY AIR MOBILITY RESEARCH AND DEVELOPMENT LABORATORY
Fort Eustis, Va. 23604

EUSTIS DIRECTORATE POSITION STATEMENT

This report presents the results of a highly complicated analytical investigation of the aeroelastic stability of a fully coupled tail rotor/tail pylon/fuselage system in the presence of perturbational aerodynamics in hover and forward flight. The resulting advanced computer program has not been verified through thorough correlation with experimental data; however, extensive evaluation of the procedures used in generating and solving the equations of motion for the elastic tail rotor system has indicated that these procedures are both efficient and accurate. Therefore, it is recommended that this new computer program be given serious consideration as a candidate technique where advanced rotor aeroelastic analysis is required.

Mr. William E. Nettles of the Technology Applications Division, Aeromechanics Area, served as Project Engineer for this effort.

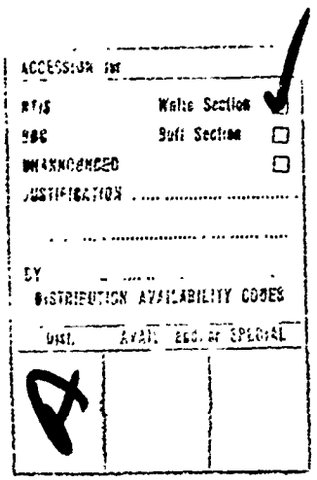

Unclassified
SECURITY CLASSIFICATION OF THIS PAGE (When Data Entered)

REPORT DOCUMENTATION PAGE

READ INSTRUCTIONS BEFORE COMPLETING FORM

1. REPORT NUMBER: USAAMRDL-TR-75-35	2. GOVT ACCESSION NO.
3. RECIPIENT'S CATALOG NUMBER	
4. TITLE (and Subtitle): THE DEVELOPMENT AND APPLICATION OF AN ANALYSIS FOR THE DETERMINATION OF COUPLED TAIL ROTOR/HELICOPTER AIR RESONANCE BEHAVIOR	5. TYPE OF REPORT & PERIOD COVERED: Final Report
	6. PERFORMING ORG. REPORT NUMBER: RASA/SRL [redacted]-75-01
7. AUTHOR(s): Lawrence R. Sutton, Santu T. Gangwani	8. CONTRACT OR GRANT NUMBER(s): DAAJ02-74-C-0026 (Mod. P00002) NEW
9. PERFORMING ORGANIZATION NAME AND ADDRESS: Rochester Applied Science Associates Div. Systems Research Laboratories, Inc. Rochester, New York 14618	10. PROGRAM ELEMENT, PROJECT, TASK AREA & WORK UNIT NUMBERS: 62209A 1F262209AH76 00 003 EK
11. CONTROLLING OFFICE NAME AND ADDRESS: Eustis Directorate, U. S. Army Air Mobility R&D Laboratory, Fort Eustis, Virginia 23604	12. REPORT DATE: Aug[redacted]75; 13. NUMBER OF PAGES: 159
14. MONITORING AGENCY NAME & ADDRESS(if different from Controlling Office)	15. SECURITY CLASS. (of this report): Unclassified
	15a. DECLASSIFICATION/DOWNGRADING SCHEDULE

16. DISTRIBUTION STATEMENT (of this Report)

Approved for public release; distribution unlimited.

DA-1-F-262209-AH-76

17. DISTRIBUTION STATEMENT (of the abstract entered in Block 20, if different from Report)

1-F-262209-AH-76

18. SUPPLEMENTARY NOTES

19. KEY WORDS (Continue on reverse side if necessary and identify by block number)

Tail Rotor
Dynamics
Helicopter
Air Resonance
Stability
Rotor
Vibration

20. ABSTRACT (Continue on reverse side if necessary and identify by block number)

An analysis and associated computer program have been developed to provide a highly sophisticated mathematical representation of coupled tail rotor/support structure systems. The coded analysis allows the consideration of an anisotropically supported flexible swashplate control system, rotor drive shaft torsional flexibility, anisotropic mounting of the gearbox about two mutually orthogonal axes, and an elastic support

DD FORM 1 JAN 73 1473 EDITION OF 1 NOV 65 IS OBSOLETE

Unclassified
SECURITY CLASSIFICATION OF THIS PAGE (When Data Entered)

20. Continued.

structure such as a fuselage-tailboom-fin structure in addition to the rotor system. As such, the analysis can also be applied to main rotor systems. The resulting analysis has the capability of predicting the air resonance (frequency, stability, and mode shape) behavior of a coupled tail rotor/support structure system in hover and forward flight where the rotor may be of a rigid, teetering, gimballed, flexstrap, or partial to fully articulated type. The blade aerodynamics representation including both quasi-steady and unsteady (Theodorsen's) terms can utilize either a uniform or a variably defined induced velocity field and up to five types of airfoil sections. All blade and fuselage-tailboom-fin structure characteristics required to adequately represent these structures in a lumped parameter form are considered, including inertia and gyroscopic damping effects. The analysis includes aerodynamic interharmonic blade coupling and interharmonic coupling due to support structure behavior. The computer program developed was applied to a helicopter configuration representative of a UTTAS model involving a flex-strap tail rotor to carry out a parametric sensitivity analysis regarding the effects of various model components on the system air resonance behavior. Also, the program is in a form suitable for modification to an analysis capable of determining the forced response behavior of the same type system.

PREFACE

This program was conducted by Rochester Applied Science Associates, a division of Systems Research Laboratories, Inc., under Contract DAAJ02-74-C-0026, and was performed under the general direction of Mr. William E. Nettles, Technology Applications Division of the Eustis Directorate, U. S. Army Air Mobility Research and Development Laboratory, Fort Eustis, Virginia.

The authors express their gratitude to Mr. Lou Bartek of the Fort Eustis Computer Facility who provided assistance with the setting up and running of the developed computer program on the Fort Eustis computer system.

TABLE OF CONTENTS

LIST OF ILLUSTRATIONS

LIST OF TABLES

INTRODUCTION

The structural dynamic behavior of tail rotors has always presented difficult design problems which have not been alleviated to any great extent in the past decade. In part these problems have been due to the lack of suitable analytical tools capable of representing the complicated cause and effect relationships associated with coupled tail rotor systems. A suitable analysis must be capable of representing the interaction of a tail rotor with its aerodynamic and support environment such that the structural dynamic behavior of a tail rotor can be adequately predicted.

There are many specific reasons for the design problems associated with tail rotor dynamic behavior. Some of the more significant reasons are outlined and discussed in Reference 1. Four major reasons are:

1. the difficulties in predicting the basic tail rotor air resonance modes (frequencies and corresponding mode shapes and associated blade motion stability);

2. the effects of tail rotor local mounting conditions on the tail rotor air resonance modes and associated blade motion stability;

3. the effects of tail rotor fuselage-tailboom-fin structural flexibility on the tail rotor air resonance modes and associated blade motion stability;

4. the nature of the harmonic and nonharmonic forcing functions associated with the main rotor wake, tail rotor wake, and elastic support structure.

As noted in Reference 1, for many years the development and/or modification of tail rotors has been accomplished by utilizing a fairly standard procedure. This procedure consists of (1) a design phase in which the isolated tail rotor blades are designed such that the blade natural frequencies are not coincident with or very close to any harmonics of the tail rotor nominal rotational speed and (2) an extensive and costly experimental phase in which the resulting tail rotor design is tested to ascertain its structural and dynamic integrity as an integral part of the overall helicopter system.

The present inadequacies of the design phase may not be due only to the lack of proper consideration of the four problem areas which have been mentioned, but are also due to restrictions inherent in exising analytical techniques. Some of the restrictions used in various natural frequency analyses, an example being the analysis developed in Reference 2, are the neglect of

1. the effects of pitch-flap and pitch-lag coupling due to mean coning and lag;

2. the nonlinear effects of large motions due to the linearizing assumption of small angles;

3. large pitch-flap coupling δ_3 and pitch-lag coupling α_1;

4. blade deflection and slope time rate of change (d/dt) effects associated with mass, inertia, and aerodynamic characteristics;

5. control load offset coupling;

6. control system cyclic stiffness.

Most, if not all, of the above restrictions are commonly used in most natural frequency analyses. Thus, accurate predictive results can only be obtained for rather simple blade, blade root, and control system designs. A more sophiscated and representative analysis than is presently available is required to obtain accurate predictive results for complicated tail rotor systems (e.g., a rotor system).

An analysis capable of adequately determining the structural dynamic modal behavior of coupled helicopter/tail rotor systems should be able to determine the air resonance modal characteristics of a tail rotor system without use of the above-noted restrictions. In addition, this analysis should adequately include the effects of control system flexibility, gearbox mounting flexibility, drive shaft torsional flexibility, and fuselage-tailboom-fin flexibility on the tail rotor behavior. It is believed that the development of such an analysis would beneficially modify the tail rotor developmental procedure by significantly reducing the corrective experimental effort that has been required previously. Realizing the advantages and the applications of such an analysis, the Eustis Directorate, U. S. Army Air Mobility Research and Development Laboratory funded the development and application

of an analysis for investigating the modal behavior of coupled helicopter/tail rotor systems. This analyses will provide a new and effective design tool for use by both government and industry in the development and modification of tail rotors.

This report will present the overall system model configurations allowed, the general theoretical concepts used to develop the analysis, the resultant analytical expressions, and the results obtained for a flexstrap tail rotor system with the computer program that was developed.

DEVELOPMENT OF MATHEMATICAL REPRESENTATION

This section of the report will first discuss the physical characteristics of the helicopter modeled and then outline the basic mathematical concepts used to develop the theoretical representation of these characteristics. Following this discussion, the mathematical representation of the helicopter and tail rotor systems that are analyzed will be given, and the mathematical method by which the eigenvalues and associated eigenvectors are obtained will be presented.

THE PHYSICAL CHARACTERISTICS OF THE HELICOPTER AND TAIL ROTOR THAT ARE MODELED

Physical Considerations Concerning Model Requirements

The development of a satisfactory analysis for the investigation of the air resonance modal behavior of coupled helicopter/tail rotor systems requires the use of a more complex representational model than those used in existing blade frequency analyses. The total coupled system model complexity results due to the blade model representational requirements and the structural models necessary for the representation of the structural support environment of a tail rotor (i.e., flexibility of the local mounting structure, fuselage-tailboom-fin support structure, and control system). The necessity of a higher degree of model sophistication is apparent upon the consideration of the physical modal behavior of coupled helicopter/tail rotor systems.

Most natural frequency analyses assume the rotor system to be operating in vacuo, whereas in reality, the blades of a rotor operate in an aerodynamic environment. This environment can have an appreciable effect on the blade frequencies, mode shapes, and blade motion stability. The aerodynamic forces and moments acting on the rotor blades alter the steady coning, sweep, and twist distributions of the blades and, therefore, have a significant effect on the coupling of the chordwise, flapwise, and torsional blade motions. This alteration of the blade deformed position due to steady aerodynamic forces also modifies the blade motion stability by changing the blade deflection and slope time rate of change (d/dt) effects associated with the blade mass and inertia characteristics. In addition to the steady aerodynamic effects, the aerodynamic environment provides oscillatory forces and moments acting on the rotor blades which are a function of the vibratory behavior of the blades. These forces and moments, besides modifying the blade

frequency and mode shapes, alter the blade motion stability thru the addition of aerodynamic damping. The effects of the aerodynamic environment on the modal behavior of a rotor system are compounded further when the rotor blades are subjected to a nonaxisymmetric flow field. In this case, significant intrablade interharmonic coupling can result (i.e., blade motion occurring at one frequency ω can couple with a motion of the same blade occurring at a frequency of $\omega + \Omega$ or $\omega - \Omega$ or both where Ω is the rotational speed of the rotor). Thus, the blade model for the development of a satisfactory analysis to determine the air resonance modal behavior of a rotor system must have the capability of the inclusion of the above-noted aerodynamic effects in addition to the effects of the elastic, geometric, and structural properties of the blade. Also, restrictions associated with blade models inherent in existing frequency analyses should be avoided.

The structural support environment of a tail rotor has a significant effect on the air resonance modal behavior of a tail rotor system since this environment allows tail rotor hub and control system motion. As a result of this additional freedom of motion, interblade interharmonic coupling (i.e., coupling of the motion of one blade to the motion of another blade thru the control system and/or hub motion) and blade-fuselage structure interharmonic coupling can occur. The necessity of representational models for the various components of the structural support environment can be shown by considering the effect of each of these components on the various types of modal behavior of a four-bladed tail rotor in forward flight with the blades cantilevered to the rotor hub. For the basic tail rotor case in which the rotor hub is not allowed motion other than that corresponding to forward flight and the control system is infinitely stiff, each blade acts independently. Thus, the air resonance eigenvalues (frequency and stability values) obtained for one blade can be construed as the air resonance eigenvalues for the basic reactionless, umbrella, forward cyclic, and backward cyclic blade motions of the four-bladed rotor. The addition of support structure flexibility will significantly alter the air resonance eigenvalues and mode shapes for some of these types of blade motion.

With the allowance of collective control system flexibility, the umbrella air resonance eigenvalues and corresponding mode shapes will not coincide with those of the reactionless and cyclic air resonance modes which remain unchanged. If an anistropic control system flexibility is allowed, the backward and forward cyclic air resonance eigenvalues and corresponding mode shapes are altered such that they are not coincident with those of the reactionless air resonance modes of the basic tail rotor case. Thus, for a control system having both anisotropic and collective flexibility, there will

be four times as many distinct air resonance eigenvalues, based on blade representation, as there are for the basic tail rotor case. Additional air resonance eigenvalues also result which are introduced due to the consideration of the control system representation. These above-noted effects of the inclusion of control system flexibilities were observed in Reference 3.

The allowance of drive shaft torsional flexibility will affect the umbrella-type blade motions and will have a very pronounced effect on the chordwise bending air resonance frequencies. A possible problem area in regard to the drive shaft torsional flexibility is the possibility that the first drive shaft-tail rotor torsional frequency may be low enough to strongly couple with a fuselage-tailboom-fin mode and create an instability. In addition to the significant change in the tail rotor chordwise modes, the drive system flexibility will modify the umbrella-type torsional and flapwise bending air resonance eigenvalues and mode shapes due to the coupling of blade elastic motions.

The inclusion of tail rotor gearbox mounting flexibility may have a significant effect on the air resonance modal behavior of the tail rotor blades, since rotational motions of the gearbox about two perpendicular axes in the plane perpendicular to the tail rotor shaft at the gearbox result in translatory and rotational motions of the tail rotor hub. Due to the gearbox rotational motions being relative to a nonrotating shaft system and the motion of the blades being relative to coordinate systems rotating at the rotor rotational speed, the basic gearbox frequencies will couple strongly with the blade cyclic air resonance frequencies at, or close to, 1/rev above or below the basic gearbox frequencies. In particular, if a forward cyclic air resonance mode has a frequency roughly 1/rev below the gearbox frequency, strong coupling will occur and significant changes in the forward cyclic air resonance eigenvalue and corresponding mode shapes will result. Similarly, if a backward cyclic air resonance mode has a frequency roughly 1/rev above the gearbox frequency, strong coupling will occur and significant changes in the backward cyclic air resonance eigenvalue and corresponding mode shapes will result.

Attachment of a tail rotor to a flexible fuselage-tailboom-fin structure complicates the determination of the air resonance modal and stability behavior of the tail rotor due to the flexibilities existing in the nonrotating system. These flexibilities will affect the cyclic and umbrella-type air resonance modes and associated stability in a manner similar to that noted for the control system and tail rotor gearbox mounting flexibilities. Besides the alteration of the basic

air resonance eigenvalues and mode shapes associated with the tail rotor due to fuselage-tailboom-fin structure, many additional air resonance modes will result due to the coupling of the basic frequencies of the fuselage-tailboom-fin structure with the rotor modes. For example, for each air resonance frequency of the fuselage-tailboom-fin structure there exists a distinct air resonance frequency and mode shape corresponding to the umbrella, forward cyclic, and backward cyclic types of rotor blade motion.

The oscillatory motion of the tail rotor hub due to the flexibility of gearbox mounting and/or the flexibility of the fuselage-tailboom-fin structure necessitates the inclusion of gyroscopic and Coriolis force effects which will have a significant effect on modal and stability results. It has been shown that the gyroscopic effects of precession are very important when the vibratory characteristics of flexible blades of prop-rotor systems attached to relatively flexible lifting surfaces are being determined (Reference 4). The importance of precession effects on the performance characteristics of a tail rotor as well was indicated in Reference 5 where it was noted that 1/3 of the total thrust required from the tail rotor can be attributed to that necessary to overcome the precession due to the yaw rate of a helicopter.

An analysis for adequate determination of the air resonance modal behavior of coupled helicopter/tail rotor systems must be based on a system model capable of including the effects of the tail rotor local support structure and fuselage-tailboom-fin structure flexibilities. The overall system model configurations allowed in the development of this analysis consist of several basic model components which when properly sequenced define the system of interest. The basic components for which mathematical models are required can be categorized as:

1. the tail rotor blade structure;
2. the tail rotor hub restraints;
3. the tail rotor control system;
4. the tail rotor control rod configuration;
5. the fuselage-tailboom-fin structure;
6. the tail rotor gearbox mounting flexibilities;
7. the tail rotor drive shaft torsional flexibility.

The analysis for the computer program has the capability to model each of these helicopter system components individually or in combination with other system components. When all of the components are included, the coupled and interdependent modal behavior for the total system depicted in Figure 1 may be predicted. A thorough description of the modelling of the individual system components is given in the following sections.

Tail Rotor Blade Model

The basic model of the blades comprising the tail rotor allows for the inclusion of all blade characteristics believed to be significant. These are as follows:

1. arbitrary orientation of the blade shear center axis by precone and presweep distributions;

2. arbitrary chordwise location of the blade shear center axis (axis about which the blade cross section will rotate when perturbed);

3. localized rigid offsets of shear center axis in the flapwise, chordwise, and spanwise directions;

4. arbitrary variable twist distribution including collective about the blade shear center axis;

5. arbitrary mass distribution and chordwise, flapwise, and torsional inertia distributions;

6. arbitrary chordwise location of the center of mass relative to the blade shear center;

7. arbitrary chordwise, flapwise, and torsional bending stiffness distributions and inclusion of centrifugal stiffening effects;

8. localized torsional spring-damper unit application about the flapwise, chordwise, and spanwise directions;

9. arbitrary structural damping coefficient;

10. gravitational perturbation moment effects;

11. arbitrary chordwise location of blade aerodynamic center axis relative to blade midchord;

12. arbitrary variable chord length distribution;

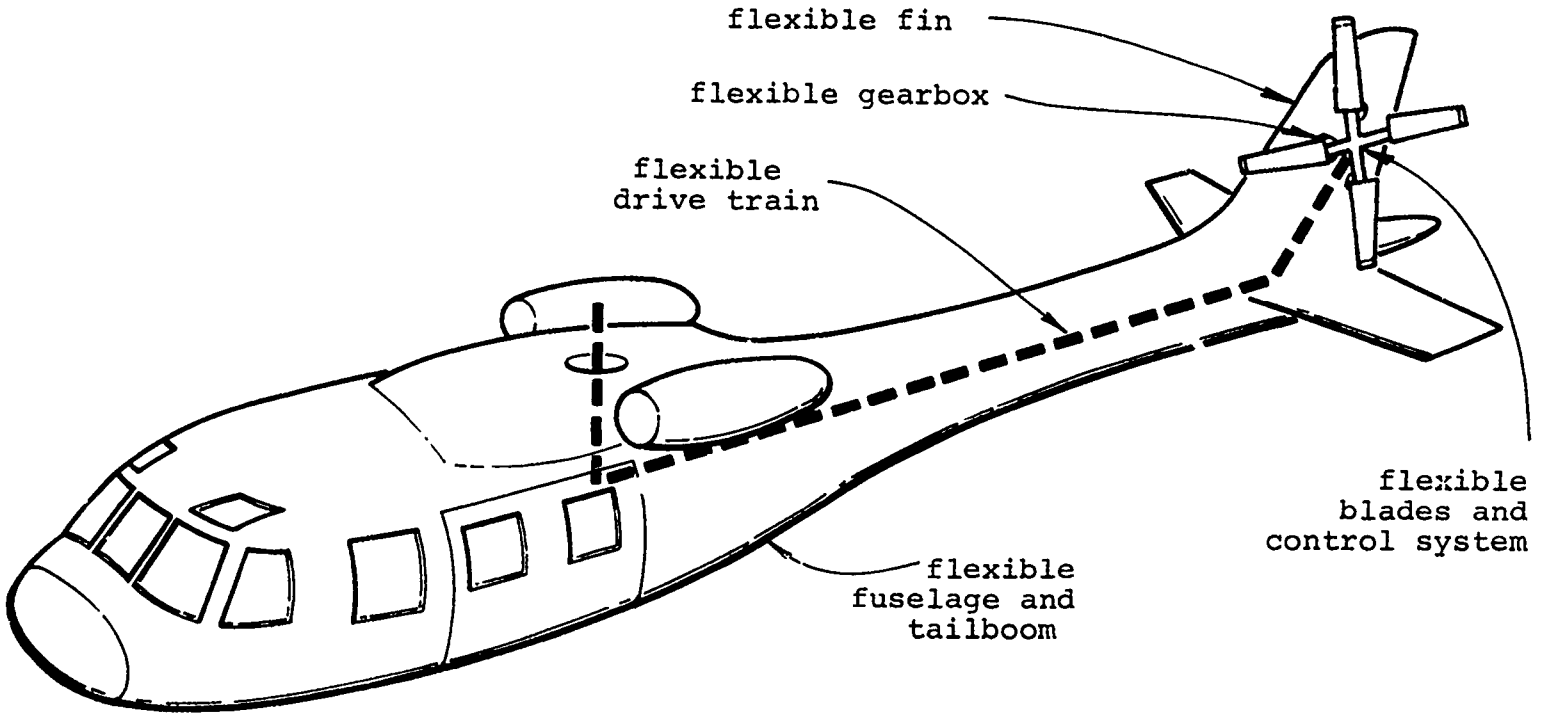

Figure 1. Representative Structure That Can Be Considered.

13. aerodynamic effects including aerodynamic damping and Theodorsen's unsteady aerodynamic effects;

14. up to five different airfoil sections along blade span with the aerodynamic coefficients determined from tables of aerodynamic coefficients versus angle of attack and Mach number.

A lumped parameter approach to the modelling of the blades is used to represent the above allowed blade characteristics. Up to 25 blade stations can be utilized to represent these various blade properties.

In addition to the modelling of the blade properties, discontinuities such as hinges and concentrated control force inputs must also be considered. Thus, the program considers two basic types of rotor systems (1) a partially to fully articulated tail rotor and (2) a flexstrap tail rotor). Through proper program control all types of commonly used rotor configurations can be represented including articulated, rigid, teetering, flexstrap, etc.

A fully articulated tail rotor requires that the blades have a flap hinge, lead-lag hinge, and pitch bearing as well as a control rod attachment restraint. The representation for a lead-lag hinge, if required, is accomplished by use of a localized torsional spring-damper unit (an allowed blade characteristic) having the required torsional stiffness and damping values. The axis of the local torsional spring-damper unit (normally, the unit acting about the local flapwise direction is used) should coincide with the axis of the lead-lag hinge. This alignment is achieved by proper location and orientation (thru the use of local precone, presweep, and pretwist angles) of the section containing the lead-lag hinge.

The representation of a flap hinge, if required in the blade model, is accomplished in either of two ways. The first way is to represent the flap hinge in a manner similar to that used for representing a lead-lag hinge. That is, a localized torsional spring-damper unit (normally, the unit acting about the local chordwise direction) may be used with the condition that the axis of the local spring-damper unit should coincide with the axis of the flap hinge The alternate way is to analytically represent the flap hinge by considering a discontinuity in the oscillatory flapping motion to occur at the flap hinge location and the condition that the local oscillatory flapwise moment must be zero at the hinge. For example, the oscillatory flapping motion of a rotating rigid blade attached to a rigid rotor hub by a flap hinge can be considered to be a flap angle discontinuity at the flap hinge. This

method of representing a flap hinge does not allow inclusion of external damping of the flap hinge motion. The analysis for both of these flap hinge models is included in the computer program to allow the user the choice of the most suitable model for particular program applications.

The representation of a pitch bearing, if required, is accomplished by considering a discontinuity in the oscillatory pitching motion to occur at the pitch bearing and the condition that the local oscillatory torque at the pitch bearing must be zero. The concept of a pitch angle discontinuity is similar to that of a flap angle discontinuity except that it occurs about the pitch bearing axis. The control rod effects on an articulated blade, if they are to be included, are represented by considering the control rod to apply an oscillatory torque (torque discontinuity) to the blade shear center axis at the effective spanwise application point of this torque. The torque discontinuity is normally considered to be applied outboard of the pitch bearing location.

The models for the flap and lead-lag hinges can represent large pitch-flap coupling δ_3 and pitch-lag coupling α_1 effects. This is possible since the flap and lead-lag hinge axes may be placed in any desired orientation by the use of local section precone, presweep, and pretwist angles. An alternate model for representing pitch-flap and pitch-lag coupling was also included in the program analysis. In this model the flap and lead-lag hinges are taken to act about the local chordwise axis and flapwise axis, respectively, with the required coupling of blade motions taken into account on specification of pitch-flap and pitch-lag coupling factors.

The other basic type of rotor system is that necessary for the consideration of a blade attached to a tail rotor hub by means of a flexible strap. In this case, flap and lead-lag hinges and a pitch bearing do not exist on the blade. Instead, the flapwise, chordwise, and torsional motions inboard of the effective pitch horn attachment point are allowed by the flexibilities inherent in the strap. While these flexibilities can be represented by the basic blade model elastic properties, the relationship between the elastic blade motions is also dependent upon the oscillatory forces and moments in three mutually orthogonal directions acting on the blade shear center axis due to the restraint provided by the control rod.

For a flexstrap blade, the control rod is assumed to be attached to a pitch horn which is described by means of its length and its flexibility and orientation in three mutually

orthogonal directions. The oscillatory forces and moments acting on the blade shear center axis at their effective application point can be expressed in terms of the pitch horn properties, local perturbation (oscillatory) slopes and deflections at the blade shear center axis, and the oscillatory deflections of the control rod attachment point to the pitch horn. The control rod attachment point deflections are considered as discontinuity quantities. The pitch-flap δ_3 and pitch-lag α_1 coupling are automatically included in this model and are directly related to the flexstrap and pitch-horn representation.

In the case of a flexstrap blade, the control rod does not remove all of the oscillatory blade torque; therefore, a significant amount of oscillatory flapwise, chordwise, and torsional elastic deflection of the strap occurs. Because of the elastic couplings, the flexstrap must be represented by more lumped parameters per unit of length than is required to properly represent the rest of the blade. Also, a sufficient knowledge of the mean orientation precone, presweep, and pretwist of the flexstrap is required since the elastic coupling is very dependent upon the rapidly changing orientation of the flexstrap elastic stiffness parameters.

Tail Rotor Configuration Models

Basically, the tail rotor configuration models considered in the development of representational analysis may consist of any number of flexible blades which can be arbitrarily located azimuthally. The computer program, however, was limited to rotor configurations consisting of identical flexible blades by the analytical coding, rotor configurations consisting of four or less blades arbitrarily spaced azimuthally or of any number of blades equally spaced azimuthally by variable dimension restrictions, and to rotor configurations consisting of any number of blades equally spaced azimuthally by additional variable dimension restrictions. These tail rotor configuration program limitations can be easily removed by increasing variable dimensions where required and modifying the analytical coding. The tail rotor configuration models allow arbitrary orientation and amplitude of the gravitational field and the rotor hub flight velocity where these orientations are specified relative to the azimuthally located reference blade position. The required analysis was developed for the several different types of rotor configurations that can be represented by the program. For purposes of discussion, the blades of all tail rotor configurations can be considered to be cantilevered to a rigid rotor hub which may have degrees of freedom relative to its attachment to the

rotor shaft. The five rotor configurations that can be represented within the program are:

1. a rigid rotor that is represented through the basic blade model (i.e., without hinges, bearings, and control rod attachments);

2. a partial to fully articulated rotor constructed from the articulated blade model;

3. a flexstrap rotor constructed from the flexstrap blade model;

4. a gimballed rotor (more than two blades) constructed from the articulated blade model;

5. a teetering rotor (two blades only) constructed from the articulated blade model.

The first three types of rotor models listed above require the rigid rotor hub to be cantilevered to the rotor shaft. The gimballed rotor model assumes the rigid rotor hub to be attached to the rotor shaft such that it is free to rotate about two mutually orthogonal axes rotating in the plane perpendicular to the rotor shaft at the rotor hub attachment point. The teetering rotor model assumes the rigid rotor hub to be attached to the rotor shaft such that it is free to rotate about one axis rotating in the plane perpendicular to the rotor shaft at the rotor hub attachment point.

Model of the Tail Rotor Control System

The model of the tail rotor control system is based upon the assumption of a swashplate-type control system. The main component of the swashplate control system model, shown in Figure 2, is represented by a flexible ring having uniform mass distribution around the circumference and consisting of upper and lower portions. Both portions of the ring are allowed to translate along the rotor shaft axis and rotate about two mutually orthogonal axes perpendicular to the rotor shaft axis. The upper portion of the ring also rotates with the blades about the rotor shaft axis. The lower portion of the ring, which does not rotate with the blades, is supported by a finite number of supports which have arbitrary linear stiffness and damping characteristics. These supports may also be arbitrarily located azimuthally around the ring so that an azimuthal distribution of control stiffness can be represented. The collective base to which the ring supports are attached is assumed to be attached to the tail rotor gearbox by a linear support having an arbitrary effective

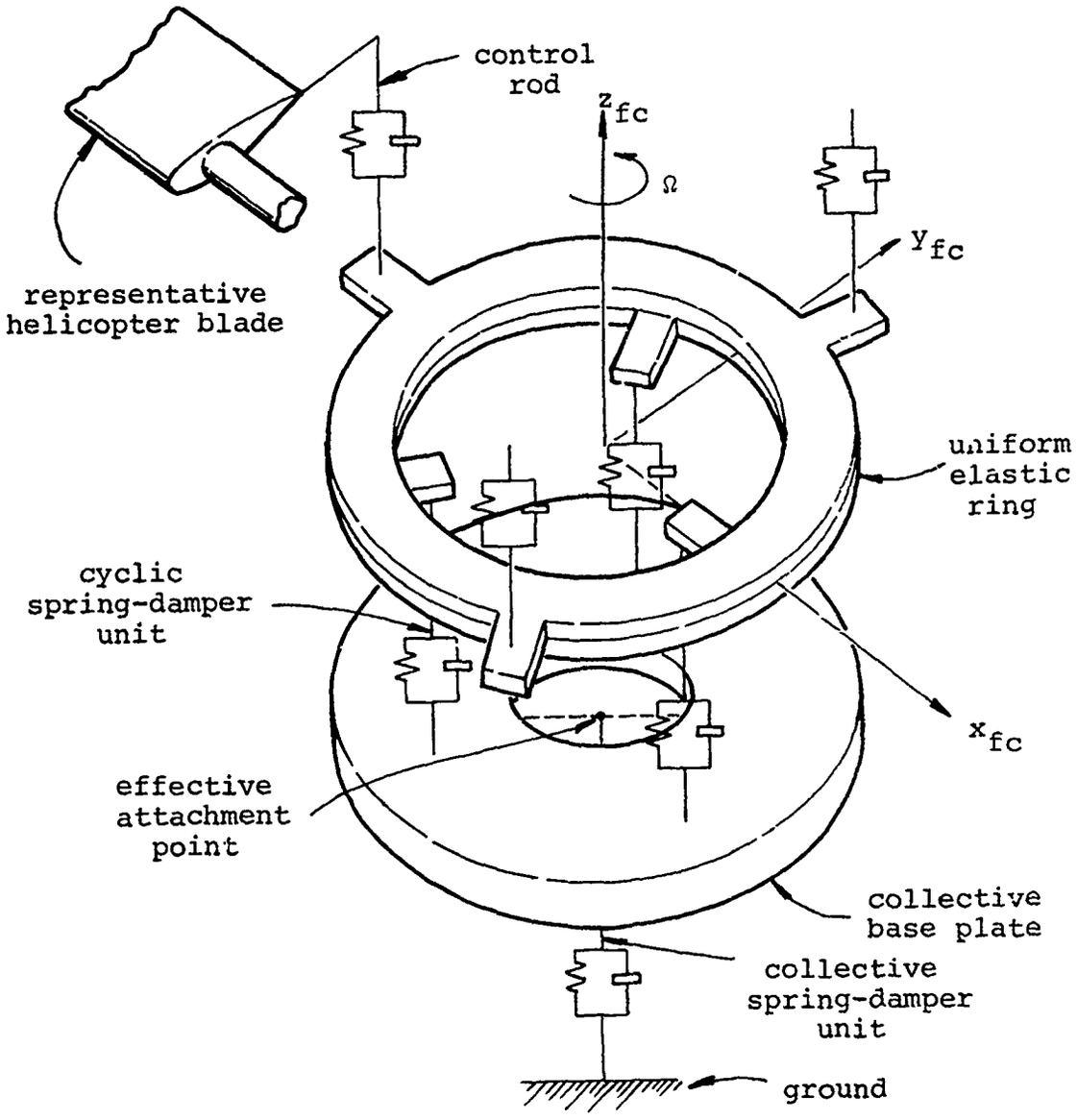

Figure 2. Swashplate Control System Model and Fixed Coordinate System for Counterclockwise Rotating Rotor.

stiffness and damping value. The forces parallel to the tail rotor drive shaft axis acting on the swashplate from the control rods are passed through the swashplate control system model and applied to the tail rotor gearbox. Thus, by variation of the stiffness and damping characteristics and azimuthal location of the supports involved, any degree of anisotropic support of the swashplate control system can be obtained.

Tail Rotor Control Rod Model

The inclusion of the tail rotor control rods is required when an articulated or flexstrap blade model is involved. In either case, the control rods are allowed to have arbitrary axial stiffness and damping characteristics and are assumed to be connected to the blade pitch horns and swashplate (or ground, if no swashplate) by swivel ball joints such that the control rods cannot carry moments or transverse loadings. For an articulated blade, the control rod is assumed to only apply a torque to the blade.

The modeling of the control rod for the flexstrap rotor system is, in general, much more complex than that which is required for the articulated rotor system. The primary reasons for the increase in model complexity are: (1) the large angularity of the control rod due to the radius at which it attaches to the blade and (2) the strong elastic coupling created by the control rod in the flexstrap flapwise, chordwise and torsional degrees of freedom. In addition, due to the angularity and offset of the control rods, blade motions in the inplane and flapwise directions are coupled through the control system. This results in a much more highly coupled system than is the case for an articulated rotor system. The stiffness and damping characteristics of the control rods are also included with those associated with the swashplate representation, discussed previously, in order to adequately represent the cyclic and collective stiffness and cyclic and collective damping acting on the blades due to the control system and control rods.

Fuselage-Tailboom-Fin Model

The basic fuselage-tailboom-fin model allows for the inclusion of all structural and aerodynamic characteristics believed to be of significance. These characteristics are essentially those which were listed for the tail rotor blade model. Since the fuselage-tailboom-fin structure is not rotating, as was the case for the blades, the representation of the mass and inertia effects and aerodynamic effects on the fuselage-tailboom-fin structure differs from the representation of these effects on a blade. For example, the mass and inertia

distribution on the fuselage-tailboom-fin structure does not provide centrifugal stiffening of elastic sections or damping effects. Also, the aerodynamic representation for the fuselage-tailboom-fin structure does not include time rate of change terms such that intrafuselage interharmonic coupling does not occur (i.e., harmonics of fuselage motion do not couple). For proper aerodynamic representation of this model, the aerodynamics for the fuselage and tailboom are based on blockage (flat plate drag) effects; whereas the fin aerodynamics are similar to that utilized for the blades. As an alternate to the use of aerodynamic coefficient tables or a complicated series representation, the aerodynamic coefficients can be based on a series representation (linear aerodynamics) for NACA 0012 airfoil. A horizontal stabilizer can be represented as an aerodynamic station on the shear center axis of the tailboom or fin. The magnitude and orientation of the flight velocity vector acting on the fuselage-tailboom-fin structure can also have an arbitrary orientation.

The fuselage-tailboom-fin structure is represented by a lumped parameter form similar to that used for the blade representation. This lumped parameter form is used to represent the entire support structure, including the tail rotor gearbox mounting flexibilities and the rotor shaft from gearbox to rotor hub attachment point. Up to 15 sections may be used to represent the entire support structure.

Tail Rotor Gearbox Mounting Model

The tail rotor gearbox mounting flexibility is represented by utilizing the localized torsional spring-damper capabilities of the fuselage-tailboom-fin model. In particular, localized torsional spring-damper units with arbitrary torsional stiffness and damping characteristics are applied about two mutually orthogonal axes at the gearbox attachment to the fuselage. The specific orientation of the two axes relative to the fuselage-tailboom-fin structure fixed coordinate system is accomplished through the use of geometric angles. By variation of the stiffness and damping characteristics of the two torsional spring-damper units, any degree of anisotrophy in tail rotor gearbox mounting can be represented.

Tail Rotor Drive Shaft Torsional Flexibility Model

In representing the drive shaft torsional flexibility, the drive shaft is assumed to be constrained in torsion at the main rotor transmission. The model of the torsional characteristics of the drive shaft system was formulated by considering a localized torsional spring at the root of each blade whose inplane flexibility is equivalent to the drive

shaft torsional flexibility. In addition, the blade chordwise moments at the hub are not allowed to provide torque to the shaft, and thereby to the fin, since the torque on the rotor shaft is removed by the transmission. This torsional spring model is considered independent of the blade model and should not be construed to be modeled as part of the basic blade model.

THEORETICAL MATHEMATICAL CONCEPTS USED IN THE PROGRAM FORMULIZATIONS

Due to the complexity of the model required to represent the tail rotor systems previously outlined, several basic theoretical mathematical techniques were used so that the formulations of all final governing equations would be compatible:

1. Laplace transformation techniques
2. transfer matrix procedures
3. Fourier analysis techniques
4. coordinate systems and transformation relationships
5. Dirac delta function representations
6. application of boundary conditions

Laplace Transformation Techniques

The application of the Laplace transformation techniques provides an effective means of converting time differential equations having first and second order time derivative terms as well as periodically varying coefficients to an algebraic form which can be efficiently manipulated to obtain the solution eigenvalues and eigenvectors. Generally, because of the nature of the problems being considered, the resulting algebraic equations involve complex variable notation; therefore, the Laplace transform variables must be allowed to be complex. In addition, a characteristic of the Laplace transformed equations can be used to develop the additional equations necessary to define the harmonically shifted variables required for the consideration of interharmonic coupling due to the control system and/or rotor hub motion and periodically varying aerodynamic coefficients.

All of the real-time equations required in the development of tail-rotor analysis were altered to a form in which the variables involved are expressible as a function of time in exponential form. These equations were then subjected to the

application of Laplace transformation techniques. In addition to the standard definition of the Laplace transform

$$\bar{F}(s) = L_T(f(t)) = \int_0^\infty e^{-st} f(t)dt$$

several other Laplace transform theorems were used: i.e., (1) the superposition theorem

$$L_T\left(\sum_n A_n f_n(t)\right) = \sum_n A_n L_T\left(f_n(t)\right)$$

where A_n are constants; (2) the basic differential theorem

$$L_T(df(t)/dt) = s\bar{F}(s)$$

assuming the quiescent initial conditions; (3) the extended differential theorem

$$L_T\left(d^n f(t)/dt^n\right) = s^n \bar{F}(s)$$

assuming quiescent initial conditions; and (4) the frequency shift theorem

$$L_T\left(e^{at} f(t)\right) = \bar{F}(s-a)$$

The latter theorem provides the means of obtaining the additional equations defining the harmonically shifted variables required when interharmonic coupling is allowed. Information concerning Laplace transform techniques is presented in References 6, 7, and 8.

Transfer Matrix Procedures

The standard transfer matrix procedure consists of the following:

1. a modeling procedure in which the distributed structure properties are converted to a lumped parameter form representing the flexible structure as (a) uniform massless elastic beam sections (centrifugally stiffened, if exposed to constant rotation) and (b) point masses, inertias, geometric bends, torsional stiffness and damping, and shear center axis offsets located at the ends of the elastic beam section, and

2. a process in which the transfer matrices associated with successive characteristics of the modeled flexible structure are combined to form the transfer or associated matrix relating the shears, moments, slopes, and deflections at a position on the flexible structure to those occurring at the end of the flexible structure at which the process was initiated.

The lumped parameter method of modeling a flexible structure is not a prerequisite for the application of transfer matrix procedures, but it is practical and convenient and is generally used.

The state variables representing the shears, moments, slopes, and deflections on one side of the lumped parameter blade representation can be related to the state variables on the other side by equations which can be written in matrix form as $\{S(t)\}^- = [G]\{S(t)\}^+$ where [G] is a real-time transfer matrix which may include time differential operators. Application of Laplace transforms to the equations prior to matrix representation with the assumption of quiescent initial conditions such that d/dt and d^2/dt^2 operators are replaced by s and s^2, respectively, yields algebraic equations which can be written in matrix form as $\{\bar{S}(s)\}^- = [\bar{G}(s)]\{\bar{S}(s)\}^+$ where $[\bar{G}(s)]$ can be denoted as a Laplace transformed transfer matrix. If the real-time state variable equations are premultiplied by $e^{ik\Omega t}$ where k is a positive or negative integer, Ω is the rotor rotational speed (rad/sec), and t is time (sec) prior to the Laplace transformation application, the resulting transformed equations can be written in matrix form as $\left\{\bar{S}_k\right\}^- = \left[\bar{G}_k\right]\left\{\bar{S}_k\right\}^+$. The k subscript denotes that the Laplace transform variable s has been replaced by $s-ik\Omega$ (k frequency shifted). This matrix equation defines the relationship of state variables at a frequency shifted $k\Omega$ relative to that specified by the imaginary part of s. Generally, any Laplace transform equation can be frequency shifted by replacing s with a frequency shifted Laplace transform variable as represented by the shifting theorem.

With the inclusion of aerodynamic forces acting on a blade, the real-time state variable equations for the transfer across an aerodynamic application point involve time varying coefficients in addition to d/dt operators. The time varying coefficients can be expressed by a Fourier series

representation in the exponential form $f(t) = \sum_{n=-\infty}^{\infty} a_n e^{in\Omega t}$. This allows the Laplace transformed equations to be written in the matrix form $\left\{\bar{S}_0\right\}^- = \sum_{n=-\infty}^{\infty} \left[\bar{G}_n\right]\left\{\bar{S}_n\right\}^+$ where $\left[\bar{G}_n\right]$ is the transformed transfer matrix specifying the contribution of the n frequency shifted state variables to the zero frequency shifted state variables due to aerodynamic considerations. This matrix equation can be frequency shifted to the matrix form $\left\{\bar{S}_k\right\}^- = \left[\bar{G}_{k,n}\right]\left\{\bar{S}_n\right\}^+$ where $\left[\bar{G}_{k,n}\right]$ is the transformed transfer matrix specifying the contributions of the n frequency shifted state variables to the k frequency shifted state variables due to aerodynamic considerations.

The Laplace transformed transfer matrices for successive lumped parameter characteristics of a structure can be combined to form the associated matrices relating the state variables at a position on the structure to the state variables at the initial end of the structure. The k frequency shifted state variables just beyond the jth lumped parameter characteristic can be expressed relative to the initial n frequency shifted state variables in the matrix form $\left\{\bar{S}_k\right\}^{j-} = \sum_{n=-\infty}^{\infty} \left[\bar{B}_{k,n}\right]^j \left\{\bar{S}_n\right\}^0$ where the $\left[\bar{B}_{k,n}\right]^j$ are associated transfer matrices.

The associated transfer matrices for the jth nonaerodynamic lumped parameter characteristic can be related to those for the (j-1)th characteristic by the expression

$$\left[\bar{B}_{k,n}\right]^j = \left[\bar{G}_k\right]^j \left[\bar{B}_{k,n}\right]^{j-1} \qquad (1)$$

If an aerodynamics lumped parameter characteristic is involved, the successive associated transfer matrices can be related by the expression

$$\left[\bar{B}_{k,n}\right]^j = \sum_{\ell=-\infty}^{\infty} \left[\bar{G}_{k,\ell}\right]^j \left[\bar{B}_{\ell,n}\right]^{j-1} \qquad (2)$$

These two associated transfer matrix relationships can be verified by replacing j in the general definition of the state variables after the jth characteristic in terms of the initial state variables by j-1 and substituting the resulting expression into the forms of the expressions for transfer across a

nonaerodynamic characteristic and an aerodynamic characteristic, respectively. Equation (2) represents the mechanism of intrablade interharmonic coupling which will occur for a rotating blade experiencing time varying aerodynamic loading. With the initial lumped parameter characteristic being other than an aerodynamic characteristic, the initial associated transfer matrix arrays are defined by $\left[\bar{B}_{k,k}\right]^1 = \left[\bar{G}_k\right]^1$ and $\left[\bar{B}_{k,n}\right]^1 = \left[0\right]$ for $k \neq n$. If the structure is in a constant aerodynamic environment such that $\left[\bar{G}_{k,\ell}\right]^j = \left[0\right]$, for $k \neq \ell$ and all values of j denoting aerodynamic application points, interharmonic coupling will not occur, with the result that $\left[\bar{B}_{k,n}\right]^j = \left[0\right]$ for $k \neq n$, as can be seen by Equations (1) and (2).

In addition to the basic formulation of the Laplace transformed transfer matrix representation of a structure, the effects of the blade discontinuities discussed in the tail rotor blade model presentation must also be considered. The general definition of the k frequency shifted state variables just beyond the jth lumped parameter characteristic can be expressed relative to the initial n frequency shifted state and discontinuity variables in the matrix form

$$\left\{\bar{S}_k\right\}^{j-} = \sum_{n=-\infty}^{\infty}\left[\left[\bar{B}_{k,n}\right]^j\left\{\bar{S}_n\right\}^0 - \left\{\bar{b}_{k,n}\right\}^j\overline{\Delta 1}_n - \left\{\bar{c}_{k,n}\right\}^j\overline{\Delta 2}_n - \left\{\bar{d}_{k,n}\right\}^j\overline{\Delta 3}_n\right] \qquad (3)$$

In this expression, $\left\{\bar{b}_{k,n}\right\}^j$, $\left\{\bar{c}_{k,n}\right\}^j$, and $\left\{\bar{d}_{k,n}\right\}^j$ are the Laplace transformed discontinuity column arrays, just beyond the jth lumped parameter characteristic, multiplying the general n frequency shifted blade discontinuity variables $\overline{\Delta 1}_n$, $\overline{\Delta 2}_n$, and $\overline{\Delta 3}_n$, respectively.

The discontinuity column matrices are introduced by considering the state variables on crossing a discontinuity to be related by the form $\left\{\bar{S}_k\right\}^- = \left\{\bar{S}_k\right\}^+ - \left\{\bar{b}_k\right\}\overline{\Delta 1}_k$ which is the relationship for the first discontinuity. For compatibility

with Equation (3), if j is less than the value of the lumped parameter index for the lumped characteristic just beyond which the first discontinuity occurs, $\left\{\bar{b}_{k,n}\right\}^j = \left\{0\right\}$ for all values of k and n. If j is the value of the lumped parameter index for the lumped characteristic just beyond which the first discontinuity occurs, $\left\{\bar{b}_{k,n}\right\}^j = \left\{0\right\}$ for $k \neq n$ and $\left\{\bar{b}_{k,k}\right\}^j = \left\{\bar{b}_k\right\}$. If j is greater than the value of the lumped parameter index for the lumped characteristic beyond which the first discontinuity occurs, $\left\{\bar{b}_{k,n}\right\}^j$ is determined by application of the relationships specified by Equations (1) and (2) with $\left\{\bar{b}_{k,n}\right\}^j$ replacing $\left[\bar{B}_{k,n}\right]^j$. The $\left\{\bar{c}_{k,n}\right\}^j$ and $\left\{\bar{d}_{k,n}\right\}^j$ discontinuity column arrays are represented in a similar manner.

The use of Laplace transforms in conjunction with the transfer matrix procedures, although simple in concept, is thought to be a fairly unique approach to representing the behavior of a structure. More detailed general information regarding the application and use of transfer matrices may be found in Reference 9.

Fourier Analysis Application

Fourier analysis techniques are utilized in the predictive program to describe the periodically varying coefficients in the representation of the blade aerodynamic forces and to develop suitable equations describing the dynamic characteristics of the swashplate.

As previously mentioned, the equations relating the state variables on one side of a lumped aerodynamic load point to the state variables on the other side may include periodically varying coefficients due to a nonaxisymmetric flow field environment acting on the blade. The periodically varying coefficients can be expressed in the exponential Fourier series form $f(t) = \sum_{n=-\infty}^{\infty} a_n e^{in\Omega t}$ where the Fourier harmonic

coefficients can be defined by the definition $a_n = (1/2\pi) \int_0^{2\pi} f(t)e^{-in\Omega t}d(\Omega t)$. An alternate definition for harmonic coefficients is $a_n = (1/NAS) \sum_{j=1}^{NAS} f(\psi_j)e^{-in\psi_j}$, where $\psi_j = 2\pi\ (j-1)/NAS$, NAS is the number of uniformly spaced azimuthal steps in one revolution, and $f(\psi_j)$ is the value of the function of interest at ψ_j. The highest harmonic coefficient a_{max} which can be determined by this method is defined by max = NAS/2-1. This latter method is employed to obtain the harmonic Fourier coefficients of the periodically varying aerodynamic coefficients of the reference blade. The periodically varying aerodynamic coefficients of additional identical blades are represented in terms of reference blade coefficients by the general form $f_m(t) = \sum_{n=-\infty}^{\infty} a_n e^{in(\Omega t+\phi_m)}$ where ϕ_m is the angle between the mth blade and the reference blade. If the mth blade is not identical to the reference blade, the above expression is valid if the a_n values for the reference blade are replaced with similar values for the mth blade, based upon the periodically varying aerodynamic coefficients of this blade as it rotates from $\psi_j = 0$ (reference blade position) to $\psi_j = 2\pi\ (NAS-1)/NAS$.

An additional use of Fourier analysis techniques is required to obtain the equations of motion of the control (swashplate) system. The time t and azimuthal θ dependent variables in the swashplate control system governing equations of motion are converted to a single dependency on time by using relationships such as

$$v_\ell(t) = (1/2\pi)\int_0^{2\pi} v(\theta,t)e^{-i\ell\theta}d\theta \qquad (4)$$

which corresponds to the definition

$$v(\theta,t) = \sum_{\ell=-\infty}^{\infty} v_\ell(t)e^{i\ell\theta} \qquad (5)$$

where the v variable utilized as an example corresponds to a

swashplate displacement variable. By multiplying all initial swashplate equations of motion by $e^{-i\ell\theta}d\theta$ and integrating over θ from 0 to 2π employing conditions of periodicity, complex variable ordinary differential equations result relating the ℓth harmonic terms (harmonics with respect to θ dependency). Use of Equation (4) and the Dirac delta function allows the determination of the applied force and moment loading acting on the swashplate ring in terms of the ring displacements and rotations at the spring-damper unit application points and the forces applied through the control rods. The use of Fourier analysis enables the development of the equations of motion in a form suitable for application of Laplace transformation techniques to obtain the final control system equations of motion compatible with the blade and fuselage-tailboom-fin related equations. Additional information regarding Fourier analysis techniques may be found in References 7 and 8.

Coordinate Systems and Transformation Relationships

The development of the analytical representation of a tail rotor attached to a local support structure and fuselage-tailboom-fin structure and the boundary condition relationships between various system components is based on the coordinate systems required to specify location and orientation of various components and system variables. A discussion of the primary coordinate systems provides a necessary background for the discussion of the analysis developed to represent the system behavior and provide the final governing matrix equation which allows solution for the system eigenvalues and associated eigenvectors. The primary coordinate systems to be discussed will be those pertaining to the blade, swashplate and fuselage-tailboom-fin structure, including the relationship between these coordinate systems at the drive shaft-hub interface. The subcoordinate systems for representing the control rod, pitch horn, gravitational field and free-stream velocity orientations will not be discussed herein, but are defined in the computer program documentation related material.

Most of the coordinate system orientations are dependent upon the direction of rotation of the tail rotor, and as such must be defined in a general sense. The basic rectangular cartesian coordinate systems associated directly with the tail rotor blades consist of a fixed (nonrotating) shaft coordinate system referenced to the first blade at $t = 0$, a rotating shaft coordinate system for each blade and a rotating local blade coordinate system for each section of each blade. The fixed shaft coordinate system has its origin at the intersection of the unperturbed shaft centerline and the rotor disc plane of the unconed, untwisted, and unswept blades. The disc

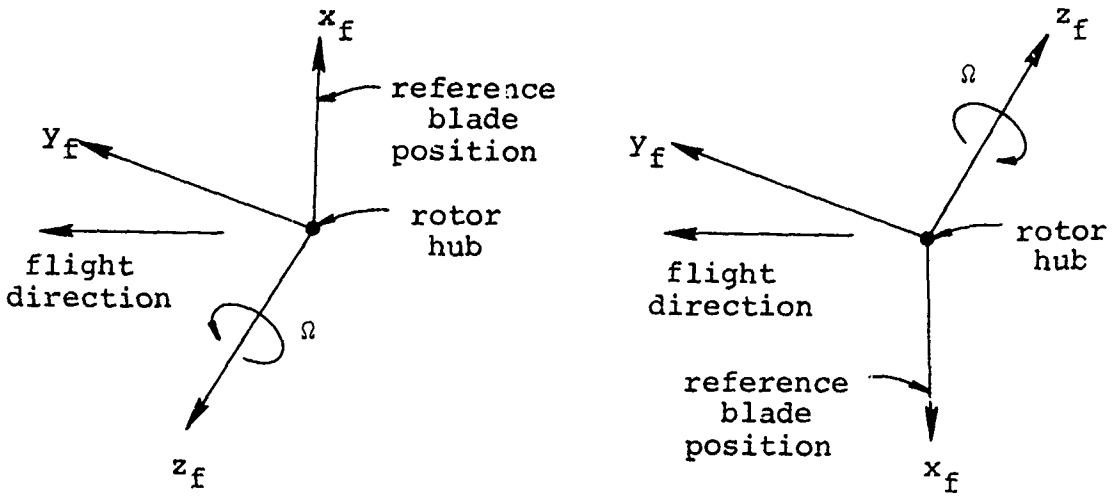

Figure 3. Fixed Shaft Coordinate Systems for Two Directions of Rotor Rotation.

plane is perpendicular to the unperturbed shaft centerline. The x-axis of this coordinate system lies in the disc plane and is perpendicular to the forward velocity of the helicopter in level forward flight such that it coincides with the spanwise axis of the unconed, untwisted, and unswept blade in the advancing blade position. This axis is positive directed away from the shaft centerline. The x-axis also denotes the azimuthal reference blade position. The z-axis coincides with the centerline of the sh ft and is positive in the direction of the rotor rotational velocity vector. The y-axis lies in the rotor plane and is mutually orthogonal to the x and z axes such as to constitute a right-handed cartesian coordinate system. The fixed coordinate system (x_f, y_f, z_f) is depicted in Figure 3 for two directions of rotational velocity. The y_f-axis has not been shown parallel to the forward velocity nor the z_f-axis perpendicular to the forward velocity since the rotor plane may be skewed with respect to the forward velocity vector. For an unconed, untwisted, and unswept blade at the reference position, the y_f-axis is parallel to the blade chord with the leading edge ahead of the x_f-axis in the positive direction of the y_f-axis. In addition, a right-handed rotation about the x_f-axis results in a positive angle

of attack of the blade airfoil.

The rotating shaft coordinate systems, one for each blade, have the same origin and z-axes as the fixed shaft coordinate system, but their x and y related axes in the basic rotor plane are rotating about the z_f-axis with a rotational speed Ω. The rotating shaft coordinate systems have their x-axis along the blade spanwise axis in the unconed, untwisted, and unswept position and can be related to the fixed shaft coordinate system by the coordinate transformation

$$\begin{Bmatrix} \bar{i}_{rm} \\ \bar{j}_{rm} \\ \bar{k}_{rm} \end{Bmatrix} = \begin{bmatrix} \cos(\Omega t+\phi_m) & \sin(\Omega t+\phi_m) & 0 \\ -\sin(\Omega t+\phi_m) & \cos(\Omega t+\phi_m) & 0 \\ 0 & 0 & 1 \end{bmatrix} \begin{Bmatrix} \bar{i}_f \\ \bar{j}_f \\ \bar{k}_f \end{Bmatrix} \qquad (6)$$

where Ωt and ϕ_m are as defined previously and $\bar{I}$, $\bar{J}$, and $\bar{K}$ are unit vectors with rm subscripts denoting the rotating shaft coordinate system for the mth blade and f subscript denoting the fixed shaft coordinate system. The rotating shaft coordinate system (x_{rm}, y_{rm}, z_{rm}) for the first blade relative to the fixed shaft coordinate is depicted in Figure 4 for the two directions of rotation.

The rotating local blade coordinate systems of each blade are located in the local blade sections in their mean deformed position. In the local blade coordinate system, the x-axis is along the local shear center axis of the blade in the mean position and positive outboard, the y-axis is along the local chord of the blade in the mean position and positive toward the blade leading edge, and the z-axis is mutually orthogonal to the x and y related axes such as to constitute a right-handed coordinate system. The blade local coordinate system (x_{bm}, y_{bm}, z_{bm}) is obtained from the associated rotating shaft coordinate system by performing three orthogonal rotations: Φ, Θ, and Ψ in consecutive order where

- Φ corresponds to local presweep in the direction of rotor rotation,
- Θ corresponds to local precone rotation about the preswept y_{rm}-axis, and
- Ψ corresponds to local pretwist and/or collective angle of attack rotation about preswept and preconed x_{rm}-axis.

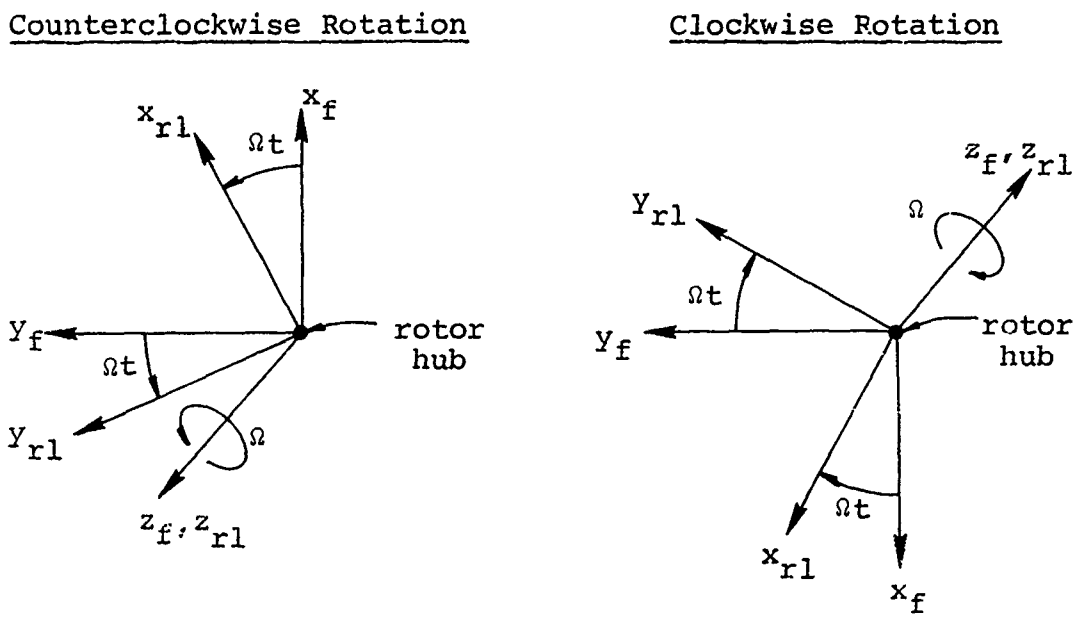

Figure 4. Rotating and Fixed Shaft Coordinate Systems for Two Directions of Rotor Rotation.

The relationship between the blade local coordinate system and its associated shaft rotating coordinate system is depicted in Figure 5, which also includes the orientation of the Laplace transformed state variables which act in the rotating local blade coordinate system and are defined as follows:

$\overline{ux}$, $\overline{uy}$, $\overline{uz}$ are the Laplace transformed blade deflections in the blade local x, y, and z directions, respectively,

$\overline{N}$, $\overline{Vy}$, $\overline{Vz}$ are the Laplace transformed axial force, chordwise shear force, and flapwise shear force in the blade local x, y, and z directions, respectively,

$\overline{\phi x}$, $\overline{\phi y}$, $\overline{\phi z}$ are the Laplace transformed torsional bending slope, flapwise bending slope and chordwise bending slope about the blade x, y, and z directions, respectively, and

$\overline{T}$, $\overline{My}$, $\overline{Mz}$ are the Laplace transformed torsional moment, flapwise bending moment, and chordwise

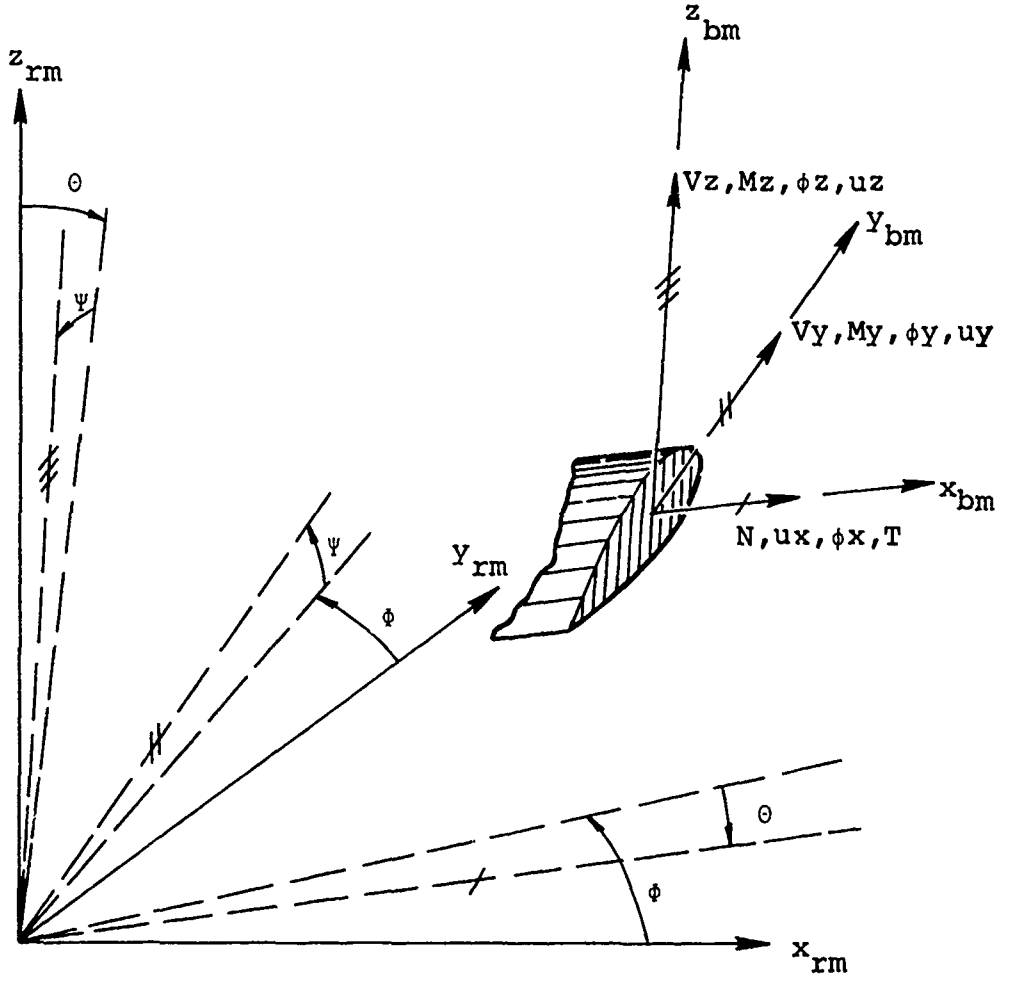

Figure 5. Blade Local Coordinate System and Laplace Transformed State Variable Orientation (slash marks refer to x_{bm}, y_{bm}, and z_{bm} blade local axes, respectively).

moment about the blade local x, y, and z directions, respectively.

The relationship between the two coordinate systems is represented by the coordinate transformation

$$\begin{Bmatrix} \bar{i}_{bm} \\ \bar{j}_{bm} \\ \bar{k}_{bm} \end{Bmatrix} = \begin{bmatrix} C\Phi\ C\Theta & S\Phi\ C\Theta & -S\Theta \\ -S\Phi\ C\Psi + C\Phi\ S\Theta\ S\Psi & C\Phi\ C\Psi + S\Phi\ S\Theta\ S\Psi & C\Theta\ S\Psi \\ S\Phi\ S\Psi + C\Phi\ S\Theta\ C\Psi & -C\Phi\ S\Psi + S\Phi\ S\Theta\ C\Psi & C\Theta\ C\Psi \end{bmatrix} \begin{Bmatrix} \bar{i}_{rm} \\ \bar{j}_{rm} \\ \bar{k}_{rm} \end{Bmatrix} \quad (7)$$

where a short form of denoting the sine and cosine functions has been utilized (e.g., $S\Phi$ represents $\sin\Phi$ and $C\Phi$ represents $\cos\Phi$. Since the transfer matrix technique relates the blade deflections, slopes, forces, and moments along the blade relative to its local coordinate system, the transformation can be used to obtain blade state variables in the basic rotor or disk plane.

The rectangular cartesian coordinate systems required for the representation of the basic swashplate control system consist of a fixed coordinate system and a rotating coordinate system corresponding to each blade. The fixed swashplate coordinate system has the same orientation in space as the fixed shaft coordinate system, but the origin of the swashplate coordinate system is on the shaft axis where the plane of the swashplate intersects it. The swashplate fixed coordinate system (x_{fc}, y_{fc}, z_{fc}) for a counterclockwise rotating rotor was depicted on Figure 2. For a clockwise rotating rotor, the fixed coordinate system y and z related axes in this figure would change direction. The rotating swashplate coordinate systems have the same orientation in space as the rotating shaft coordinate systems for the blades, but they have their origin at the origin of the fixed swashplate coordinate system. The rotating swashplate coordinate systems (x_{rc}, y_{rc}, z_{rc}) can be related to the fixed swashplate coordinate system (x_{fc}, y_{fc}, z_{fc}) by the transformation

$$\begin{Bmatrix} \bar{i}_{rc} \\ \bar{j}_{rc} \\ \bar{k}_{rc} \end{Bmatrix} = \begin{bmatrix} \cos(\Omega t+\phi_m) & \sin(\Omega t+\phi_m) & 0 \\ -\sin(\Omega t+\phi_m) & \cos(\Omega t+\phi_m) & 0 \\ 0 & 0 & 1 \end{bmatrix} \begin{Bmatrix} \bar{i}_{fc} \\ \bar{j}_{fc} \\ \bar{k}_{fc} \end{Bmatrix} \quad (8)$$

where the transformation array is identical to that of Equation (6).

The rectangular cartesian coordinate systems required for the representation of the fuselage-tailboom-fin structure parameters consist of a fixed coordinate system and local coordinate systems which are conceptually similar to the fixed and local blade coordinate systems, except that the local fuselage-tailboom-fin structure coordinate systems are not rotating. The fixed coordinate system is a reference coordinate system with its origin on the shear center axis at the nose of the fuselage. For convenience, the x-axis of the fixed coordinate system is taken to be parallel to the forward velocity of the helicopter in level forward flight, positive aft; the y-axis is taken to be perpendicular to the x-axis and in the vertical plane of the fuselage (positive toward top of helicopter); and the z-axis is mutually orthogonal to the x and y related axes such as to constitute a right-handed coordinate system. The fixed fuselage-tailboom-fin structure coordinate system and examples of local fuselage-tailboom-fin structure coordinate systems are shown in Figure 6. It should be noted that the tail rotor shaft is treated as part of the fuselage-tailboom-fin structure.

The local fuselage-tailboom-fin structure coordinate systems are obtained by application of the geometric angles Φ, Θ, and Ψ in the same manner as in the rotating local blade coordinate systems. Thus, the relationship between the local structure coordinate systems (x_s, y_s, z_s) and the fixed structure coordinate system (x_{fs}, y_{fs}, z_{fs}) is represented by matrix Equation (7) with the bm and rm subscripts replaced by s and fs subscripts, respectively. The matching of conditions at the interface of the tail rotor shaft and the rotor hub requires a defined relationship between the local fuselage-tailboom-fin structure coordinate system at the end of the tail rotor shaft and the fixed nonrotating blade reference coordinate system. The orientation of the local structure coordinate system at the end of the tail rotor shaft is accomplished through the use of the Φ, Θ, and Ψ angles at that position.

The relationship between the two coordinate systems used for the matching of boundary conditions is that at the hub-shaft interface point, in terms of unit vectors

$$\bar{i}_s = \bar{k}_f$$

$$\bar{j}_s = \bar{j}_f$$

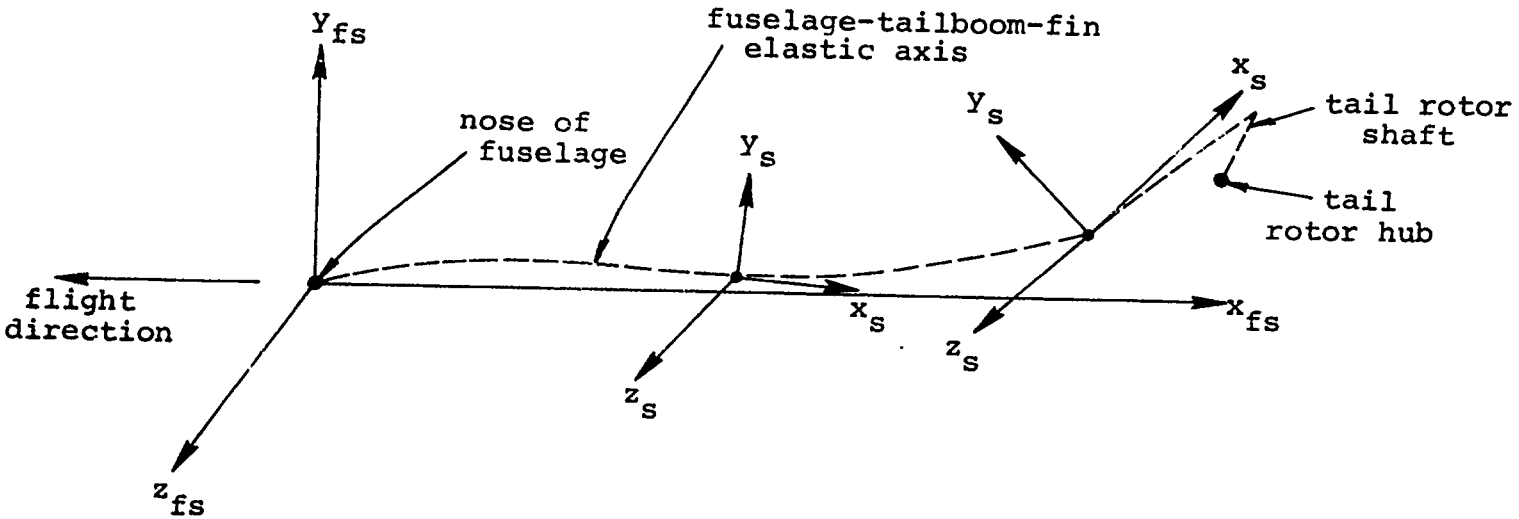

Figure 6. Fixed Fuselage Structure Coordinate System and Examples of Local Fuselage Structure Coordinate Systems.

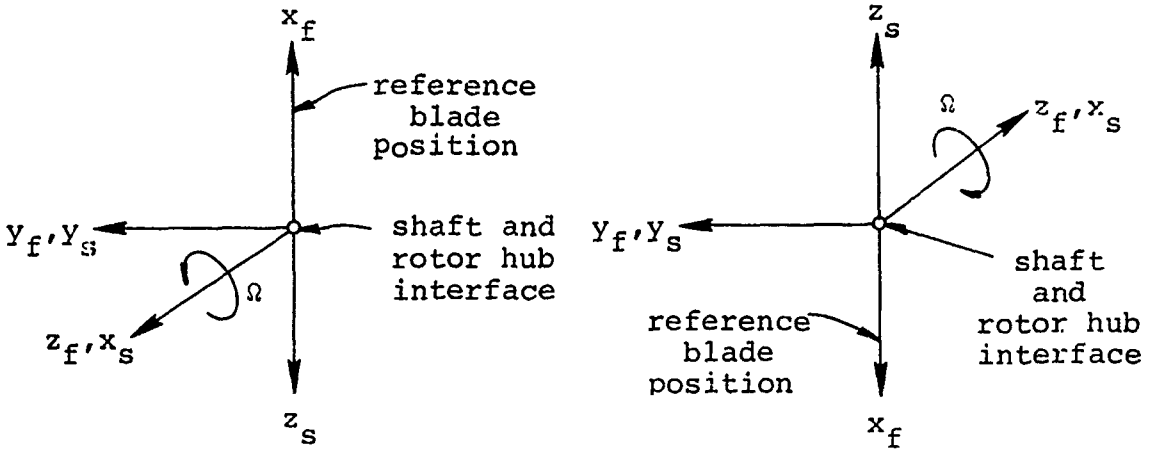

Counterclockwise Rotation Clockwise Rotation

Figure 7. Relationship of the Local Fuselage Structure Coordinate System and Fixed Shaft Coordinate System Required at Shaft and Rotor Hub Interface.

$$\bar{k}_s = \bar{i}_f$$

Thus, the required relationship between the fuselage-tailboom-fin structure coordinate system and the fixed shaft coordinate system at the hub-shaft interface is as depicted in Figure 7 for the two directions of rotor rotation. This coordinate system relationship, which is dependent upon the direction of rotor rotation, must be satisfied irrespective of whether the tail rotor drive shaft is modeled on the positive or negative z_f-axis side of the tail rotor hub.

Dirac Delta Functions

The governing differential equations of motion for the ring of the swashplate control system consist of equilibrium, stress-strain, and strain-displacement equations. These equations involve variables which are a function of θ, the azimuthal location of a point of interest on the ring relative to the x_{fc}-axis of the ring, and time t. Three of the variables involved are the applied loading distributions $Q(\theta,t)$, $\beta(\theta,t)$, and $\sigma(\theta,t)$ (see Figure 9), which are defined as the shear loading on the ring parallel to the z_f-axis of the ring, the torque loading on the ring about the circumferential ring axis, and the bending moment loading on the ring about a local

radial axis, respectively. In the control system configuration, these loadings are applied at discrete points on the ring by the control rods and the linear spring-damper supports. As noted in Figure 2, the applied forces from the control rods may be offset from the ring radius, as are the forces applied by the set of linear spring-damper support units.

A standard method of treating discrete loading points in an elastic structure is to utilize a Dirac delta representation of the form $\delta(\theta-\theta_0)$ where this multiplier specifies that the function being multiplied does not exist until $\theta \geq \theta_0$. In application to the definitions of the applied loading functions above, two forms are involved. For the control rod contributions to the applied loadings, $\delta(\theta-\Omega t-\phi_m)$ is used, and for the spring-damper support unit contributions to the applied loadings, $\delta(\theta-\chi_j)$ is used. χ_j is the azimuthal angle of the jth spring-damper support unit relative to the x_f-axis of the control system. The Dirac delta function $\delta(\theta-\theta_0)$ is defined such that

$$\int_0^{2\pi} f(\theta)\ \delta(\theta-\theta_0)\ R d\theta = f(\theta_0) \qquad (9)$$

where θ_0 is an arbitrary angle and R is the radius of the swashplate ring. This expression is also valid if the function is of the form $f(\theta,t)$ where the variable θ is independent of the variable t. The form of Equation (9) results when Equation (4) is utilized to obtain the Fourier harmonic coefficients of the exponential Fourier analysis form of the loadings acting on the swashplate ring ($Q_\ell(t)$, $\beta_\ell(t)$, and $\phi_\ell(t)$) and thus enables the definition of these coefficients as a function of χ_j and ϕ_m as required.

Application of Boundary Conditions

The equations, used to construct the final governing matrix equation whose solution yields the coupled tail rotor system eigenvalues and corresponding eigenvectors, are based on the consideration of the boundary conditions occurring on the structural components (i.e., blades, control system, etc.) of the helicopter/tail rotor system model. In general, the application of boundary conditions, as used in the development of analysis, has four basic forms. These are: (1) the use of the boundary conditions at the unattached end of a structural component (e.g., blade tip) to reduce the number of unknowns

associated with the component; (2) the matching of the boundary conditions at an interface between structural components (e.g., shaft-hub interface) to directly provide equations relating system unknowns; (3) a combination of the use of the boundary conditions acting on a structural component (e.g., control system), due to the attachment to other structural components, with the equations of motion of the structural component to provide the equations relating system unknowns; and (4) the use of the conditions occurring at blade model articulation characteristics (e.g., flap hinge) to provide equations defining blade discontinuity unknowns. The boundary condition application will be discussed first for various conditions of tail rotor hub restraint. The blade and fuselage unknowns must be initially considered in the form of real-time variables, i.e., a function of time, to properly apply the boundary conditions.

In real-time notation, there initially exist twelve blade tip unknown state variables for each blade and twelve unknown state variables for the fuselage-tailboom-fin structure. The blade tip loadings - three shears and three moments - can be taken as zero in value for each blade, since the blade tip is a free end. This reduces the number of blade tip unknown state variables per blade to six: three deflections and three slopes. In a similar manner, the nose of the fuselage-tailboom-fin structure can be considered as a cantilevered or a free end such that either the three slopes and three deflections or three moments and three shears at the nose end may be taken as zero, depending upon the condition of interest. This reduces the number of fuselage-tailboom-fin structure nose unknown state variables to six. Thus, for a system of Nb blades and a fuselage-tailboom-fin structure, 6 times (Nb+1) unknowns exist, not including discontinuity type unknowns, which requires the same number of equations for defining the unknowns. These equations are obtained by matching the moments, shears, deflections, and slopes of the blades at their attachment to the rotor shaft to the moments, shears, deflections, and slopes of the fuselage-tailboom-fin structure at the same point.

For a tail rotor hub cantilevered to the shaft, as is the case for a rigid, articulated, or flexstrap tail rotor, part of the necessary equations are obtained by properly matching the slopes and deflections of the blades to the shaft slopes and deflections at the blade attachment point. The matching of these boundary conditions is done in the rotating shaft coordinate system and provides the equations necessary for the determination of blade tip unknowns. From the relationship between the fuselage local system at the end of the shaft and the fixed blade reference coordinate system discussed

previously and shown in Figure 7, the shaft deflections at the interface end of the fuselage-tailboom-fin structure can be defined relative to the fixed blade reference coordinate system in the deflection vector form $\bar{u}_s = uz_s\bar{i}_f + uy_s\bar{j}_f + ux_s\bar{k}_f$. The s subscripted deflection variables above denote the shaft deflections of the fuselage-tailboom-fin structure with respect to the local fuselage-tailboom-fin structure coordinate system at the end of the shaft. The blade deflections at the same point can be defined in the deflection vector form $\bar{u}_m = ux_m\bar{i}_{rm} + uy_m\bar{j}_{rm} + uz_m\bar{k}_{rm}$ where the m subscripted deflection variables denote the blade deflections of the mth blade at the interface with respect to the rotating shaft coordinate system of the mth blade. The shaft deflection vector $\bar{u}_s$ can be expressed relative to the shaft rotating coordinate system for a specific blade by use of the inverse coordinate system transformation associated with Equation (6). Thus, for the mth blade the expression $\bar{u}_m - \bar{u}_s = 0$, where both vectors are defined relative to the rotating shaft coordinate system of the mth blade, is used to relate the shaft deflections and blade root deflections in the three orthogonal directions. Each direction provides a separate equation, for a total of three deflection relating equations per blade. Using a similar procedure for the blade and shaft slopes, the expression $\bar{\phi}_m - \bar{\phi}_s = 0$ provides three slope relating equations for each blade. Thus, six equations for each blade can be obtained, with the result that a total of 6 x Nb equations are obtainable corresponding to the number of blade state variable unknowns. Due to physical considerations, the equation for each blade involving the blade inplane slope ϕz_m is altered to $\phi z_m = 0$; which, on the inclusion of consideration of drive shaft torsional flexibility is replaced by $\phi z_m - Mz_m/kd = 0$ where Mz_m is the blade chordwise moment at the root of the mth blade and kd is the torsional stiffness of the drive shaft.

The remaining set of 6 equations corresponding to the number of fuselage-tailboom-fin unknowns is obtained by matching the forces and moments of all blades to the shaft forces and moments in the fixed reference blade coordinate system. The moments at the interface end of the fuselage-tailboom-fin structure can be defined in the vector form $\bar{M}_s = -Mz_s\bar{i}_f + My_s\bar{j}_f + T_s\bar{k}_f$ where T_s, My_s, and Mz_s are the moments in the local fuselage-tailboom-fin structure coordinate system about its x, y, and z axes, respectively, at the end of the shaft. The blade root moments in the rotating shaft coordinate system

can be written in the vector form $\bar{M}_m = T_m \bar{i}_{rm} + My_m \bar{j}_{rm} + Mz_m \bar{k}_{rm}$ where T_m, My_m, and Mz_m are moments about the x, y, and z axes, respectively, of the mth blade's rotating shaft coordinate system. The moment vector $\bar{M}_m$ can be expressed relative to the fixed coordinate system by the transformation specified in Equation (6). The expression $\sum_{m=1}^{Nb} \bar{M}_m - \bar{M}_s = 0$, where both vectors are defined relative to the fixed reference blade coordinate system, is used to obtain the expressions for the moment boundary conditions in three directions. The expression for the moment boundary condition equation in the $\bar{k}_f$ direction must be replaced by $T_s = 0$ since the torque due to the blades is not allowed to be applied to the shaft from which it would be transferred to the fin, but is considered to be removed by the tail rotor drive shaft transmission. Using a similar procedure for blade and shaft shear forces, three additional equations are obtained from the expression $\sum_{m=1}^{Nb} \bar{V}_m - \bar{V}_s = 0$. Thus, six equations in real-time notation corresponding to the six fuselage-tailboom-fin structure unknowns are obtained. In combination with those corresponding to the blade tip unknowns, a sufficient number of equations in real-time notation are available to completely represent the problem if control system and discontinuity representations are not involved.

The previous discussion was restricted to the situation of a rotor hub cantilevered to the tail rotor shaft. When considering a gimballed or teetering rotor system, some of the previous boundary condition equations must be modified to allow for the additional hub degrees of freedom which occur. For a gimballed rotor, the rotor hub is assumed to be attached to the rotor shaft by a swivel joint such that the rotor cannot physically apply transverse bending moments to the rotor shaft. It is also assumed that the torsional and flapwise blade bending slopes are independent of the bending slopes of the end of the rotor shaft. As a result of the nontransmittal of the blade moments, the moment boundary condition equations for the moments about the $\bar{i}_f$ and $\bar{j}_f$ axes reduce to $Mz_s = 0$ and $My_s = 0$. The components of the vector $\sum_{m=1}^{Nb} \bar{M}_m$ in the direction of the $\bar{i}_f$ and $\bar{j}_f$ axes must also be

zero in value, providing two additional boundary condition equations which are not required (if a phasing relationship between blade behavior is not assumed) but are automatically satisfied by the final solutions that are obtained. The slope boundary conditions for ϕx_m and ϕy_m are no longer coupled to the shaft slopes and are not necessarily zero in value; rather, the slopes of each blade are related to the slopes of the other blades because each blade is cantilevered to a hub that is free to rotate out of the reference rotor plane. Transformation of the blade root slope vectors for each blade in their individual shaft rotating coordinate system to the shaft rotating coordinate system for the first blade and separating vector components provides the condition that the terms $(\phi x_m \cos\phi_m - \phi y_m \sin\phi_m)$ and $(\phi x_m \sin\phi_m + \phi y_m \cos\phi_m)$ each represent a function of time which is independent of the value chosen for m. Thus, for each blade, these two terms can be set equal to those corresponding to the next azimuthally located blade, with the result that a sufficient number of real-time boundary condition equations are obtained to replace the rigid hub ϕx_m and ϕy_m related boundary condition equations.

In the case of a teetering rotor which is allowed to have only two blades equally spaced azimuthally and free to rotate about the rotating $\bar{j}_{r1}$ axis; i.e., $\bar{j}_{rm}$ axis of the first blade, the blade root moment My_m and slope ϕy_m are independent of the shaft moments and slopes. Thus, in the moment boundary condition equations corresponding to the fuselage unknowns for the rigid hub conditions, the contribution of My_m must be removed. In a manner similar to that discussed for the gimballed rotor system, the component of the vector $\sum_{m=1}^{2} M_m$ in the direction of the $\bar{j}_{r1}$ axis must be zero in value. This equation is necessary to replace one of the two ϕy_m related boundary condition equations (one for each blade) since the ϕy_m related boundary condition equation for a teetering rotor will only provide a single equation. The blade slope boundary condition equation for ϕy_m for the first blade in the rigid hub case is replaced by $\phi y_1 + \phi y_2 = 0$, using the form of the second slope term for the gimballed system, dropping the ϕx_m contribution and taking $\phi_1 = 0$ and $\phi_2 = \pi$ radians. For the second blade, use of this term would result in $\phi y_2 + \phi y_1 = 0$ which is identical to that

for the first blade and cannot be used. Thus, the expression $My_1 - My_2 = 0$, obtained from the summation vector, is used to replace the ϕy_m related boundary condition equation for the second blade.

There may also exist up to three discontinuity unknowns resulting from consideration of a flexstrap or articulated blade. For a flexstrap blade, the discontinuity unknowns are the three mutually orthogonal perturbation deflections of the control rod attachment point to the pitch horn in the directions of the axes of the rotating shaft coordinate system. Two of the three equations corresponding to these unknowns are obtained by using the conditions that the control rod can only carry an axial load, thereby requiring that the perturbation forces applied to the control rod at its attachment point to the pitch horn in two mutually orthogonal directions perpendicular to the control rod must be zero. The third equation is obtained by requiring the perturbation forces acting axially on the ends of the control rod from the pitch horn and the control system and/or ground to be such that the control rod is in dynamic equilibrium. The discontinuity unknowns allowed for an articulated blade are associated with the perturbation torque, pitch angle, and flap angle. The required equations are obtained by utilizing the conditions that the perturbation flapwise moment at a flap hinge must be zero, the perturbation torque at the pitch bearing must be zero, and the perturbation torque applied by the control rod is a function of the blade perturbation rotation angle ϕx at the torque application point and the deflection of control system such that the control rod is in dynamic force equilibrium.

Additional system real-time unknowns corresponding to swashplate control system variables result on consideration of the control system model. By simultaneous solution of the equilibrium, stress-strain, and strain-displacement equations for a ring with applied loading, a swashplate governing equation of motion is obtained. This equation involves the azimuthally dependent harmonics of the ring deflection in the rotating swashplate coordinate system and the base plate deflection. The base plate collective motion and the boundary conditions occurring at the attachment point of each control rod to its associated blade pitch horn are used in conjunction with the characteristic of the spring-damper units attached to the swashplate ring to properly represent the ring applied loading in terms of the swashplate unknowns. The boundary conditions at the attachment of the collective spring-damper support unit to the tail rotor gearbox or to ground are used to obtain an expression for the collective base plate motion.

This expression involves time differential operators such that this deflection unknown cannot be replaced in the swashplate governing equation of motion without the application of Laplace transforms.

The application of boundary conditions has been discussed on a real-time variable basis. The use of Laplace transformation techniques on the real-time equations obtained from boundary condition considerations provides equations involving shifted and unshifted Laplace transform variables. These variables are, in turn, defined as functions of shifted and unshifted Laplace transform variables due to the representation necessary for the inclusion of interharmonic coupling. For example, a Laplace transformed blade state variable at a radial position on the blade and a function of s is defined by the form of Equation (3) with k = 0 to be dependent upon the shifted and unshifted blade tip state variables. Thus, the use of Laplace transformations increases the number of unknowns associated with the system. By frequency shifting the Laplace transform variables in all of the basic boundary condition equations, the additional equations required for the shifted Laplace transform variable unknowns can be obtained. However, the expressions for a given frequency shifted equation will involve variables of a higher or lower frequency shift which, in turn, must be defined. Thus, to be practical in the construction of the final governing matrix, a limit must be applied to the number of frequency shifted sets of equations (truncation of frequency shifted variables). In addition, the application of Laplace transforms allows the replacement of the base plate Laplace transformed deflection unknowns with their equivalents in the transformed swashplate governing equations.

BASIC RESULTANT ANALYTICAL FORMULATION

This section will be concerned with the general form of the analytical expressions utilized to obtain (1) the final governing matrix equations which must be solved to obtain the solution complex variable eigenvalues and eigenvectors and (2) the fuselage-tailboom-fin structure and blade state variable mode shapes corresponding to the solution eigenvalues.

Blade State Variable Representation

The general transfer matrix representation of the k frequency shifted blade state variables just beyond the jth lumped parameter was given previously in Equation (3). In actual application, this equation is modified to a form in which the blade is divided into sections representing the lumped parameter characteristics in the blade.

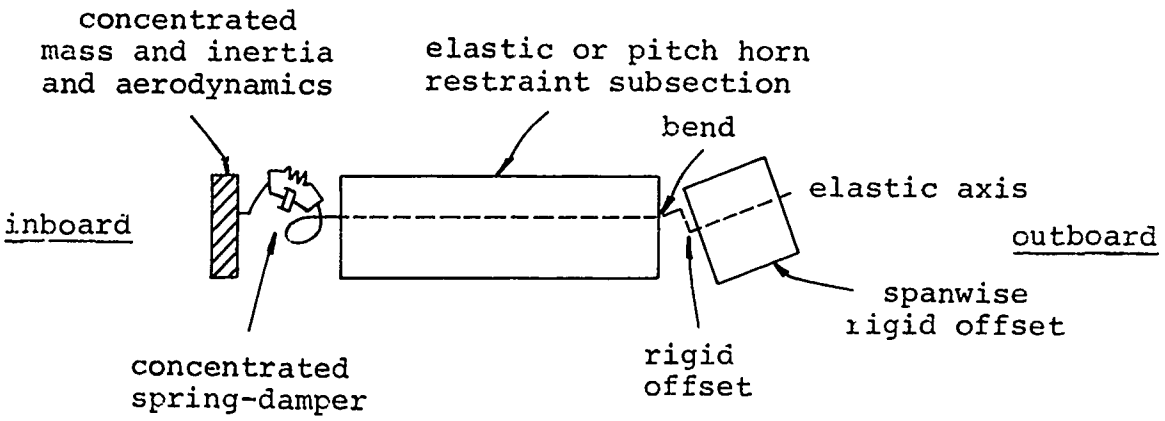

Figure 8. A General Blade Section.

In the sectional representation, the blade is divided into a finite number of sections in which each section may have the following characteristics: rigid offsets in the shear center axis, bending of the shear center axis at a point, a centrifugally stiffened elastic length or flexstrap pitch horn restraints, concentrated torsional spring-damper units, mass and inertias, and aerodynamics as depicted in Figure 8. The concentrated torsional spring-damper units, bends, and rigid offsets are allowed in three mutually perpendicular directions. The Laplace transformed transfer arrays for each of the above-listed characteristics, except for aerodynamics, in the order mentioned above, can be denoted by

$$\left[\overline{R}\right]_m^i,\ \left[\overline{BE}\right]_m^i,\ \left[\overline{E}\right]_m^i,\ \left[\overline{L}\right]_m^i,\ \left[\overline{SK}_k\right]_m^i,\ \text{and}\ \left[\overline{A}_k\right]_m^i$$

where i and m denote the ith section of the mth blade. These arrays are equivalent to the previously defined $\left[\overline{G}_k\right]^j$ arrays. The k subscript denoting s replaced by $(s-ik\Omega)$ is only involved in matrices originally containing differential operators. The arrays without a k subscript consist of numerical constants only. For an aerodynamics application point, the previously used $\left[\overline{G}_{k,n}\right]^j$ is replaced by $\left[\overline{C}_{n-k,n}\right]_m^i e^{i(n-k)\phi_m}$

for the mth blade. This array is defined by the matrix expression

$$\left[\bar{C}_{n-k,n}\right]_m^i = (s-in\Omega)\left[\bar{C}_{n-k}\right]_m^i + \left[\bar{D}_{n-k}\right]_m^i \qquad (10)$$

in which $(s-in\Omega)$ is a multiplier which results due to the periodic aerodynamic coefficients multiplying a differential operator acting on a blade state variable.

The application of the individual transfer matrices to the associated transfer matrices for the characteristics involved in each section is carried out as they are encountered in the same manner as Equations (1) and (2). However, after transferring across the ith section using the specific i superscripted transfer matrices defined previously, the associated transfer matrix at the inboard end of the ith section is denoted by $\left[\bar{B}_{k,n}\right]_m^i$. The same concept of transfer matrix application occurs in regard to the discontinuity column vectors such that they also can be referred to as

$$\left\{\bar{b}_{k,n}\right\}_m^i, \left\{\bar{c}_{k,n}\right\}_m^i \text{ and } \left\{\bar{d}_{k,n}\right\}_m^i.$$

The blade tip conditions that the moments and shears acting on the blade tip are zero allows the associated transfer arrays $\left[\bar{B}_{k,n}\right]_m^i$ to be redefined as 12 x 6 arrays. This reduction of array size significantly reduces the number of computations necessary to define the state variables acting at any blade section and to solve the final governing matrix. The reduction in associated matrix size can be represented by defining the Laplace transformed state variables at the mth blade tip by the form $\left\{\bar{S}_k\right\}_m^0 = \sum_{n=-\infty}^{\infty}\left[\bar{B}_{k,n}\right]_m^0\left\{\bar{S}_n\right\}_m^*$ where $\left\{\bar{S}_k\right\}_m^0$ is the k frequency shifted state variable column vector consisting of the twelve Laplace transformed state variables defined previously in real-time form whose order in the cclumn vector is defined by the form $\left\{\bar{S}\right\} =$ $\left\{\overline{ux}\ \overline{N}\ \overline{\phi x}\ \overline{T}\ \overline{uy}\ \overline{\phi z}\ \overline{Mz}\ -\overline{Vy}\ -\overline{uz}\ \overline{\phi y}\ \overline{My}\ \overline{Vz}\right\}$, $\left\{\bar{S}_n\right\}_m^*$ is the n frequency shifted mth blade unknown state variable column vector

consisting of the six unknowns at the mth blade tip such that $\left\{\overline{S}_n\right\}_m^* = \left\{\overline{ux}\ \overline{\phi x}\ \overline{uy}\ \overline{\phi z}\ -\overline{uz}\ \overline{\phi y}\right\}_{n,m}^*$, and $\left[\overline{B}_{k,n}\right]_m^0$ for $k \neq n$ is a 12 x 6 array of zero elements and for $k = n$ is defined by the expression

$$\left[\overline{B}_{k,n}\right]_m^0 = \begin{bmatrix} 1 & 0 & 0 & 0 & 0 & 0 \\ 0 & 0 & 0 & 0 & 0 & 0 \\ 0 & 1 & 0 & 0 & 0 & 0 \\ 0 & 0 & 0 & 0 & 0 & 0 \\ 0 & 0 & 1 & 0 & 0 & 0 \\ 0 & 0 & 0 & 1 & 0 & 0 \\ 0 & 0 & 0 & 0 & 0 & 0 \\ 0 & 0 & 0 & 0 & 0 & 0 \\ 0 & 0 & 0 & 0 & 1 & 0 \\ 0 & 0 & 0 & 0 & 0 & 1 \\ 0 & 0 & 0 & 0 & 0 & 0 \\ 0 & 0 & 0 & 0 & 0 & 0 \end{bmatrix} \qquad (11)$$

It is impossible to consider the harmonic summation limits from $-\infty$ to $+\infty$ in actual application of this complicated analysis; therefore, the summation was truncated to the range of -Nf to Nf, where Nf represents the number of harmonics above and below the main eigenvalue which are allowed to couple with the main eigenvalue related behavior. For example, if Nf is 1, then the 1/rev and -1/rev shifted frequencies will be allowed to couple with the 0 shifted frequencies. On the basis of analyses conducted by RASA, it has been determined that these limits are very realistic and the answers that are obtained are within a few percent of those obtained using higher values of Nf. Combining all of the above-noted items, the frequency shifted state variable vector at the inboard end of the ith section of the mth blade can be defined by the expression

$$\left\{\overline{S}_k\right\}_m^i = \sum_{n=-Nf}^{Nf}\left[\left[\overline{B}_{k,n}\right]_m^i\left\{\overline{S}_n\right\}_m^* - \left\{\overline{b}_{k,n}\right\}_m^i(\overline{\Delta 1}_n)_m - \left\{\overline{c}_{k,n}\right\}_m^i(\overline{\Delta 2}_n)_m - \left\{\overline{d}_{k,n}\right\}_m(\overline{\Delta 3}_n)_m\right] . \qquad (12)$$

The associated transfer matrices and discontinuity column vectors for additional blades, if they are identical to the first blade and ϕ_1 is zero, can be related to the first blade

associated transfer matrices and discontinuity column vectors by the form

$$\left[\overline{B}_{k,n}\right]^{i}_{m} = \left[\overline{B}_{k,n}\right]^{i}_{1} e^{i(n-k)\phi_m}$$

where the exponential relationship results from the application of the aerodynamic transfer matrices. Equation (12) provides the definition of the blade state variables at any blade section in terms of the blade tip unknowns and also provides the means to obtain the blade state variable mode shapes once the blade tip unknowns are obtained for a solution eigenvalue.

Fuselage-Tailboom-Fin Structure State Variable Representation

The overall concept of the transfer matrix representation of the k frequency shifted fuselage-tailboom-fin structure state variables is similar to that pertaining to the k frequency shifted blade state variables. Differences at the basic level do occur as a result of the direction of transfer matrix application and the conditions to which the fuselage structure is exposed. The direction of transfer matrix application for the blades is along the local blade negative x-axis (tip to root), whereas for the fuselage-tailboom-fin structure the direction of transfer matrix application is along the local fuselage-tailboom-fin structure positive x-axis (nose to tail). As a result, the individual characteristic transfer matrices for the fuselage structure, without considering any alterations due to different conditions, would differ from those for the blade characteristics due to required changes in sign of some of the matrix elements. Although the direction of transfer matrix application is different for the fuselage-tailboom-fin structure, the individual characteristics of a section (i.e., mass, bend, elastic, etc.) are considered in the same order as the blade characteristics.

The conditions for the fuselage-tailboom-fin structure which differ from those on the blades are that the fuselage structure is not rotating and the aerodynamic forces for the fuselage are due to flat plate drag effects resulting from crossflow. Not having a constant rotational speed associated with the fuselage-tailboom-fin structure drastically reduces the complexity of the transfer matrices associated with mass and inertia parameters, elastic parameters, and aerodynamic parameters. In the mass and inertia transfer matrices, all terms which include Ω are dropped, thereby removing mass and inertia related damping terms, structural damping, and Ω^2 effects. The elastic transfer matrix is modified by not

including centrifugal stiffening of the section elastic length. Without a constant rotating speed of the fuselage-tailboom-fin structure, the aerodynamic transfer representation does not involve periodically time variant coefficients, with the result that intrafuselage interharmonic coupling does not occur. Thus, the aerodynamic transfer matrix can be represented by

$$\left[\overline{G}_k\right]_s^i = \left[\overline{C}_k\right]_s^i = (s-ik\Omega)\left[\overline{C}_0\right]_s^i + \left[\overline{D}_0\right]_s^i$$

where the subscript s denotes the fuselage-tailboom-fin structure and can be added as a subscript to the other types of fuselage structure transfer arrays to denote the same. The above expression can be obtained by letting n = k in Equation (10).

In applying the transfer matrix procedure in going across a fuselage-tailboom-fin structure characteristic, the associated transfer matrix for the fuselage-tailboom-fin structure would be defined in terms of the previous associated fuselage-tailboom-fin structure transfer matrix by the form of Equation (1). Thus, since the fuselage is not exposed to any discontinuities or intraharmonic coupling, the fuselage-tailboom-fin structure state variables just beyond the ith section can be defined by the expression

$$\left\{\overline{S}_k\right\}_s^i = \left[\overline{S}_k\right]_s^i \left\{\overline{S}_k\right\}_s^* \qquad (13)$$

where the general state variables and general k shifted state variable vector are defined as for the blades except they are on the fuselage-tailboom-fin structure and $\left[\overline{S}_k\right]_s^i$ is a 12 x 6 array representing the k frequency shifted associated fuselage-tailboom-fin structure transfer matrix. The k frequency shifted unknown column vector of six variables at the initial transfer matrix application point will consist of either initial fuselage-tailboom-fin structure slopes and deflections, as is the case for the blades with free end conditions, or initial fuselage-tailboom-fin structure moments and shears corresponding to cantilevered end conditions. In the latter case, the initial associated fuselage-tailboom-fin structure matrix is defined by

$$\left[\overline{S}_k\right]_s^0 = \begin{bmatrix} 0 & 0 & 0 & 0 & 0 & 0 \\ 1 & 0 & 0 & 0 & 0 & 0 \\ 0 & 0 & 0 & 0 & 0 & 0 \\ 0 & 1 & 0 & 0 & 0 & 0 \\ 0 & 0 & 0 & 0 & 0 & 0 \\ 0 & 0 & 0 & 0 & 0 & 0 \\ 0 & 0 & 1 & 0 & 0 & 0 \\ 0 & 0 & 0 & 1 & 0 & 0 \\ 0 & 0 & 0 & 0 & 0 & 0 \\ 0 & 0 & 0 & 0 & 0 & 0 \\ 0 & 0 & 0 & 0 & 1 & 0 \\ 0 & 0 & 0 & 0 & 0 & 1 \end{bmatrix} \qquad (14)$$

and $\left\{\overline{S}_k\right\}_s^* = \left\{\overline{N}_s \ \overline{T}_s \ \overline{Mz}_s - \overline{Vy}_s \ \overline{My}_s \ \overline{Vz}_s\right\}_k^*$.

Equation (13) provides the definition of the fuselage-tailboom-fin structure state variables at any fuselage-tailboom-fin section in terms of fuselage-tailboom-fin structure unknowns and also provides the means to obtain the fuselage-tailboom-fin structure state variable mode shapes once the fuselage-tailboom-fin structure unknowns are determined for a solution eigenvalue.

Rotor Hub-Shaft Interface Conditions

The Laplace transformed form of the interface boundary conditions corresponding to the mth blade unknowns for a hub cantilevered to the shaft can be given in terms of the state variables at the interface by the expressions

$$(\overline{ux}_m)_k + \left[-(-\overline{uz}_s)_{k+1} + i(\overline{uy}_s)_{k+1}\right]e^{i\phi_m/2} + \left[-(-\overline{uz}_s)_{k-1} - i(\overline{uy}_s)_{k-1}\right]e^{-i\phi_m/2} = 0$$

$$(\overline{\phi x}_m)_k + \left[(\overline{\phi z}_s)_{k+1} + i(\overline{\phi y}_s)_{k+1}\right]e^{i\phi_m/2} \left[(\overline{\phi z}_s)_{k-1} - i(\overline{\phi y}_s)_{k-1}\right]e^{-i\phi_m/2} = 0$$

$$(\overline{uy}_m)_k + \left[-i(-\overline{uz}_s)_{k+1} - (\overline{uy}_s)_{k+1}\right]e^{i\phi_m/2} + \left[+i(-\overline{uz}_s)_{k-1} - (\overline{uy}_s)_{k-1}\right]e^{-i\phi_m/2} = 0$$

$$(\overline{\phi z}_m)_k - (\overline{Mz}_m)_k/kd = 0$$

$$(-\overline{uz}_m)_k + (\overline{ux}_s)_k = 0 \qquad (15)$$

$$(\overline{\phi y}_m)_k + \left[i(\overline{\phi z}_s)_{k+1} - (\overline{\phi y}_s)_{k+1}\right] e^{i\phi_m/2} + \left[-i(\overline{\phi z}_s)_{k-1} - (\overline{\phi y}_s)_{k-1}\right] e^{-i\phi_m/2} = 0$$

which are obtained by (1) matching the real-time variables at the hub relative to the mth blade rotating shaft coordinate system, (2) replacing sine and cosine terms involving $(\Omega t + \phi_m)$ by exponential equivalents, (3) Laplace transforming the resulting expressions, and (4) applying a k frequency shift on the Laplace transform variables.

The expressions of Equation (15) can be represented in the array form

$$\left[\alpha R\right] \left\{\overline{S}_k\right\}_m^{NS} + \sum_{I=-1}^{1} \left[\beta R_I\right]_m \left\{\overline{S}_{k+I}\right\}_s^{NSF} = 0 \qquad (16)$$

The variables NS and NSF are the number of blade and fuselage-tailboom-fin structure sections, respectively, and the matrices $\left[\alpha R\right]$ and $\left[\beta R_I\right]_m$ are defined by

$$\left[\alpha R\right] = \begin{bmatrix} 1 & 0 & 0 & 0 & 0 & 0 & 0 & 0 & 0 & 0 & 0 & 0 \\ 0 & 0 & 1 & 0 & 0 & 0 & 0 & 0 & 0 & 0 & 0 & 0 \\ 0 & 0 & 0 & 0 & 1 & 0 & 0 & 0 & 0 & 0 & 0 & 0 \\ 0 & 0 & 0 & 0 & 0 & 1 & -1/kd & 0 & 0 & 0 & 0 & 0 \\ 0 & 0 & 0 & 0 & 0 & 0 & 0 & 0 & 1 & 0 & 0 & 0 \\ 0 & 0 & 0 & 0 & 0 & 0 & 0 & 0 & 0 & 1 & 0 & 0 \end{bmatrix}$$

$$\left[\beta R_I\right]_m = \begin{bmatrix} 0 & 0 & Iie_{I,m} & 0 & -e_{I,m} & 0 \\ 0 & 0 & 0 & e_{I,m} & 0 & Iie_{I,m} \\ 0 & 0 & -e_{I,m} & 0 & -Iie_{I,m} & 0 \\ 0 & 0 & 0 & 0 & 0 & 0 \\ \delta_I^0 & 0 & 0 & 0 & 0 & 0 \\ 0 & 0 & 0 & Iie_{I,m} & 0 & -e_{I,m} \end{bmatrix} \left[\alpha\right]$$

where $\left[\alpha\right]$ is the same as $\left[\alpha_R\right]$ except the 1/kd term is replaced by zero, i equals $\sqrt{-1}$, δ_b^a is Kronecker's delta, and

$$e_{I,m} \triangleq e^{Ii\phi_m}(\delta_1^I + \delta_{-1}^I)/2.$$

On application of a similar procedure to the real-time boundary condition equations corresponding to the fuselage-tailboom-fin structure unknowns, the Laplace transformed equations can be given in terms of the state variables at the interface by the expressions

$$\left.\begin{aligned}
&(\bar{N}_s)_k - \sum_{m=1}^{Nb} (\overline{Vz}_m)_k = 0 \\
&(\bar{T}_s)_k = 0 \\
&(\overline{Mz}_s)_k + \sum_{m=1}^{Nb}\left[\left[(\bar{T}_m)_{k+1} + i(\overline{My}_m)_{k+1}\right]e^{i\phi_m/2}\right. \\
&\qquad\left. + \left[(\bar{T}_m)_{k-1} - i(\overline{My}_m)_{k-1}\right]e^{-i\phi_m/2}\right] = 0 \\
&(-\overline{Vy}_s)_k = \sum_{m=1}^{Nb}\left[\left[-i(\bar{N}_m)_{k+1} - (-\overline{Vy}_m)_{k+1}\right]e^{i\phi_m/2}\right. \\
&\qquad\left. + \left[i(\bar{N}_m)_{k-1} - (-\overline{Vy}_m)_{k-1}\right]e^{-i\phi_m/2}\right] = 0 \\
&(\overline{My}_s)_k + \sum_{m=1}^{Nb}\left[\left[i(\bar{T}_m)_{k+1} - (\overline{My}_m)_{k+1}\right]e^{i\phi_m/2}\right. \\
&\qquad\left. - \left[i(\bar{T}_m)_{k-1} + (\overline{My}_m)_{k-1}\right]e^{-i\phi_m/2}\right] = 0 \\
&(\overline{Vz}_s)_k + \sum_{m=1}^{Nb}\left[\left[(\bar{N}_m)_{k+1} - i(-\overline{Vy}_m)_{k+1}\right]e^{i\phi_m/2}\right. \\
&\qquad\left. + \left[(\bar{N}_m)_{k-1} + i(-\overline{Vy}_m)_{k-1}\right]e^{-i\phi_m/2}\right] = 0
\end{aligned}\right\} \quad (17)$$

which can be represented in matrix equation form as

$$\left[\gamma\right]\left\{\overline{S}_k\right\}_s^{NSF} + \sum_{I=-1}^{1}\sum_{m=1}^{Nb}\left[\Delta R_I\right]_m\left\{\overline{S}_{k+I}\right\}_m^{NS} = 0 \qquad (18)$$

where

$$\left[\gamma\right] = \begin{bmatrix} 0 & 1 & 0 & 0 & 0 & 0 & 0 & 0 & 0 & 0 & 0 & 0 \\ 0 & 0 & 0 & 1 & 0 & 0 & 0 & 0 & 0 & 0 & 0 & 0 \\ 0 & 0 & 0 & 0 & 0 & 0 & 1 & 0 & 0 & 0 & 0 & 0 \\ 0 & 0 & 0 & 0 & 0 & 0 & 0 & 1 & 0 & 0 & 0 & 0 \\ 0 & 0 & 0 & 0 & 0 & 0 & 0 & 0 & 0 & 0 & 1 & 0 \\ 0 & 0 & 0 & 0 & 0 & 0 & 0 & 0 & 0 & 0 & 0 & 1 \end{bmatrix}$$

and

$$\left[\Delta R_I\right]_m = \begin{bmatrix} 0 & 0 & 0 & 0 & 0 & -\delta_I^0 \\ 0 & 0 & 0 & 0 & 0 & 0 \\ 0 & e_{I,m} & 0 & 0 & Iie_{I,m} & 0 \\ -Iie_{I,m} & 0 & 0 & -e_{I,m} & 0 & 0 \\ 0 & Iie_{I,m} & 0 & 0 & -e_{I,m} & 0 \\ e_{I,m} & 0 & 0 & -Iie_{I,m} & 0 & 0 \end{bmatrix} \left[\gamma\right]$$

The matrix Equations (16) and (18) provide the necessary boundary conditions corresponding to blade and fuselage-tailboom-fin state variable unknowns in terms of the state variables at the interface for a flexstrap, articulated or rigid rotor system.

The consideration of a gimballed rotor system results in a modification of the boundary condition expressions provided by Equations (16) and (18). The boundary co· ition matrix equation involving moments, Equation (18), is modified to a gimballed situation by simply removing the contributions due to $\overline{T}_m$ and $\overline{My}_m$ terms which is achieved by replacing $\left[\Delta R_I\right]_m$ with $\left[\Delta G_I\right]_m$. This matrix is obtained when the second and fifth columns of $\left[\Delta R_I\right]_m$ are taken to consist of zeroes only.

Slope relationships are not as easily modified. The two terms presented previously in the discussion of the slope boundary conditions for a gimballed rotor system can be replaced by the two terms $(\phi x_m + i\phi y_m)e^{+i\phi_m}$ and $(\phi x_m - i\phi y_m)e^{-i\phi_m}$ which are

each a function of time independent of the blade considered; for example, $(\phi x_1 + i\phi y_1)e^{i\phi_1} = (\phi x_2 + i\phi y_2)e^{i\phi_2}$ and $(\phi x_1 - i\phi y_1)e^{-i\phi_1} = (\phi x_2 - i\phi y_2)e^{-i\phi_2}$. In general, on taking the Laplace transform and shifting the Laplace transform variable by $ik\Omega$, the relationships

$$\left.\begin{aligned}\left[(\overline{\phi x}_p)_k + i(\overline{\phi y}_p)_k\right]e^{i\phi_p} - \left[(\overline{\phi x}_{p+1})_k + i(\overline{\phi y}_{p+1})_k\right]e^{i\phi_{p+1}} = 0 \\ \left[(\overline{\phi x}_p)_k - (\overline{\phi y}_p)_k\right]e^{-i\phi_p} - \left[(\overline{\phi x}_{p+1})_k - i(\overline{\phi y}_{p+1})_k\right]e^{-i\phi_{p+1}} = 0\end{aligned}\right\} \quad (19)$$

result where p denotes the blade of interest; and if p is taken as equal to the number of blades, then p+1 is taken as 1.

The boundary condition matrix equation involving slopes, Equation (16), is modified to a gimballed situation by replacing $\left[\alpha R\right]$ with $\left[\alpha G\right]_m$ and $\left[\beta R_I\right]_m$ with $\left[\beta G_I\right]_m$, and introducing a new term on the left side of Equation (16) of the form $\left[\alpha G'\right]_{m+1}\left\{\bar{S}_k\right\}_{m+1}^{NS}$ where if $m + 1 = Nb + 1$, then $m + 1$ is taken as 1 corresponding to the first blade. The matrix $\left[\alpha G\right]_m$ is obtained by modifying the second and sixth rows of $\left[\alpha R\right]$ to the form $\left(0\ 0\ e^{i\phi_m}\ 0\ 0\ 0\ 0\ 0\ 0\ ie^{i\phi_m}\ 0\ 0\right)$ and $\left(0\ 0\ e^{-i\phi_m}\ 0\ 0\ 0\ 0\ 0\ 0\ -ie^{-i\phi_m}\ 0\ 0\right)$, respectively, where $(\ )$ denotes a row array. The matrix $\left[\beta G_I\right]_m$ is the same as $\left[\beta R_I\right]_m$ except that its second and sixth rows consist of zeroes only. The matrix $\left[\alpha G'\right]_{m+1}$ has the same dimensions as $\left[\alpha R\right]$, with only nonzero elements appearing in the second and sixth rows of the

form $\left(0\ 0\ -e^{i\phi_{m+1}}\ 0\ 0\ 0\ 0\ 0\ 0\ -ie^{i\phi_{m+1}}\ 0\ 0\right)$ and

$\left(0\ 0\ -e^{-i\phi_{m+1}}\ 0\ 0\ 0\ 0\ 0\ 0\ +ie^{-i\phi_{m+1}}\ 0\ 0\right)$, respectively. These modifications represent the replacement of the cantilevered boundary condition $(\overline{\phi x}_m)_k$ and $(\overline{\phi y}_m)_k$ equations in Equation (15) with the gimballed slope boundary conditions exemplified by Equation (19).

The final hub interface boundary conditions that must be considered are those for a teetering rotor system. In this case, the My_m moments are not passed to the shaft such that $\left[\Delta R_I\right]_m$ is replaced by $\left[\Delta T_I\right]_m$ which is obtained when the fifth column of $\left[\Delta R_I\right]_m$ is taken to consist of only zero elements. In regard to the slope boundary condition alteration due to a teetering rotor, only the $(\overline{\phi y}_m)_k$ definition must be changed. However, on dropping $(\overline{\phi x}_m)_k$ from Equation (19) and noting that $\phi_1 = 0$ and $\phi_2 = \pi$, only one equation results. Thus, for a teetering rotor the equation corresponding to the second blade $(\overline{\phi y}_m)_k$ equation must be based on the summation of moments $(\overline{My}_m)_k$ acting on the hub becoming zero. Thus, corresponding to the first and second blades, respectively,

$$-i(\overline{\phi y}_p)_k e^{-i\phi_p} + i(\overline{\phi y}_{p+1})_k e^{-i\phi_{p+1}} = 0$$

$$(\overline{My}_p)_k e^{i\phi_p} + (\overline{My}_{p+1})_k e^{i\phi_{p+1}} = 0$$

where p can only have a value of 1.

The boundary condition matrix equation involving slopes, Equation (16), is modified to a teetering situation by replacing $\left[\alpha R\right]$ with $\left[\alpha T1\right]_m \delta_m^1 + \left[\alpha T2\right]_m \delta_m^2$ and $\left[\beta R_I\right]_m$ with $\left[\beta T_I\right]_m$, and adding the two terms $\left[\alpha T'\right]_{m+1} \left\{\overline{S}_k\right\}_{m+1}^{NS} \delta_m^1$ and

$\left[\alpha T''\right]_{m-1}\left\{\bar{S}_k\right\}_{m+1}^{NS}\delta_m^2$ to the left side of Equation (16). The $\left[\alpha T1\right]_m$ and $\left[\alpha T2\right]_m$ matrices are defined by modifying the sixth row of $\left[\alpha R\right]$ to the form $\left(0\ 0\ 0\ 0\ 0\ 0\ 0\ 0\ 0\ -ie^{-i\phi_m}\ 0\ 0\right)$ and $\left(0\ 0\ 0\ 0\ 0\ 0\ 0\ 0\ 0\ 0\ e^{i\phi_m}\ 0\right)$, respectively. The matrix $\left[\beta T_I\right]_m$ is the same as $\left[\beta R_I\right]_m$ except the sixth row consists of zeroes. The $\left[\alpha T'\right]_{m+1}$ and $\left[\alpha T''\right]_{m-1}$ matrices have the same dimensions as $\left[\alpha R\right]$ with only nonzero elements appearing in the sixth row of the forms $\left(0\ 0\ 0\ 0\ 0\ 0\ 0\ 0\ 0\ ie^{-i\phi_{m+1}}\ 0\ 0\right)$ and $\left(0\ 0\ 0\ 0\ 0\ 0\ 0\ 0\ 0\ 0\ e^{i\phi_{m-1}}\ 0\right)$, respectively.

On combination of the forms of Equations (16) and (18) required for rigid, gimballed, and teetering hub conditions, the general boundary condition equations corresponding to the fuselage-tailboom-fin structure and blade unknowns can be given in the matrix form

$$\left[B1\right]_m\left\{\bar{S}_k\right\}_m^{NS} + \left[B2\right]_m^{m+1}\left\{\bar{S}_k\right\}_{m+1}^{NS} + \left[B0\right]_m^{m-1}\left\{\bar{S}_k\right\}_{m-1}^{NS} + \sum_{I=-1}^{1}\left[DI\right]_m\left\{\bar{S}_{k+I}\right\}_s^{NSF} = 0 \qquad (20)$$

$$\left[\gamma\right]\left\{\bar{S}_k\right\}_s^{NSF} + \sum_{I=1}^{1}\sum_{m=1}^{Nb}\left[M_I\right]_m\left\{\bar{S}_{k+I}\right\}_m^{NS} = 0 \qquad (21)$$

where IBC = 0, 1, 2 for cantilevered hub, gimballed hub, and teetering hub, respectively, and

$$\left[B1\right]_m = \left[\alpha R\right]\delta^0_{IBC} + \left[\alpha G\right]_m\delta^1_{IBC} + \left[\alpha T1\right]_m\delta^2_{IBC}\delta^1_m + \left[\alpha T2\right]_m\delta^2_{IBC}\delta^2_m$$

$$\left[B2\right]^{m+1}_m = \left[\alpha G'\right]_{m+1}\delta^1_{IBC} + \left[\alpha T'\right]_{m+1}\delta^2_{IBC}\delta^1_m$$

$$\left[B0\right]^{m-1}_m = \left[\alpha T''\right]_{m-1}\delta^2_{IBC}\delta^2_m$$

$$\left[D_I\right]_m = \left[\beta R_I\right]_m\delta^0_{IBC} + \left[\beta G_I\right]_m\delta^1_{IBC} + \left[\beta T_I\right]_m\delta^2_{IBC}$$

and

$$\left[M_I\right]_m = \left[\Delta R_I\right]_m\delta^0_{IBC} + \left[\Delta G_I\right]_m\delta^1_{IBC} + \left[\Delta T_I\right]_m\delta^2_{IBC}$$

Final boundary condition matrix equations corresponding to the blade and fuselage-tailboom-fin structure unknowns in terms of these unknowns are obtained by substituting the form of Equation (12) with i = NS for the NS superscripted (blade) interface state variables and Equation (13) with i = NSF for the NSF superscripted (fuselage-tailboom-fin) state variables, exercising caution in replacing the k subscripts with k+1 and the m subscripts with m+1 or m-1 as required. These final expressions provide the necessary boundary condition relationships for a given value of k and m, including the interharmonic coupling effects due to blade aerodynamics and fuselage-tailboom-fin structure behavior.

Swashplate Control System Final Governing Equations

The governing equations for the deflection behavior of the swashplate in the swashplate rotating coordinate system are obtained by considering the governing differential equations of motion of a flexible ring in terms of swashplate variables defined relative to the fixed swashplate coordinate system and the equations which define the applied loadings acting on the ring at discrete azimuthal locations. The loading representation requires a knowledge of the displacement behavior of the base plate which can only be defined explicitly through the use of Laplace transforms. Due to this fact and the coupling between the blades and swashplate through the control rods and the coupling between base plate motion and gearbox motion, the final control system equations must be in a Laplace transformed form compatible with the fuselage-tailboom-fin structure and blade representation. Due to the complexity of the analysis involved pertaining to the swashplate

representation, the initial equations followed by a rough sketch of how the final equations are obtained and the final equations will be presented.

The governing differential equations for the motion of an elastic ring - which involve variables that are a function of both the azimuthal location of a point of interest on the ring relative to the fixed coordinate system x-axis θ, and time t - consist of the equilibrium, stress-strain, and strain-displacement equations. These equations for θ increasing as the point of interest moves counterclockwise around the ring from the fixed x-axis are:

$$\left.\begin{aligned}
\frac{\partial Vy(\theta,t)}{R\,\partial\theta} &= \mu\,\frac{\partial^2 v(\theta,t)}{\partial t^2} - Q(\theta,t) \\
\frac{\partial Mz(\theta,t)}{R\,\partial\theta} &= -Vy(\theta,t) - \frac{T(\theta,t)}{R} - \sigma(\theta,t) \\
\frac{\partial T(\theta,t)}{R\,\partial\theta} &= \frac{Mz(\theta,t)}{R} - \beta(\theta,t) \\
\frac{\partial \Theta(\theta,t)}{R\,\partial\theta} &= \frac{\Phi(\theta,t)}{R} + \frac{Mz(\theta,t)}{EI} \\
\frac{\partial v(\theta,t)}{R\,\partial\theta} &= \Theta(\theta,t) \\
\frac{\partial \Phi(\theta,t)}{R\,\partial\theta} &= \frac{\Theta(\theta,t)}{R} + \frac{T(\theta,t)}{GJ}
\end{aligned}\right\} \quad (22)$$

where $Vy(\theta,t)$, $Mz(\theta,t)$, and $T(\theta,t)$ are local shear force, bending moment, and torque acting on the ring, respectively;

$v(\theta,t)$ is the local displacement of the ring;

μ is the mass per unit arc length of the ring;

$\Theta(\theta,t)$ and $\Phi(\theta,t)$ are the local bending slope and twist angle of the ring;

R is the ring radius;

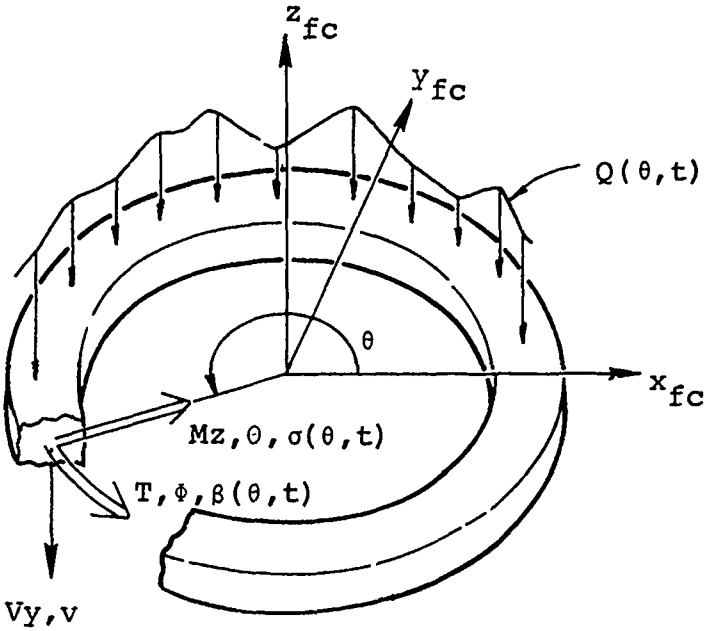

Figure 9. Coordinates of Swashplate Variables.

EI is the bending stiffness of the ring;

GJ is the torsional stiffness of the ring;

$\sigma(\theta,t)$ is the applied moment per unit length acting on the ring;

$\beta(\theta,t)$ is the applied torque per unit length acting on the ring; and

$Q(\theta,t)$ is the applied force per unit length acting on the ring.

The orientation of each of the θ and t dependent variables in Equation (22) is shown in Figure 9.

The applied loading distributions as a function of θ and t can be written on consideration of the forces and moments applied to the ring by the control rods and the spring-damper units supporting the ring by using a Dirac delta representation such that

$$
\left.
\begin{aligned}
\beta(\theta,t) &= \sum_{m=1}^{Nb} P_m(t)\, d_m \delta(\theta - \Omega t - \phi_m) \\
&\quad + \sum_{j=1}^{Ns} \delta(\theta - \chi_j)\, b_j \left(k_j + c_j \frac{\partial}{\partial t}\right) d(\theta,t) \\
&\quad - \sum_{j=1}^{Ns} \delta(\theta - \chi_j) \left(k\phi_j + c\phi_j \frac{\partial}{\partial t}\right) \Phi(\theta,t) \\
Q(\theta,t) &= \sum_{m=1}^{Nb} P_m(t)\, \delta(\theta - \Omega t - \phi_m) \\
&\quad - \sum_{j=1}^{Ns} \delta(\theta - \chi_j) \left(k_j + c_j \frac{\partial}{\partial t}\right) d(\theta,t) \\
\sigma(\theta,t) &= - \sum_{j=1}^{Ns} \sigma(\theta - \chi_j) \left(k\theta_j + c\theta_j \frac{\partial}{\partial t}\right) \Theta(\theta,t)
\end{aligned}
\right\} \qquad (23)
$$

where $d(\theta,t) = v(\theta,t) - b_j\Phi(\theta,t) - u_0(t)$ represents the distance a linear spring-damper unit is compressed at time t if the unit is at θ, and

Nb is the number of blades,

$P_m(t)$ is the force acting on the ring in the negative z_{fc}-axis direction due to the mth control rod,

d_m is the rigid offset of the mth control rod attachment point from the neutral axis of the ring, positive outward,

ϕ_m is the azimuthal location of the mth control rod relative to the reference blade position and defined by $\phi_m = \frac{(m-1)2\pi}{Nb}$ for equal spacing between control rods,

Ns is the number of linear spring-damper units supporting the ring,

χ_j is the azimuthal angle locating the jth support relative to ring x_{fc}-axis,

b_j is the offset of the jth linear spring attachment point from the neutral axis of the ring, positive inward,

k_j and c_j are the linear stiffness and damping values for the jth spring-damper unit,

$k\theta_j$ and $c\theta_j$ are the torsional stiffness and damping values for the jth torsional spring-damper unit counteracting local lateral rotation,

$\kappa\phi_j$ and $c\phi_j$ are the torsional stiffness and damping values for the jth torsional spring-damper unit counteracting local longitudinal ring rotation,

$u_0(t)$ is the displacement of the base which supports the spring-damper units in the negative z_{fc} direction.

Substituting the Fourier analysis representation of the θ and t dependent variables, as was specified by the form of Equation (5) into Equations (22), and carrying out the derivative operations with respect to θ and then assuming the resulting equations to be valid for each harmonic component denoted by ℓ, a set of six complex variable equations is obtained. These can be simultaneously solved to obtain a time differential equation for $v_\ell(t)$ in terms of the applied loading harmonics. The resulting differential equation is

$$\left[\mu \frac{\partial^2}{\partial t^2} + \frac{F(\ell)}{R^3}\right] v_\ell(t) = Q_\ell(t) - \frac{i\ell}{R}\sigma_\ell(t) + S_\ell \beta_\ell(t) \qquad (24)$$

where for convenience

$$F(a) = \frac{a^2 (a^2-1)^2 GJ EI}{(EI + a^2 GJ) R}$$

$$S_a = \frac{a^2 (GJ + EI)}{(a^2 GJ + EI) R}$$

The above definitions for a = 0 or = ±1 are independent of the ring stiffnesses, as would be expected, since $v_1(t)$, $v_0(t)$, and $v_{-1}(t)$ correspond to rigid body degrees of freedom of the ring.

The fixed frame displacement variables $v_\ell(t)$ can be related to the rotating frame displacement variables $w_\ell(t)$ by the relationship

$$v_\ell(t) = e^{-i\ell\Omega t} w_\ell(t) \tag{25}$$

which can be directly substituted into Equation (24) to yield the following expression:

$$\left[\left(\mu \frac{\partial^2}{\partial t^2} - 2i\ell\Omega \frac{\partial}{\partial t} - \ell^2\Omega^2\right) + \frac{F(\ell)}{R^3}\right] w_\ell(t)$$

$$= e^{i\ell\Omega t}\left(Q_\ell(t) - \frac{i\ell}{R}\sigma_\ell(t) + S_\ell\beta_\ell(t)\right) \tag{26}$$

when the time differential operators are applied and the equation is multiplied by $e^{i\ell\Omega t}$. The Laplace transform of Equation (26) is

$$\left[\mu(s^2 - 2i\ell\Omega s - \ell^2\Omega^2) + \frac{F(\ell)}{R^3}\right] \bar{w}_\ell(s)$$

$$= L_T\left(e^{i\ell\Omega t} Q_\ell(t) - e^{i\ell\Omega t} \frac{i\ell}{R} \sigma_\ell(t) + e^{i\ell\Omega t} S_\ell\beta_\ell(t)\right). \tag{27}$$

The expressions for $\beta_\ell(t)$, $Q_\ell(t)$, and $\sigma_\ell(t)$ are obtained by substituting the $\beta(\theta,t)$, $Q(\theta,t)$, and $\sigma(\theta,t)$ definitions of Equation (23) into the Fourier analysis equation exemplified by Equation (4) and integrating utilizing the characteristics of the Dirac delta integral as specified in Equation (9). The resulting expressions involve the χ_j dependent variables $\Phi(\chi_j,t)$, $\Theta(\chi_j,t)$ and $d(\chi_j,t)$, where $d(\chi_j,t) = v(\chi_j,t) - b_j\Phi(\chi_j,t) - u_0(t)$. These variables can be defined as

$$v(\chi_j,t) = \sum_{p=-\infty}^{\infty} w_p(t)e^{ip(\chi_j-\Omega t)}$$

$$\Phi(\chi_j,t) = \sum_{p=-\infty}^{\infty} S_p w_p(t)e^{ip(\chi_j-\Omega t)}$$

$$O(\chi_j,t) = \sum_{p=-\infty}^{\infty} i_p w_p(t)e^{ip(\chi_j-\Omega t)}/R$$

$$d(\chi_j,t) = \sum_{p=-\infty}^{\infty}\left[(1-b_j S_p)w_p(t)e^{ip(\chi_j-\Omega t)}\right] - u_0(t)$$

which can be substituted as required into the expressions for $\beta_\ell(t)$, $Q_\ell(t)$, and $\sigma_\ell(t)$ such that these applied loading harmonics can be defined in terms of $w_p(t)$ and $u_0(t)$.

The definition of the base plate displacement $u_0(t)$ involved time derivative operators and can only be algebraically defined in the Laplace transformed notation by

$$\bar{u}_0(s-i\ell\Omega) = \frac{\sum_{p=-\infty}^{\infty}\sum_{j=1}^{Ns}(1-b_j S_p)\overline{KC}_\ell e^{ip\chi_j}\,\bar{w}_p(s-i\ell\Omega+ip\Omega)}{K + (s-i\ell\Omega)C + \sum_{j=1}^{Ns}\overline{KC}_\ell}$$

$$- \frac{[K + (s-i\ell\Omega)C]\,\overline{uxs}(s-i\ell\Omega)}{K + (s-i\ell\Omega)C + \sum_{j=1}^{Ns}\overline{KC}_\ell} \qquad (28)$$

where $\overline{KC}_a = k_j + (s-ia\Omega)\,c_j$, K and C are the stiffness and damping values associated with the base plate spring-damper support, and $\overline{uxs}(s-i\ell\Omega)$ is the ℓ frequency shifted rotor shaft motion in the shaft axis direction. Thus, the expressions for the applied loading harmonics must be inserted into their respective terms of Equation (27) and Laplace transformed prior to use of Equation (28) to obtain the governing swashplate equations as a function of the Laplace transformed displacement and load variables: $\bar{w}_\ell(s)$, $\bar{w}_\ell(s-i\ell\Omega+p\Omega)$, $\overline{uxs}(s-i\ell\Omega)$, and $\bar{P}_m(s)$. The equation resulting from the

execution of the above operation and insertion of Equation (28) is modified initially by replacing the index ℓ with q, then the index p with ℓ, and multiplying thru by $2\pi R$ such that $2\pi R\mu = M$ which is the total mass of the swashplate ring. The resulting equation is further modified by introducing a summation over an index n of the terms involving the swashplate displacement variables which are taken as $\bar{w}_\ell(s-in\Omega)$, where Kronecker's delta is utilized to determine the values of n for which terms are to be included. This equation is further extended to provide additional equations by frequency shifting the Laplace transform variable by $ik\Omega$ such that the resulting governing equation for swashplate displacements can be written in the form

$$\sum_{n=-\infty}^{\infty}\left[\sum_{\ell=-\infty}^{\infty}\bar{z}_n^{\ell}\,\delta_q^{\ell}\,\delta_k^{n}+\sum_{\substack{\ell=-\infty\\ \ell\neq q}}^{\infty}\bar{x}_{q,\ell}^{k,n}\,\delta_{k+q}^{n+\ell}\right]\bar{w}_\ell(s-in\Omega)$$

$$+\sum_{n=-\infty}^{\infty}\bar{u}_n^{q}\,\delta_{q+k}^{n}\,\overline{uxs}(s-in\Omega)-\sum_{m=1}^{Nb}(1+d_mS_q)\overline{P_m}(s-ik\Omega)e^{-iq\phi_m}=0 \quad (29)$$

where

$$\bar{z}_n^{\ell}=M\left[(s-in\Omega)^2-2i\ell\Omega(s-in\Omega)-\ell^2\Omega^2\right]+\frac{2\pi F(\ell)}{R^2}$$

$$-\left[\overline{K1}_{\ell,-}^{\ell+n}\,\overline{K1}_{\ell,+}^{\ell+n}\,/\,\overline{K3}^{\ell+n}\right]+\overline{K2}_{\ell,\ell}^{\ell+n}$$

$$\bar{x}_{q,\ell}^{k,n}=-\left[\overline{K1}_{q,-}^{\ell+n}\,\overline{K1}_{\ell,+}^{\ell+n}\,/\,\overline{K3}^{\ell+n}\right]+\overline{K2}_{\ell,q}^{\ell+n}$$

$$\bar{U}_n^{q}=\overline{K4}_q^{q+k}$$

$$\overline{K1}_{b,c}^{a}=\sum_{j=1}^{Ns}(1-b_jS_b)\overline{KC}_a e^{cib\chi_j},\ c \text{ denotes sign}$$

$$\overline{K2}_{b,c}^{a}=\sum_{j=1}^{Ns}\left[(1-b_jS_b)(1-b_jS_c)\overline{KC}_a+bc\overline{KC\theta}_a/R^2\right.$$

$$\left.+S_cS_b\overline{KC}\phi_a\right]e^{-i\chi_j(c-b)}$$

$$\overline{K3}^a = K + (s-ia\Omega)C + \sum_{j=1}^{Ns} \overline{KC}_a$$

$$\overline{K4}^a_b = \left[K + (s-ia\Omega)C\right] \overline{K1}^a_{b,-} \; / \overline{K3}^a .$$

$$\overline{KC\phi}_a = k\phi_j + (s-ia\Omega)c\phi_j$$

$$\overline{KC\theta}_a = k\theta_j + (s-ia\Omega)c\theta_j .$$

The expression presented in Equation (29) provides the swashplate equations of motion for a given value of k and q and is in a coefficient form suitable for inclusion with the array coefficient form that results for the blade and fuselage structure final equations. To confine the coupling to a range that can be handled, the summation over n is truncated to the range of -Nf to +Nf and the summation over ℓ is truncated to the range of -Nmax to +Nmax. The governing equation for a given value of q and k is obtained by substituting their values into Equation (29) and carrying out the summations indicated. For each value of k, q is taken to have values from -Nmax to +Nmax such that 2Nmax+1 equations result. In addition, k is taken to have values from -Nf to +Nf such that a total of (2Nmax+1)(2Nf+1) control system governing equations result.

The definition of $(\overline{P}_k)_m$ or $\overline{P}_m(s-ik\Omega)$ is dependent upon whether the rotor is comprised of articulated or flexstrap blades. For articulated blades, $(\overline{P}_k)_m = (\overline{\Delta T}_k)_m/a_m$ where a_m is the control rod pitch horn attachment point offset aft of the mth blade shear center axis and $(\overline{\Delta T}_k)_m$ is the k frequency shifted torque applied to the mth blade in an opposite sense to the blade torque due to the mth control rod. $(\overline{\Delta T}_k)_m$ corresponds to the $(\overline{\Delta I}_k)_m$ discontinuity for an articulated blade. For flexstrap blades, the force applied to the ring $(\overline{P}_k)_m$ is defined in terms of the transfer matrix parameters used for crossing the effective application point of the pitch horr forces on the blade shear center axis. In particular,

$$(\bar{P}_k)_m = \sum_{n=-Nf}^{Nf} \left(\overline{CVz}_{k,n}\right)_m \left\{\bar{S}_n\right\}_m^* - C_{3,m}(\overline{\Delta 1}_k)_m$$

$$- C_{8,m}(\overline{\Delta 2}_k)_m + C_{12,m}(\overline{\Delta 3}_k)_m \qquad (30)$$

where the $C_{i,m}$ quantities are the elastic influence coefficients of the restraint transfer matrix of the mth blade; $(\overline{\Delta 1}_k)_m$, $(\overline{\Delta 2}_k)_m$ and $(\overline{\Delta 3}_k)_m$ are the k frequency shifted discontinuity deflection variables of the mth blade corresponding to the $\overline{ux}_r$, $\overline{uy}_r$ and $\overline{uz}_r$ deflections of the control rod attachment point; and

$$\left(\overline{CVz}_{k,n}\right)_m = \left(C_3\ C_{13}\ C_8\ C_{15} - C_{12}\ C_{14}\right)_m \left[\alpha\right] \left[\bar{B}_{k,n}\right]_m^{Nr}$$

where $\left[\alpha\right]$ was defined previously in regard to blade-fuselage tailboom-fin interface boundary conditions and Nr denotes the section at which the restraint application occurs. Thus, depending on the type of blades involved in the rotor, the $(\bar{P}_k)_m$ forces acting on the ring are definable in terms of the blade state variables and discontinuity unknowns such that in combination with Equation (29) the swashplate control system representation is complete.

Discontinuity Representation

The remaining equations necessary to construct the final governing matrix equation are those which define the discontinuity terms $(\overline{\Delta 1}_k)_m$, $(\overline{\Delta 2}_k)_m$, and $(\overline{\Delta 3}_k)_m$. For articulated blades, these variables correspond to $(\overline{\Delta T}_k)_m$, $(\overline{\Delta \phi x}_k)_m$, and $(\overline{\Delta \phi y}_k)_m$, respectively. If a control torque is to be applied to the blade by the control rod (Mct = 1) at the inboard end of section Nct, the torque opposite in direction to the blade torque can be defined in terms of real-time variables by

$$(\Delta T)_m = a_m k_m (1 + \tau_m d/dt)\left[a_m(\phi x_m)^{Nct} - \sum_{\ell=-\infty}^{\infty} S_{m,\ell} w_\ell(t)\right]$$

where k_m and τ_m are the linear stiffness and damping retardation time of the mth control rod, respectively, and

$S_{m,\ell} = (1 + d_m S_\ell) e^{i\ell\phi_m}$. By applying Laplace tranformations, including k frequency shifting of the Laplace transform variable, to the real-time torque discontinuity equation and dividing by k_m, the torque discontinuity expression

$$(\overline{\Delta T}_k)_m/k_m \quad \overline{Y}_{k,m}\left[a_m(\overline{\phi x}_m)_k^{Nct} - \sum_{\ell=-\infty}^{\infty} S_{m,\ell}\overline{w}_\ell(s-ik\Omega)\right] = 0$$

is obtained where $\overline{Y}_{k,m} = a_m(1 + (s-ik\Omega)\tau_m)$. The variable $(\overline{\phi x}_m)_k^{Nct}$ is equivalent to the third element of the k frequency shifted mth blade state variable vector at the section denoted by Nct such that $(\overline{\phi x}_m)_k^{Nct} = \left[r_3\right]\left\{\overline{S}_k\right\}_m^{Nct}$ where the form $\left[r_i\right]$, for i an integer, denotes a twelve-element row matrix with the ith element equal unity and all others zero. Using the form of Equation (12) with the assumption that the pitch bearing, if included, occurs inboard of the control torque application point, i.e., $\left\{\overline{c}_{k,n}\right\}_m^{Nct} = 0$, and the fact that $\left[r_3\right]\left\{\overline{b}_{k,n}\right\}_m^{Nct} = 0$, $(\overline{\phi x}_m)_k^{Nct}$ can be defined in terms of the n frequency shifted mth blade tip unknowns and flap discontinuities. By substituting this definition into the torque discontinuity expression,

$$(\overline{\Delta T}_k)_m/k_m - a_m\overline{Y}_{k,m}\left[r_3\right]\sum_{n=-Nf}^{Nf}\left[\left[\overline{B}_{k,n}\right]_m^{Nct}\left\{\overline{S}_n\right\}_m^{*} - \left\{\overline{d}_{k,n}\right\}_m^{Nct}(\overline{\Delta\phi y}_k)_m\right]$$

$$+ \overline{Y}_{k,m}\sum_{\ell=-Nmax}^{Nmax} S_{m,\ell}\overline{w}_\ell(s-ik\Omega) = 0 \qquad (31)$$

At the pitch bearing, if included in the blade model (Mfea = 1) and located at the inboard end of section Nfea, the condition exists that the torque must go to zero which is represented by $\left[r_4\right]\left\{\overline{S}_k\right\}_m^{Nfea} = 0$. However, to take into account pitch-lag coupling, if not handled by blade modeling, the condition $(\overline{T}_k)_m^{Nfea} + PLC(\overline{Mz}_k)_m^{Nfea} = 0$ or $\left[r_{PLC}\right]\left\{\overline{S}_k\right\}_m^{Nfea} = 0$ has been

allowed where $\left[r_{PLC}\right]$ is the row vector

$\left[0\ 0\ 0\ 1\ 0\ 0\ PLC\ 0\ 0\ 0\ 0\ 0\right]$ and PLC is the pitch-lag coupling factor. Thus, utilizing Equation (12)

$$\left[r_{PLC}\right] \sum_{n=-Nf}^{Nf} \left[\left[\bar{B}_{k,n}\right]_m^{Nfea} \left\{\bar{S}_n\right\}_m^* - \left\{\bar{b}_{k,n}\right\}_m^{Nfea} \left(\overline{\Delta T}_k\right)_m - \left\{\bar{d}_{k,n}\right\}_m^{Nfea} \left(\overline{\Delta \phi y}_k\right)_m\right] = 0 \quad (32)$$

where use has been made of the fact that $\left[r_{PLC}\right]\left\{\bar{c}_{k,n}\right\}_m^{Nfea} = 0.$

At the flap hinge, if included in the blade model (Nflap = 1) and located at the inboard end of section Nflap, the condition exists that the flapwise moment must go to zero which is represented by $\left[r_{11}\right]\left\{\bar{S}_k\right\}_m^{Nflap} = 0.$ However, to take into account pitch-flap coupling, if not handled by blade modeling, the condition $\left(My_k\right)_m^{Nflap} + PFC\left(\bar{T}_k\right)_m^{Nflap} = 0$ or $\left[r_{PFC}\right]\left\{\bar{S}_k\right\}_m^{Nflap} = 0$ has been allowed where $\left[r_{PFC}\right]$ is the row vector $\left[0\ 0\ 0\ PFC\ 0\ 0\ 0\ 0\ 0\ 0\ 1\ 0\right]$ and PFC is the pitch-flap coupling factor. Thus, utilizing Equation (12)

$$\left[r_{PFC}\right] \sum_{n=-Nf}^{Nf} \left[\left[\bar{B}_{k,n}\right]_m^{Nflap} \left\{\bar{S}_k\right\}_m^* - \left\{\bar{b}_{k,n}\right\}_m^{Nflap} \left(\overline{\Delta T}_k\right)_m - \left\{\bar{c}_{k,n}\right\}_m^{Nflap} \left(\overline{\Delta \phi x}_k\right)_m\right] = 0 \quad (33)$$

where use has been made of the fact that $\left[r_{PFC}\right]\left\{\bar{d}_{k,n}\right\}_m^{Nflap} = 0.$

Equations (31), (32), and (33) can be used to define the k

shifted discontinuity variables.

The discontinuity related equations for the flexstrap blades are based upon the requirement that a control rod cannot carry transverse loading and that the axial force in a control rod is a function of the linear stiffness and damping characteristics of the control rod and the relative change in control rod length. The forces acting on a control rod at its attachment point to the pitch horn in the same orientation as the rotating shaft coordinate system for the mth blade are defined by

$$(\overline{N2}_k)_m = -\sum_{n=-Nf}^{Nf}\left(\overline{CN}_{k,n}\right)_m\left\{\overline{S}_n\right\}_m^* + C_{1,m}(\overline{\Delta 1}_k)_m + C_{2,m}(\overline{\Delta 2}_k)_m - C_{3,m}(\overline{\Delta 3}_k)_m$$

$$(\overline{Vy2}_k)_m = -\sum_{n=-Nf}^{Nf}\left(\overline{CVy}_{k,n}\right)_m\left\{\overline{S}_n\right\}_m^* + C_{2,m}(\overline{\Delta 1}_k)_m + C_{7,m}(\overline{\Delta 2}_k)_m - C_{8,m}(\overline{\Delta 3}_k)_m$$

$$(\overline{Vz2}_k)_m = -\sum_{n=-Nf}^{Nf}\left\{\overline{CVz}_{k,n}\right\}_m\left\{\overline{S}_n\right\}_m^* + C_{3,m}(\overline{\Delta 1}_k)_m + C_{8,m}(\overline{\Delta 2}_k)_m - C_{12,m}(\overline{\Delta 3}_k)_m$$

where $\left(\overline{CN}_{k,n}\right)_m = \left(C_1\ C_4\ C_2\ C_6\ -C_3\ C_5\right)_m\left[\alpha\right]\left[\overline{B}_{k,n}\right]_m^{Nr}$, $\left(\overline{CVy}_{k,n}\right)_m = \left(C_2\ C_9\ C_7\ C_{11}\ -C_8\ C_{10}\right)_m\left[\alpha\right]\left[\overline{B}_{k,n}\right]_m^{Nr}$ and the definition of other quantities was given following Equation (30).

The forces acting in the mth control rod local coordinate system can be defined by

$$\begin{Bmatrix}\overline{FX2}_k\\ \overline{FY2}_k\\ \overline{FZ2}_k\end{Bmatrix}_m = \begin{bmatrix}\alpha_1 & \alpha_2 & \alpha_3\\ \alpha_4 & \alpha_5 & 0\\ -\alpha_3\alpha_5 & \alpha_3\alpha_4 & \alpha_6\end{bmatrix}_m\begin{Bmatrix}\overline{N2}_k\\ \overline{Vy2}_k\\ \overline{Vz2}_k\end{Bmatrix}_m = \begin{Bmatrix}0\\ 0\\ \kappa_k x_e\end{Bmatrix}_m \qquad (34)$$

where $\kappa_{k,m} = K_{c,m} + (s-ik\Omega)C\tau_{c,m}$ with $K_{c,m}$ and $C\tau_{c,m}$ representing the linear stiffness and damping coefficient for the

mth control rod spring-damper unit, respectively, and $x_{e,m}$ is the extension of the control rod. In Equation (34), the 3 x 3 array, consisting of $\alpha_{i,m}$ quantities representing sines and cosines of control rod orientation angles, corresponds to the transformation array for defining the local control rod unit vectors in terms of the rotating shaft unit vectors. The control rod extension can be expressed in terms of the deflections of the control rod attachment point to the pitch horn ($(\overline{uxa}_k)_m$, $(\overline{uya}_k)_m$, and $(\overline{uza}_k)_m$) and the deflections of the control rod attachment point to the swashplate ($(\overline{uxp}_k)_m$, $(\overline{uyp}_k)_m$, and $(\overline{uzp}_k)_m$) by the expression

$$x_{e,m} = -\alpha_{3,m}\alpha_{5,m}\left[(\overline{uxa}_k)_m - (\overline{uxp}_k)_m\right]$$

$$+ \alpha_{3,m}\alpha_{4,m}\left[(\overline{uya}_k)_m - (\overline{uyp}_k)_m\right] + \alpha_{6,m}\left[(\overline{uza}_k)_m - (\overline{uzp}_k)_m\right].$$

The control rod attachment point deflections associated with the mth blade are defined in coordinate systems oriented the same as the mth blade rotating coordinate system. Two of the three equations required to represent the flexstrap discontinuity terms are obtained from the $(\overline{FX2}_k)_m$ and $(\overline{FY2}_k)_m$ definitions in Equation (34). The remaining equation is obtained from the $(\overline{Vz2}_k)_m$ definition resulting when the middle and right side terms of Equation (34) are premultiplied by the inverse of the transformation array in Equation (34). The three equations obtained on substitution of the definition of the various deflections and force terms are

$$-\sum_{n=-Nf}^{Nf}\left[\overline{DX}_{k,n}\right]_m\left\{\overline{S}_n\right\}_m^* + DX1_m(\overline{\Delta 1}_k)_m + DX2_m(\overline{\Delta 2}_k)_m - DX3_m(\overline{\Delta 3}_k)_m = 0$$

$$-\sum_{n=-Nf}^{Nf}\left[\overline{DY}_{k,n}\right]_m\left\{\overline{S}_n\right\}_m^* + DY1_m(\overline{\Delta 1}_k)_m + DY2_m(\overline{\Delta 2}_k)_m - DY3_m(\overline{\Delta 3}_k)_m = 0$$

$$-\sum_{n=-Nf}^{Nf}\left[\overline{DZ}_{k,n}\right]_m\left\{\overline{S}_n\right\}_m^* + DZ1_{k,m}(\overline{\Delta 1}_k)_m + DZ2_{k,m}(\overline{\Delta 2}_k)_m$$

$$- DZ3_{k,m}(\overline{\Delta 3}_k)_m + \left[DB\right]_m\left\{\overline{S}_k\right\}_m^{NS}$$

$$-\sum_{\ell=-Nmax}^{Nmax}(1 + d_m S_\ell)w_\ell(s-ik\Omega)e^{i\ell\phi_m}\delta^1_{NSP} = 0 \qquad (35)$$

where the row vectors consisting of 12 elements are defined by

$$\left(\overline{DX}_{k,n}\right)_m = \alpha_{1,m}\left(\overline{CN}_{k,n}\right)_m + \alpha_{2,m}\left(\overline{CVy}_{k,n}\right)_m + \alpha_{3,m}\left(\overline{CVz}_{k,n}\right)_m$$

$$\left(\overline{DY}_{k,n}\right)_m = \alpha_{4,m}\left(\overline{CN}_{k,n}\right)_m + \alpha_{5,m}\left(\overline{CVy}_{k,n}\right)_m$$

$$\left(\overline{DZ}_{k,n}\right)_m = \left(\overline{CVz}_{k,n}\right)_m \; / \; (\alpha_{6,m}\alpha_{6,m}\kappa_{k,m})$$

$$\left(\overline{DB}\right)_m = \alpha_{3,m}\alpha_{4,m}\left(r_5\right) + L12_m\left(r_3\right)/\alpha_{6,m} - \left(r_9\right)\delta^0_{NSP}$$

$$- \alpha_{3,m}\alpha_{5,m}\left(r_1\right) - L12_m\left(r_{10}\right)/\alpha_{6,m}$$

in which $L12_m$ is the distance from the hub center to the mth control rod attachment point on the swashplate ring which is used in conjunction with the slopes and deflections at the hub to determine the transverse motion of the control rod attachment points, and NSP is an integer variable equal to 1 if the swashplate is allowed to move along the shaft axis, otherwise equal to zero. The single element variables in Equation (35) are defined by the expressions

$$DX1_m = \alpha_{1,m}C_{1,m} + \alpha_{2,m}C_{2,m} + \alpha_{3,m}C_{3,m}$$

$$DX2_m = \alpha_{1,m}C_{2,m} + \alpha_{2,m}C_{7,m} + \alpha_{3,m}C_{8,m}$$

$$DX3_m = \alpha_{1,m}C_{3,m} + \alpha_{2,m}C_{8,m} + \alpha_{3,m}C_{12,m}$$

$$DY1_m = \alpha_{4,m}C_{1,m} + \alpha_{5,m}C_{2,m}$$

$$DY2_m = \alpha_{4,m}C_{2,m} + \alpha_{5,m}C_{7,m}$$

$$DY3_m = \alpha_{4,m}C_{3,m} + \alpha_{5,m}C_{8,m}$$

$$DZ1_{k,m} = \alpha_{3,m}\alpha_{5,m}/\alpha_{6,m} + C_{3,m}/(\alpha_{6,m}\alpha_{6,m}\kappa_{k,m})$$

$$DZ2_{k,m} = -\alpha_{3,m}\alpha_{4,m}/\alpha_{6,m} + C_{8,m}/(\alpha_{6,m}\alpha_{6,m}\kappa_{k,m})$$

$$DZ3_{k,m} = -1 + C_{12,m}/(\alpha_{6,m}\alpha_{6,m}\kappa_{k,m}).$$

The last equation of Equation (35) utilizes the swashplate displacements which are defined relative to the nonperturbed position of the swashplate to define the shaftwise deflection

of the control rod attachment point if the swashplate is allowed to move along the shaft. If there is no motion of the swashplate relative to the shaft, the deflection of the control rod attachment point is based on the motion of the hub. All of the necessary equations for construction of the final matrix have been presented and may now be arranged in the final matrix form.

Final Matrix Equation

Equations (20), (21), (29), (30), (31), (32), (33), and (35), in conjunction with Equations (12) and (13), allow the construction of the final governing equations for any value of k denoting the k frequency shifted equations which can be represented in the form

$$\sum_{n=Nf}^{Nf} \left[\overline{T}_{k,n}\right]\left\{\overline{q}_n\right\}^* = 0 \qquad (36)$$

where $\left[\overline{T}_{k,n}\right]$ contains the terms relating the contribution of n frequency shifted unknown quantities in the column vector $\left\{\overline{q}_n\right\}^*$ to the k frequency shifted governing equations. The construction of the $\left[\overline{T}_{k,n}\right]$ matrix can be represented using a three-bladed rotor as an example and integers for blade subscripts and superscripts in the form

$$\left[\overline{T}_{k,n}\right] = \begin{array}{|c|c|c|c|c|} \hline \left[\overline{SW}_{k,n}\right] & \left[\overline{SF}_{k,n}\right] & \left[\overline{SB}_{k,n}\right]1 & \left[\overline{SB}_{k,n}\right]2 & \left[\overline{SB}_{k,n}\right]3 \\ \hline 0 & \left[\overline{FU}_k\right]\delta_n^k & \left[\overline{FB}_{k,n}\right]1 & \left[\overline{FB}_{k,n}\right]2 & \left[\overline{FB}_{k,n}\right]3 \\ \hline \left[\overline{BS}_k\right]1\ \delta_n^k & \left[\overline{BF}_{k,n}\right]1 & \left[\overline{BB}_{k,n}\right]\begin{matrix}1\\1\end{matrix} & \left[\overline{BB}_{k,n}\right]\begin{matrix}2\\1\end{matrix} & \left[\overline{BB}_{k,n}\right]\begin{matrix}3\\1\end{matrix} \\ \hline \left[\overline{BS}_k\right]2\ \delta_n^k & \left[\overline{BF}_{k,n}\right]2 & \left[\overline{BB}_{k,n}\right]\begin{matrix}1\\2\end{matrix} & \left[\overline{BB}_{k,n}\right]\begin{matrix}2\\2\end{matrix} & \left[\overline{BB}_{k,n}\right]\begin{matrix}3\\2\end{matrix} \\ \hline \left[\overline{BS}_k\right]3\ \delta_n^k & \left[\overline{BF}_{k,n}\right]3 & \left[\overline{BB}_{k,n}\right]\begin{matrix}1\\3\end{matrix} & \left[\overline{BB}_{k,n}\right]\begin{matrix}2\\3\end{matrix} & \left[\overline{BB}_{k,n}\right]\begin{matrix}3\\3\end{matrix} \\ \hline \end{array} \qquad (37)$$

If the number of spacial harmonics retained in the swashplate representation is limited by letting q and ℓ range from -Nmax to Nmax, for Nmax equals 1 in Equation (39), the swashplate impedances are represented by

$$\left[\overline{SW}_{k,n}\right] = \left[\begin{array}{c|c|c} \overline{Z}_n^{-1}\ \delta_k^n & \overline{X}_{-1,0}^{k,n}\ \delta_{k-1}^n & \overline{X}_{-1,1}^{k,n}\ \delta_{k-1}^{n+1} \\ \hline \overline{X}_{0,-1}^{k,n}\ \delta_k^{n-1} & \overline{Z}_n^0\ \delta_k^n & \overline{X}_{0,1}^{k,n}\ \delta_k^{n+1} \\ \hline \overline{X}_{1,-1}^{k,n}\ \delta_{k+1}^{n-1} & \overline{X}_{1,0}^{k,n}\ \delta_{k+1}^n & \overline{Z}_n^1\ \delta_k^n \end{array}\right]$$

the swashplate to fuselage-tailboom-fin coupling is represented by

$$\left[\overline{SF}_{k,n}\right] = \left[\begin{array}{c} \overline{U}_n^{-1}\ \left(r_1\right)\left[\overline{S}_{k-1}\right]_s^{NSF}\ \delta_{k-1}^n \\ \hline \overline{U}_n^0\ \left(r_1\right)\left[\overline{S}_k\right]_s^{NSF}\ \delta_k^n \\ \hline \overline{U}_n^1\ \left(r_1\right)\left[\overline{S}_{k+1}\right]_s^{NSF}\ \delta_{k+1}^n \end{array}\right]$$

and the swashplate to blade coupling is represented by either

$$\left[\overline{SB}_{k,n}\right]_m = \left[\begin{array}{c|c|c} & -S_{m,-1}/a_m & \\ \hline \leftarrow 6\ \text{cols.} \rightarrow \text{ of zeroes} & -S_{m,0}/a_m & \leftarrow 2\ \text{cols.} \rightarrow \text{ of zeroes} \\ \hline & -S_{m,1}/a_m & \end{array}\right]$$

for an articulated blade or

$$\left[\overline{SB}_{k,n}\right]_m =$$

$$\left[\begin{array}{c|c|c|c} -S_{m,-1}\left(\overline{CVz}_{k,n}\right)_m & S_m\ {}_{-1}C_{3,m}\ \delta_n^k & S_{m,-1}C_{8,m}\ \delta_n^k & -S_{m,-1}C_{12,m}\ \delta_n^k \\ \hline -S_{m,0}\left(\overline{CVz}_{k,n}\right)_m & S_{m,0}C_{3,m}\ \delta_n^k & S_{m,0}C_{8,m}\ \delta_n^k & -S_{m,0}C_{12,m}\ \delta_n^k \\ \hline -S_{m,1}\left(\overline{CVz}_{k,n}\right)_m & S_{m,1}C_{3,m}\ \delta_n^k & S_{m,1}C_{8,m}\ \delta_n^k & -S_{m,1}C_{12,m}\ \delta_n^k \end{array}\right]$$

From Equation (21), the diagonal fuselage-tailboom-fin array $\left[\overline{FU}_k\right]$ is defined by

$$\left[\overline{FU}_k\right] = \left[\gamma\right]\left[\overline{S}_k\right]_s^{NSF}$$

and the fuselage-tailboom-fin coupling to the blades is defined by

$$\left[\overline{FB}_{k,n}\right]_m = \left[\left[\overline{FBB}_{k,n}\right]_m \middle| -\left\{\overline{FBb}_{k,n}\right\}_m \middle| -\left\{\overline{FBc}_{k,n}\right\}_m \middle| -\left\{\overline{FBd}_{k,n}\right\}_m\right]$$

where

$$\left[\overline{FBB}_{k,n}\right]_m = \sum_{I=-1}^{1}\left[M_I\right]_m\left[\overline{B}_{k+I,n}\right]_m^{NS}$$

$$\left\{\overline{FBb}_{k,n}\right\}_m = \sum_{I=-1}^{1}\left[M_I\right]_m\left\{\overline{b}_{k+I,n}\right\}_m^{NS}$$

and $\left\{\overline{FBc}_{k,n}\right\}_m$ and $\left\{\overline{FBd}_{k,n}\right\}_m$ are defined in a similar form with b in the last expression replaced by c and d, respectively. From Equations (20), (31), (32), and (33), which represent an articulated blade, the diagonal blade arrays $\left[\overline{BB}_{k,n}\right]_m^m$ are defined by

$$\left[\overline{BB}_{k,n}\right]_m^m = \left[\begin{array}{c|c} \left[\overline{BBB}_{k,n}\right]_m & \left[\overline{BBR}_{k,n}\right]_m \\ \hline \left[\overline{BBC}_{k,n}\right]_m & \left[\overline{BBD}_{k,n}\right]_m \end{array}\right]$$

where

$$\left[\overline{BBB}_{k,n}\right]_m = \left[Bl\right]_m \left[\overline{B}_{k,n}\right]_m^{NS}$$

$$\left[\overline{BBR}_{k,n}\right]_m = \left[-\left[Bl\right]_m \left\{\overline{b}_{k,n}\right\}_m^{NS} \middle| - \left[Bl\right]_m \left\{\overline{c}_{k,n}\right\}_m^{NS} \middle| - \left[Bl\right]_m \left\{\overline{d}_{k,n}\right\}_m^{NS}\right]$$

$$\left[\overline{BBC}_{k,n}\right]_m = \left[\begin{array}{c} \left[-a_m \, \overline{Y}_{k,m}\left(r_3\right) \left[\overline{B}_{k,n}\right]_m^{Nct}\right] \\ \hline \left[\left(r_{PLC}\right) \left[\overline{B}_{k,n}\right]_m^{Nfea}\right] \\ \hline \left[\left(r_{PFC}\right) \left[\overline{B}_{k,n}\right]_m^{Nflap}\right] \end{array}\right]$$

$$\left[\overline{BBD}_{k,n}\right]_m =$$

$$\left[\begin{array}{c|c|c} 1/k_m & 0 & +a_m \, \overline{Y}_{k,m} \left\{\overline{d}_{k,n}\right\}_m^{Nct} \\ \hline -\left(r_{PLC}\right)\left\{\overline{b}_{k,n}\right\}_m^{Nfea} & 0 & -\left(r_{PLC}\right)\left\{\overline{d}_{k,n}\right\}_m^{Nfea} \\ \hline -\left(r_{PFC}\right)\left\{\overline{b}_{k,n}\right\}_m^{Nflap} & -\left(r_{PFC}\right)\left\{\overline{c}_{k,n}\right\}_m^{Nflap} & 0 \end{array}\right]$$

and the off diagonal blade arrays $\left[\overline{BB}_{k,n}\right]_m^j$ are defined by

$$\left[\overline{BB}_{k,n}\right]_{m}^{j} = \left[\begin{array}{c|c} \left[\overline{BBJ1}_{k,n}\right]_{m}^{j} & \left[\overline{BBJ2}_{k,n}\right]_{m}^{j} \\ \hline & \begin{array}{c}\uparrow \\ 3 \text{ rows} \\ \text{of} \\ \text{zeroes} \\ \downarrow\end{array} \end{array}\right]$$

$j \neq m$

where

$$\left[\overline{BBJ1}_{k,n}\right]_{m}^{j} = \left[\begin{array}{l} \left[B2\right]_{m}^{j} \left[\overline{B}_{k,n}\right]_{j}^{NS} \Delta_{j-m} \\ + \left[B0\right]_{m}^{j} \left[\overline{B}_{k,n}\right]_{j}^{NS} \delta_{j-m}^{-1} \end{array}\right]$$

$$\left[\overline{BBJ2}_{k,n}\right]_{m}^{j} =$$

$$\left[\begin{array}{l|l|l} -\left[B2\right]_{m}^{j}\left\{\overline{b}_{k,n}\right\}_{j}^{NS} \Delta_{j-m} & -\left[B2\right]_{m}^{j}\left\{\overline{c}_{k,n}\right\}_{j}^{NS} \Delta_{j-m} & -\left[B2\right]_{m}^{j}\left\{\overline{d}_{k,n}\right\}_{j}^{NS} \Delta_{j-m} \\ -\left[B0\right]_{m}^{j}\left\{\overline{b}_{k,n}\right\}_{j}^{NS} \delta_{j-m}^{-1} & -\left[B0\right]_{m}^{j}\left\{\overline{c}_{k,n}\right\}_{j}^{NS} \delta_{j-m}^{-1} & -\left[B0\right]_{m}^{j}\left\{\overline{d}_{k,n}\right\}_{j}^{NS} \delta_{j-m}^{-1} \end{array}\right]$$

and $\Delta_{j-m} = \delta_{j-m}^{1} + \delta_{j-m}^{-Nb+1}\,\delta_{IBC}^{1}$, the latter term required for the Nbth blade equations, Nb being the total number of blades being considered. The blade to fuselage-tailboom-fin coupling arrays are defined by

$$\left[\overline{BF}_{k,n}\right]_{m} = \left[\begin{array}{c} \sum_{I=-1}^{1} \left[D_I\right]_{m} \left[\overline{S}_{k+I}\right]_{s}^{NSF} \delta_{n-k}^{I} \\ \hline \begin{array}{c}\uparrow \\ 3 \text{ rows} \\ \text{of} \\ \text{zeroes} \\ \downarrow\end{array} \end{array}\right]$$

and the blade to swashplate coupling is defined by

$$\left[\overline{BS}_k\right]_m = \begin{bmatrix} & \uparrow \\ & \text{6 rows of zeroes} \\ & \downarrow & \\ \hline \bar{Y}_{k,m}\, S_{m,-1} & \bar{Y}_{k,m}\, S_{m,0} & \bar{Y}_{k,m}\, S_{m,1} \\ 0 & 0 & 0 \\ 0 & 0 & 0 \end{bmatrix}$$

For a flexstrap tail rotor, using Equation (35) instead of Equations (31), (32) and (33), the diagonal blade arrays and blade to swashplate coupling arrays are altered to the form

$$\left[\overline{BB}_{k,n}\right]_m =$$

$$\begin{bmatrix} \left[Bl\right]_m\left[B_{k,n}\right]_m^{NS} & -\left[Bl\right]_m\left\{\bar{b}_{k,n}\right\}_m^{NS} & -\left[Bl\right]_m\left\{\bar{c}_{k,n}\right\}_m^{NS} & -\left[Bl\right]_m\left\{\bar{d}_{k,n}\right\}_m^{NS} \\ -\left\{\overline{DX}_{k,n}\right\}_m & DX1_m & DX2_m & -DX3_m \\ -\left\{\overline{DY}_{k,n}\right\}_m & DY1_m & DY2_m & -DY3_m \\ -\left\{\overline{DZ}_{k,n}\right\}_m & DZ1_{km} & DZ2_{km} & -DZ3_{km} \\ +\left\{DB\right\}_m\left[\bar{E}_{k,n}\right]_m^{NS} & -\left\{DB\right\}_m\left[\bar{b}_{k,n}\right]_m^{NS} & -\left\{DB\right\}_m\left\{\bar{c}_{k,n}\right\}_m^{NS} & -\left\{DB\right\}_m\left\{\bar{d}_{k,n}\right\}_m^{NS} \end{bmatrix}$$

$$\left[\overline{BS}_k\right]_m =$$

$$\begin{bmatrix} & \uparrow \\ & \text{8 rows of zeroes} \\ & \downarrow & \\ \hline -S_{m,-1} & -S_{m,0} & -S_{m,1} \end{bmatrix}$$

The column vector of unknowns is defined by

$$\left\{\bar{q}_n\right\}^* = \begin{Bmatrix} \left\{\bar{r}_n\right\} \\ \left\{\bar{S}_n\right\}_s^* \\ \left\{\bar{P}_n\right\}_1 \\ \left\{\bar{P}_n\right\}_2 \\ \left\{\bar{P}_n\right\}_3 \end{Bmatrix}$$

where in general

$$\left\{\bar{r}_n\right\} = \begin{Bmatrix} \bar{w}_{-Nmax}(s-in\Omega) \\ \cdot \\ \cdot \\ \bar{w}_{-1}(s-in\Omega) \\ \bar{w}_0(s-in\Omega) \\ \bar{w}_1(s-in\Omega) \\ \cdot \\ \cdot \\ \bar{w}_{Nmax}(s-in\Omega) \end{Bmatrix} \text{ and } \left\{\bar{P}_n\right\}_m = \begin{Bmatrix} \left\{\bar{S}_n\right\}_m^* \\ \left\{\overline{\Delta 1}_n\right\}_m \\ \left\{\overline{\Delta 2}_n\right\}_m \\ \left\{\overline{\Delta 3}_n\right\}_m \end{Bmatrix}$$

Equation (37) has been given for a system consisting of all possible components of coupling. Considering this array to be made up of five columns and five rows, the exclusion of a swashplate from the system results in the removal of the first column and first row, the exclusion of a fuselage-tailboom-fin structure results in the removal of the second column and second row, and the exclusion of a blade results in the removal of the row and column containing the associated diagonal blade array. For teetering rotors, only two blades are allowed such that blade matrices for m greater than two do not exist.

The k frequency shifted equations represented by Equation (36) involve n frequency shifted variables which can be defined by considering values of k from $-N_f$ to $+N_f$ such that the final matrix required for solution may be obtained in the form

$$\begin{bmatrix} \bar{T}_{-1,-1} & \bar{T}_{-1,0} & \bar{T}_{-1,1} \\ \bar{T}_{0,-1} & \bar{T}_{0,0} & \bar{T}_{0,1} \\ \bar{T}_{1,-1} & \bar{T}_{1,0} & \bar{T}_{1,1} \end{bmatrix} \begin{Bmatrix} \bar{q}_{-1} \\ \bar{q}_0 \\ \bar{q}_1 \end{Bmatrix}^* = 0 \qquad (38)$$

for NF = 1. In general, the number of $\left[\bar{T}_{k,n}\right]$ matrices required to construct the final governing matrix is defined by $(2Nf+1)^2$ such that for Nf equal to 2 the resulting governing matrix would consist of five rows and five columns of $\left[\bar{T}_{k,n}\right]$ matrices.

Throughout the development of the analysis, the degree of interharmonic coupling (due to periodically varying coefficients) used in obtaining the governing equations and the final governing matrix were limited by the truncation of the summations involved to the range of -Nf to +Nf. If this truncation procedure is not applied, an infinite set of governing equations is obtained. Thus, in matrix form, an infinite final matrix results such that there are an infinite number of roots which satisfy the final matrix determinant. This characteristic of equations resulting from consideration of periodically varying coefficients in a ground resonance helicopter analysis was encountered by Coleman and Feingold in Reference 10. It was also noted in Reference 10 that with the inclusion of periodically varying coefficients, system motions are defined by a form which involves the term $\sum_{n=-\infty}^{\infty} a_n e^{i(\omega+n\Omega)t}$ such that the value of ω is not uniquely determinate, since $\omega \pm n\Omega$ will also satisfy the determinant. Thus, the infinite number of roots to the infinite determinant will consist of the principal values of ω plus all of their harmonics. The roots of Equation (38) in an infinite form as well as in the truncated form exhibit the above-noted behavior. In the truncated form, the number of harmonics of the principal frequencies which are solutions to the determinant of the final matrix are dependent upon the magnitude of Nf.

In the application of Equation (38) to a physical system,

Nf equal to 1 is probably sufficient on the basis of (1) results obtained in a similar, but not as complex dynamic response analysis and (2) consideration of the interharmonic coupling that occurs for umbrella, reactionless, forward cyclic, and backward cyclic blade motion. During use of the dynamic response analysis of Reference 11, the difference in steady response results obtained with and without including the -2/rev and +2/rev effects were slight. In the air resonance modal analysis, developed herein, the harmonics to which the blade motions couple in the various types of blade modes noted above are dependent upon the type of mode such that the truncation procedure does not signicantly affect the results obtained.

In order to provide some insight into the method of developing the final governing matrix equation and the truncation involved, a simple example is presented in Appendix A.

Blade Phasing Assumption Modification and Advantages

If all blades comprising the tail rotor are assumed to be identical and equally spaced azimuthally, the relative behavior of the tail rotor blade can be specified corresponding to the types of basic tail rotor modes possible for the rotor being considered. For example, an umbrella, backward cyclic, forward cyclic, or reactionless blade mode can be specified. With the relative motion of the blades specified, the contributions to the final governing equations provided by blades other than the first blade can be defined in terms of the corresponding contributions of the first blade. This allows the $\left[\overline{T}_{k,n}\right]$ array, as defined in Equation (37), to be reduced in size by the removal of the arrays corresponding to blades other than the first blade such that for the representation shown in Equation (37) the last two rows and columns of arrays are not required. The swashplate to blade coupling array $\left[\overline{SB}_{k,n}\right]_1$ and the blade moment and shears contribution array $\left[\overline{FB}_{k,n}\right]_1$ must be altered to include the contributions of the additional blades. In the case of a gimballed or teetering rotor, modifications are also necessary in the blade array $\left[\overline{BB}_{k,n}\right]_1^1$ since with a phasing relationship specified, the slope related boundary condition equations corresponding to pinned blade root conditions may be automatically satisfied for certain situations and must be replaced with moment

related equations.

The assumption of identical blades allows the blade transfer arrays and blade discontinuity column arrays of the mth blade to be related to those of the first blade. This relationship is exemplified by

$$\left[\bar{B}_{k,n}\right]_m^i = \left[\bar{B}_{k,n}\right]_1^i e^{i(n-k)\phi_m} \text{ and}$$

$$\left[\bar{b}_{k,n}\right]_m^i = \left[\bar{b}_{k,n}\right]_1^i e^{i(n-k)\phi_m}$$

This exponential relationship results due to the introduction of the exponential term when the first aerodynamic transfer matrix is applied and is maintained by subsequent transfer matrix application. On insertion of the relationships specified above into Equation (13) for the blade root variables, the expression

$$\left\{\bar{S}_k\right\}_m^{NS} = \sum_{n=-Nf}^{Nf} e^{i(n-k)\phi_m}\left[\left[\bar{B}_{k,n}\right]_1^{NS}\left\{\bar{S}_n\right\}_m^* - \left\{\bar{b}_{k,n}\right\}_1^{NS}(\overline{\Delta 1}_n)_m - \left\{\bar{c}_{k,n}\right\}_1^{NS}(\overline{\Delta 2}_n)_m - \left\{\bar{d}_{k,n}\right\}_1^{NS}(\overline{\Delta 3}_n)_m\right] \quad (39)$$

is obtained.

The relationship of the mth blade tip unshifted state variables to the 1st blade tip unshifted state variables (corresponding to the k = 0 equations) can be defined by the form

$$\left\{\bar{S}_0\right\}_m^* = \left\{\bar{S}_0\right\}_1^* e^{-iNps\phi_m}$$

where Nps is an integer denoting the type of relative blade motion. In particular, for four blades, Nps = 1, 0, 1, and 2 corresponds to backward cyclic, umbrella, forward cyclic, and reactionless type modes, respectively. It can be shown that this expression can be extended to $\left\{\bar{S}_n\right\}_m^* = \left\{\bar{S}_n\right\}_1^* e^{-i(n+Nps)\phi_m}$ for the n frequency shifted tip vector variables. The same type of relationship is valid for the blade discontinuity variables. Thus, Equation (39) can be altered to a form in

which the blade state variables at the blade root for the mth blade can be defined in terms of the variables for the first blade. This form is

$$\left\{\bar{S}_k\right\}_m^{NS} = \sum_{n=-Nf}^{Nf} e^{-i(Nps+k)\phi_m}\left[\left[\bar{B}_{k,n}\right]_1\left\{\bar{S}_n\right\}_1^* - \left\{\omega_{k,n}\right\}_1^{NS}\left(\overline{\Delta 1}_n\right)_1 - \left\{\bar{c}_{k,n}\right\}_1^{NS}\left(\overline{\Delta 2}_n\right)_1 - \left\{\bar{d}_{k,n}\right\}_1^{NS}\left(\overline{\Delta 3}_n\right)_1\right]. \quad (40)$$

The blade root moment and shear state variable terms involved in Equation (17) can be expressed by utilizing their definitions from Equation (40) and the characteristic that

$$\sum_{m=1}^{Nb} e^{-i(Nps+k)\phi_m} = Nb \quad (Nps+k) = 0, Nb, -Nb, \text{ etc})$$

$$\sum_{m=1}^{Nb} e^{-i(Nps+k)\phi_m} = 0 \quad (Nps+k) \neq 0, Nb, -Nb, \text{ etc})$$

This exponential dependency results since the integer shifts, in addition to the k shift, cancel the $e^{i\phi_m}$ and $e^{-i\phi_m}$ dependencies in Equation (17). Thus, with the phasing assumption the $\left[\overline{FB}_{k,n}\right]_1$ as defined previously will be multiplied by Nb if Nps+k is equal to zero or plus or minus an integer multiple of Nb, and will otherwise be an array consisting of zeroes.

In addition, the swashplate to blade coupling term in Equation (29) is represented as a summation over the forces applied by each blade $(\bar{P}_k)_m$. The $(\bar{P}_k)_m$ definitions, when blade phasing is assumed, can be related to the $(\bar{P}_k)_1$ definition in a manner similar to that employed for the moment and shear terms above. This exponential relationship, in combination with the exponential $e^{-iq\phi_m}$ term involved in the summation, results in a summation over m of $e^{-i(Nps+k+q)\phi_m}$ which is defined as Nb if Nps+k+q equals zero of plus or minus an integer multiple of Nb, and equal to zero otherwise. Thus, the $\left[\overline{SB}_{k,n}\right]_1$ array is defined previously will be modified such

that a row for which Nps+k+q = 0, -Nb, +Nb, etc., is multiplied by Nb; and if this condition is not met, then the row is altered to consist of zeroes.

The previous discussion presented the alterations required for the assumption of specified blade phasing relationships for the types of tail rotors allowed, with the exception of the modifications to the main blade array $\left[\overline{BB}_{k,n}\right]_1^1$. These modifications are required for gimballed and teetering rotor systems due to the modified slope boundary condition equations automatically being satisfied for certain conditions on the assumption of blade phasing. For a gimballed tail rotor, the second and sixth rows of $\left[\overline{BB}_{k,n}\right]_1^1$ represent the n frequency shifted contribution to $(\overline{\phi x}_1)_k^{NS} + i(\overline{\phi y}_1)_k^{NS}$ and $(\overline{\phi x}_1)_k^{NS} - i(\overline{\phi y}_1)_k^{NS}$, respectively. It can be shown that with the assumption of blade phasing, the first term being zero is a valid boundary condition equation for Nps+k-1 not equal to zero or plus or minus an integer multiple of the total number of blades Nb such that the second row of the blade array would be unaltered. If this condition is not satisfied, the contributions of this term must be replaced by the representation of the n frequency shifted contribution to $(\overline{T}_1)_k^{NS} + i(\overline{My}_1)_k^{NS}$. which is equal to zero if Nps+k-1 equals zero of plus or minus an integer multiple of Nb. The second term being zero is a valid boundary condition equation for Nps+k+1 not equal to zero or plus or minus an integer multiple of Nb such that the sixth row of the blade array would be unaltered. If Nps+k+1 is equal to zero or plus or minus an integer multiple of Nb, then the sixth row must be replaced by the representation for the n frequency shifted contribution to $(\overline{T}_1)_k^{NS} - i(\overline{My}_1)_k^{NS}$ which is equal to zero.

For a teetering rotor, the same type of modification occurs for only the sixth row of the blade array with only $-i(\overline{\phi y}_1)_k^{NS} = 0$ and $-i(\overline{My}_1)_k^{NS} = 0$ conditions involved.

The advantages of utilizing the blade phasing assumption are significant. Basically, the size of the $\left[\bar{T}_{k,n}\right]$ matrices is significantly reduced. For instance, for a four-bladed rotor attached to a fuselage-tailboom-fin structure, and a swashplate with Nmax equal to one, the $\left[\bar{T}_{k,n}\right]$ matrix would be a 45 x 45 matrix which, when put in final form for N_f equal to one, would result in a final governing matrix that would be 135 x 135. On the other hand, with the phasing assumption, the $\left[\bar{T}_{k,n}\right]$ matrix would only be an 18 x 18 matrix and the final governing matrix 54 x 54. The smaller size of these arrays allows a significant reduction in running time, primarily dependent on the solution of the final governing matrix, as well as a greater accuracy of results; since the larger the array, the more error in solution values. Also, if only the blade phasing assumption is to be used, the dimensioning of these and related arrays can be based on that required for blade phasing such that a significant reduction in core requirements is obtained.

EIGENVALUE AND EIGENVECTOR SOLUTION METHOD

The solution method applied to the final governing matrix equation to obtain the eigenvalues and eigenvectors is based on an approach referred to in Reference 9 as the modified transfer-matrix method. The primary purpose of the method used is to avoid the numerical accuracy problems due to the taking of small differences of large numbers, which generally occurs in transfer matrix techniques, particularly when the frequency determinant is computed for higher natural frequencies. The solution method employed iterates the eigenvector corresponding to the unknowns of the system simultaneously with the iteration on the eigenvalue until the desired degree of convergence of the eigenvalue is achieved.

The final governing matrix equation can be expressed in the form $\left[\bar{A}_{ij}\right]\left\{\bar{X}_j\right\} = 0$, where $\left[\bar{A}_{ij}\right]$ consists of the $\left[\bar{T}_{k,n}\right]$ matrices located in the form shown in Equation (38) and $\left\{\bar{X}_j\right\}$ consists of the $\left\{\bar{q}_n\right\}^*$ column vectors located in the form shown in Equation (38). The $\left\{\bar{X}_j\right\}$ column vector can be

defined in general as $\{\bar{X}_j\} = \{\bar{\lambda}_j\} + \{\bar{\varepsilon}_j\}$ where $\{\bar{\lambda}_j\}$ represents trial values for the unknown eigenvector and $\{\bar{\varepsilon}_j\}$ represents corrections to the trial eigenvector. By substitution of this definition for $\{\bar{X}_j\}$ into the equation involving $[\bar{A}_{ij}]$, the expression $[\bar{A}_{ij}]\{\bar{\varepsilon}_j\} = -[\bar{A}_{ij}]\{\bar{\lambda}_j\} = -\{\bar{F}_j\}$ results from which $\{\bar{\varepsilon}_j\} = -\{\bar{\lambda}_j\}$ or $\{\bar{X}_j\} = 0$ by premultiplication of both sides of the matrix equation by the inverse of $[\bar{A}_{ij}]$. This problem of indeterminate equations is overcome by normalization of a particular $\{\bar{X}_j\}$ quantity to a value of unity such that the corresponding $\{\bar{\lambda}_j\}$ and $\{\bar{\varepsilon}_j\}$ quantities are equal to unity and zero, respectively. This allows the removal of the column of $[\bar{A}_{ij}]$ which multiplies the particular $\bar{\varepsilon}_j$ which is zero and the row of $[\bar{A}_{ij}]$ corresponding to the j index of the $\bar{\varepsilon}_j$ which is zero such that a reduced array $[\bar{A}'_{ij}]$ results. Also, the element of $\{\bar{\varepsilon}_j\}$ and $\{\bar{F}_j\}$ corresponding to the row removed from $[\bar{A}_{ij}]$ is removed such that the reduced column arrays $\{\bar{\varepsilon}'_j\}$ and $\{\bar{F}'_j\}$ result. Thus, the resulting equation relating the correction values and trial values for the unknowns is $[\bar{A}'_{ij}]\{\bar{\varepsilon}'_j\} = -\{\bar{F}'_j\}$, which on premultiplication by the inverse of $[\bar{A}'_{ij}]$ provides the expression for $\{\bar{\varepsilon}'_j\}$ as

$$\{\bar{\varepsilon}'_j\} = -[\bar{A}'_{ij}]^{-1}\{\bar{F}'_j\} \qquad (41)$$

The validity of this equation can be demonstrated by considering a simple 3 x 3 final governing matrix equation expressed as

$$\begin{bmatrix} \bar{A}_{11} & \bar{A}_{12} & \bar{A}_{13} \\ \bar{A}_{21} & \bar{A}_{22} & \bar{A}_{23} \\ \bar{A}_{31} & \bar{A}_{32} & \bar{A}_{33} \end{bmatrix} \begin{Bmatrix} \bar{X}_1 \\ \bar{X}_2 \\ \bar{X}_3 \end{Bmatrix}$$

which on replacing the $\{\bar{X}_j\}$ by $\{\bar{\lambda}_j\} + \{\bar{\varepsilon}_j\}$ provides the expression

$$\begin{bmatrix} \bar{A}_{11} & \bar{A}_{12} & \bar{A}_{13} \\ \bar{A}_{21} & \bar{A}_{22} & \bar{A}_{23} \\ \bar{A}_{31} & \bar{A}_{32} & \bar{A}_{33} \end{bmatrix} \begin{Bmatrix} \bar{\varepsilon}_1 \\ 0 \\ \bar{\varepsilon}_3 \end{Bmatrix} = - \begin{bmatrix} \bar{A}_{11} & \bar{A}_{12} & \bar{A}_{13} \\ \bar{A}_{21} & \bar{A}_{22} & \bar{A}_{23} \\ \bar{A}_{31} & \bar{A}_{32} & \bar{A}_{33} \end{bmatrix} \begin{Bmatrix} \bar{\lambda}_1 \\ 1 \\ \bar{\lambda}_3 \end{Bmatrix}$$

where the quantity $\bar{X}_2$ was considered to be the unknown variable normalized to unity. Removal of the second row of this equation and the quantities in the second column of the $[\bar{A}_{ij}]$ matrix involved in the terms on the left side of this equation (which are quantities multiplying zero) provides the expression

$$\begin{bmatrix} \bar{A}_{11} & \bar{A}_{13} \\ \bar{A}_{31} & \bar{A}_{33} \end{bmatrix} \begin{Bmatrix} \bar{\varepsilon}_1 \\ \bar{\varepsilon}_3 \end{Bmatrix} = - \begin{bmatrix} \bar{A}_{11} & \bar{A}_{12} & \bar{A}_{13} \\ \bar{A}_{31} & \bar{A}_{32} & \bar{A}_{33} \end{bmatrix} \begin{Bmatrix} \bar{\lambda}_1 \\ 1 \\ \bar{\lambda}_3 \end{Bmatrix}$$

Premultiplication of both sides of this expression by the inverse of the array on the left side of the expression provides the following relationship:

$$\begin{Bmatrix} \bar{\varepsilon}_1 \\ \bar{\varepsilon}_3 \end{Bmatrix} = - \begin{bmatrix} \bar{A}_{11} & \bar{A}_{13} \\ \bar{A}_{31} & \bar{A}_{33} \end{bmatrix}^{-1} \begin{bmatrix} \bar{A}_{11} & \bar{A}_{12} & \bar{A}_{13} \\ \bar{A}_{31} & \bar{A}_{32} & \bar{A}_{33} \end{bmatrix} \begin{Bmatrix} \bar{\lambda}_1 \\ 1 \\ \bar{\lambda}_3 \end{Bmatrix}$$

which shows in general that the $\bar{\varepsilon}_j$ quantities are not necessarily equal to the $\bar{\lambda}_j$ quantities.

The object of the solution method is to obtain a value for the eigenvalue for which the determinant of $\left[\bar{A}_{ij}\right]$ and the $\left\{\bar{\varepsilon}_j'\right\}$ quantities approach zero. This method consists of considering trial eigenvalues until the convergence criteria based on the changes in trial eigenvalues are satisfied or the number of allowed iterations have occurred. In particular, for a given starting trial eigenvalue and a set of parameters required for the analysis, the determinant of $\left[\bar{A}_{ij}\right]$ and the correction quantities $\bar{\varepsilon}_j$ by Equation (41) are determined based on the $\left\{\bar{\lambda}_j\right\}$ trial eigenvector quantities all being equal to unity. The $\bar{\varepsilon}_j$ quantities are then added to the $\bar{\lambda}_j$ quantities to define a new $\left\{\bar{\lambda}_j\right\}$. The new trial eigenvalue is obtained by increasing the starting trial eigenvalue by a specified percentage and a new determinant of $\left[\bar{A}_{ij}\right]$ and a new set of $\bar{\varepsilon}_j$ quantities calculated where the latter are used to update the $\left\{\bar{\lambda}_j\right\}$. From this point on the new trial eigenvalues are based upon a slope interpolation scheme based on the previous two eigenvalues and corresponding determinant values of the form

$$s_{NE} = s_{CU} - \bar{\Delta}_{CU}\,(s_{CU} - s_{LA})/(\bar{\Delta}_{CU} - \bar{\Delta}_{LA})$$

where $\bar{\Delta}$ denotes the determinant value of $\left[\bar{A}_{ij}\right]$ and CU, LA, and NE subscripts denote the values for the iteration just completed, the iteration just prior to the one just completed, and the next iteration, respectively. For the new eigenvalue the determinant and set of $\bar{\varepsilon}_j$ are calculated and in turn are used to update the $\left\{\bar{\lambda}_j\right\}$. After each iteration after the first two trial eigenvalues have been used a convergence criteria test is applied such that a sufficient eigenvalue and eigenvector have been obtained if $\left|(s_{NE} - s_{CU})/s_{CU}\right| \leq .1^{Mer}$ where $|\ |$ denotes the complex absolute value and Mer is an integer defining the convergence limit desired. With the

satisfaction of the convergence criteria or occurrence of maximum number of iterations allowed, the blade and fuselage-tailboom-fin structure transfer matrix procedures are applied to the corresponding resultant eigenvector to obtain the state variables at the inboard end of each lumped parameter section in the section local coordinate systems which are then transformed to the disc plane for the blades and fixed coordinate system for the fuselage-tailboom-fin structure.

The resultant eigenvalue and eigenvector values represent the behavior of the total system investigated. The analysis developed and the solution thereof provide the fundamental and harmonic coefficients in a complex variable form of the real-time swashplate, blade, and fuselage-tailboom-fin state variables. The fuselage-tailboom-fin structure state variables at the ith section, after it has been transferred across as a function of time, can be expressed in the general form

$$f(t)^{(i)} = \sum_{p=-\infty}^{\infty} (X_p^{(i)} + iY_p^{(i)})\, e^{\sigma t}\, e^{i(\omega t + p\Omega t)} \qquad (42)$$

where $X_p^{(i)}$ and $y_p^{(i)}$ are the real and imaginary part, respectively, of the state variable of interest and p is an integer which when positive in value denotes an oscillatory behavior at a frequency $p\Omega$ radians per second higher than that corresponding to ω. A negative value of k denoting the k frequency shifted Laplace transformed state variables in the development of the analysis previously discussed corresponds to a positive value of p of the same absolute value. Also, in the resulting computer program the output of the state variable is in the order of p going from positive to negative where the headings are in terms of k/rev and not p/rev. By conversion of the exponential function with the imaginary argument in Equation (42) to a sine and cosine equivalent representation, the form of this equation can be modified to

$$f(t)^{(i)} = \sum_{p=-\infty}^{\infty} R_p^{(i)}\, e^{\sigma t} \cos(\omega t + p\Omega t + \beta_p^{(i)}) \qquad (43)$$

where $R_p^{(i)} = \sqrt{(X_p^{(i)})^2 + (Y_p^{(i)})^2}$ and $\beta_p^{(i)} = \arctan(Y_p^{(i)}/X_p^{(i)})$.

To be practical, the summation can be truncated to the range -Nf to Nf.

The above state variable representation can be modified to represent a blade state variable at the inboard end of the ith section when the blade phasing assumption is not employed by adding m subscripts to all blade-related variables. The behavior of the mth blade is relative to the rotating coordinate system of the mth blade. Thus, at t equal to zero, the value of a state variable for the mth blade defined by the form of Equation (43) is for the blade ϕ_m radians azimuthally ahead of the fixed reference blade location. The variable ϕ_m is not involved in the nonphased blade state variable definition of the form of Equation (43) since the contribution of this variable has been included in the blade tip state variables by the analysis developed.

For the case of blade phasing, state variable coefficients are obtained for the first blade such that the definition for additional blades is obtained by use of the phasing relationship $\left\{\bar{S}_n\right\}_m^{(i)} = \left\{\bar{S}_n\right\}_1^{(i)} e^{i(-n-Nps)\phi_m}$. From this relationship the p related coefficients for a state variable of the mth blade can be defined as the corresponding state variable of the first blade multiplied by $e^{i(p-Nps)\phi_m}$. Thus, for blade phasing the representation used for a fuselage-tailboom-fin state variable would be modified with the blade related quantities having a subscript of 1 except for $f(t)^{(i)}$ which would have an m subscript added and $p\Omega t$ replaced with $p(\Omega t+\phi_m) - Nps\phi_m$. The resulting mth blade state variables are referenced to their own rotating coordinate system as discussed for the blades without phasing assumption.

The swashplate rotating frame displacement variable $w_\ell(t)$ can be defined in the same form of representation as for the fuselage-tailboom-fin structure with $f(t)^{(i)}$ replaced by $w_\ell(t)$ and $X_p^{(i)}$ and $Y_p^{(i)}$ replaced by $X_{\ell,p}$ and $Y_{\ell,p}$, respectively, which correspond to the coefficients of ℓth spatial harmonic of swashplate motion in the rotating swashplate coordinate system at a frequency of $\omega + p\Omega$.

The basic iterative method of solution used to obtain the solution eigenvalues and eigenvectors may require reasonably good guesses for the starting eigenvalue in order to achieve the required convergence within a reasonable number of iterations or to avoid converging on an eigenvalue obtained

previously. To aid in estimating these initial values, a scanning procedure was developed to automatically estimate the starting eigenvalues for the basic iterative method of solution within a range of stability and frequency values. Basically, the desired frequency and stability value ranges are divided into incremental steps. For each frequency, the stability value is stepped from the lower range limit to the upper range limit with the determinant of the $\left[\bar{A}_{ij}\right]$ matrix determined for each stability value. If the imaginary part of the determinant value changes sign during the stepping of the stability value, the stability value and real part of the determinant corresponding to the imaginary part of the determinant being zero in value are obtained by interpolation. The resulting real parts of the determinant corresponding to the stability values which yield imaginary parts of the determinant close to zero are then scanned with respect to frequency values to determine if changes in sign of the real part of the determinant occur. If so, then the stability and frequency values corresponding to the real and imaginary parts of the determinant close to zero in value are determined by interpolation and can be utilized as starting values for the normal iterative solution method. This procedure is not foolproof, however, since a reasonable step size of both frequency and stability value is required to avoid missing possible roots to the analysis developed.

DESCRIPTION OF OVERALL COMPUTER PROGRAM

The analysis discussed previously was utilized to develop a digital computer program for the determination of air resonance eigenvalues and corresponding mode shapes of a tail rotor attached to a flexible fuselage-tailboom-fin structure. The resultant computer program which was developed for use on IBM 360 systems consists of several basic steps:

1. input of system parameters,
2. determination of intermediate terms,
3. blade transfer matrix application,
4. fuselage-tailboom-fin structure transfer matrix application,
5. construction of $\left[\bar{T}_{k,n}\right]$ arrays and trial eigenvector forcing functions to yield $\left[\bar{A}_{ij}\right]$ and $\left\{\bar{F}_{j}\right\}$ arrays,
6. solution for determinant and eigenvector correction array $\left\{\bar{\varepsilon}_{j}\right\}$,
7. trial eigenvalue scanning procedure,
8. main program logic control.

These steps will be clarified to various degrees. The system parameters, which include model structural parameters necessary to define the model configuration of interest, environmental parameters necessary to define the operational environment of the model, program logic control parameters such as starting eigenvalues, convergence criteria and scanning procedure variables, and aerodynamic data, are required as input for the program. All of this data except aerodynamic data is read into a storage array by defining the variable array location and the variable value in floating point form. This array of 2800 elements is constructed by utilizing the first 200 elements for storage of environmental, logic control, and model representation control parameters; the next 2000 elements for storage of blade and fuselage-tailboom-fin structure sectional data (50 elements per section); and the last 600 elements for a radial and azimuthally varying induced velocity distribution, if desired. The concept of this input form was to eliminate the necessity of

a defined order of input such that input cards out of order would not result in erroneous results or aborted computer runs and also to allow several model configurations to be considered consecutively with only system variables inputted for those that altered from the previous configuration. During parametric investigations with the program, an additional capability of this form of input was utilized. This capability is the allowance of a variable to be modified to a new value after previously being defined in the same set of input, such that a basic input deck followed by input modifications can be used for the specific configuration of interest. The airfoil coefficient tables are required as input for each configuration.

As a mechanism for reducing running time of the program for a system configuration, some of the terms not a function of the Laplace transform variables and coefficients multiplying Laplace transform variables (intermediate terms) are computed and stored so that these calculations do not have to be repeated for each iteration eigenvalue.

The blade transfer matrix applications consist of two similar forms; that used during the iterative procedure to obtain solution eigenvalues and eigenvectors or scanning procedure, and that used to obtain the blade state variables at the inboard end of each blade section. During the iterative procedure, the representation of the blade variables at the hub - in terms of the blade tip and discontinuity unknowns - is obtained for each trial eigenvalue by successive multiplication of the initial blade tip associated transfer matrices and discontinuity columns by the individual lumped parameter characteristic transfer arrays as each characteristic is crossed in transferring from blade tip to hub. The individual transfer matrices are obtained by utilizing the stored intermediate terms and the value of the trial eigenvalue. Also, during the application of transfer matrices, the representation of the blade state variables at the discontinuity locations, as required for the blade discontinuity equations, is stored.

A trial eigenvalue is taken to be a solution eigenvalue when either the difference between the trial eigenvalue and the next predicted eigenvalue satisfies the convergence criteria or the trial eigenvalue is that of the last allowed iteration. When the solution eigenvalue is obtained, the blade transfer matrix procedure is repeated for the solution eigenvalue in the same manner as during an iteration, except that the associated transfer matrices and discontinuity columns obtained at the inboard end of each section are applied to the pertinent solution eigenvector variables to

define the frequency unshifted and shifted section state variables. The solution eigenvector is equivalent to the sum of the trial eigenvector and correction eigenvector associated with the iteration using the solution eigenvalue.

The fuselage-tailboom-fin structure transfer matrix applications are similar in concept to the blade transfer matrix application, except that the transfer process proceeds in the direction toward the tail rotor, the individual lumped parameter transfer matrices are simpler for certain characteristics, and interharmonic coupling is not involved. The representation of the shifted and unshifted blade and fuselage-tailboom-fin structure state variables for a trial eigenvalue provides the majority of terms necessary in the $\left[\bar{T}_{k,n}\right]$ matrices as defined in Equation (37). The remaining terms, which are related to the swashplate representation and discontinuity definition equations, can be obtained by direct substitution of just the configurational parameters or in combination with the matrix definitions of blade and fuselage-tailboom-fin structure variables. The numerical construction of the $\left[\bar{T}_{k,n}\right]$ matrices is dependent on the degrees of freedom of the hub-rotor shaft interface, as previously discussed. The $\left[\bar{T}_{k,n}\right]$ matrices and the trial eigenvalue are used to generate the $\left[\bar{A}_{ij}\right]$ and $\left\{\bar{F}_{j}\right\}$ arrays.

The determinant of the final matrix and the correction vector $\left\{\bar{\epsilon}_{j}\right\}$ for a given trial eigenvalue are obtained simultaneously by utilizing a sophisticated triangularization technique. This technique operates on the total final governing matrix and trial eigenvector forcing function in a manner such that an iterative procedure to obtain the determinant and a matrix inversion for the eigenvector correction array are not required. This technique has proven to be much faster in execution time and more accurate than the technique that is utilized for a similar matrix manipulation in Reference 3. It should be noted that the matrix solution technique is carried out in double precision.

The scanning procedure to obtain initial starting eigenvalues, as described previously, has been incorporated into the program mainline as an independent control segment such that

it is bypassed if the scanning procedure is not desired. If the scanning procedure is utilized, the analysis equivalent to a normal iteration loop is carried out for each eigenvalue of a grid defined by the specification of the lowest stability and frequency values to be considered, the size of the steps in stability and frequency values, and the number of stability and frequency steps to be taken to obtain the corresponding determinant values. An interpolation scheme is employed to determine possible roots to the polynomial which the final matrix represents. These possible roots are then used as starting values for the remaining control segment of the program mainline pertaining to the determination of solution eigenvalues and corresponding eigenvectors and mode shapes.

The main program logic control initially determines, on the basis of input parameters, whether or not the scanning segment is to be employed prior to the iteration control segment; and, if so, specifies the operational procedure to be employed for scanning. The main program logic control then, on the basis of the number of starting eigenvalues inputted or from the scanning procedure, convergence criteria, and iteration limits, specifies the operational procedure to be employed for the iteration control segment. The overall iterative system flow for the program is depicted in Figure 10.

Although the mathematical analysis for the representation of coupled helicopter/tail rotor systems was developed for nonidentical blades arbitrarily spaced azimuthally, the development of the computer program analytical coding was based on the assumption of identical blades arbitrarily spaced azimuthally. This assumption was employed to avoid the higher core and tape (or disc) storage requirements necessary to store and manipulate the blade-related information arrays for nonidentical blades. Since this computer program will be primarily used in the design or modification of coupled tail rotor systems in which the blades are constructed as close to identical as possible, the assumption of identical blades will be sufficient for most applications. The program modifications which are required for considering rotor systems with nonidentical blades, whether due to damage (e.g., ballistic damage or partial blade failure) or design (e.g., variable geometry rotor with nonidentical sets of blades), are not complicated and can be easily added to the program. The computer program blade representational capabilities were further limited by the use of two sets of restrictions on the dimension size of program array variables. The first set of dimensional restrictions limits the maximum number of arbitrarily azimuthally spaced blades that can be considered without use of the assumption of blade phasing to four by restricting the size of the control rod-related arrays, the

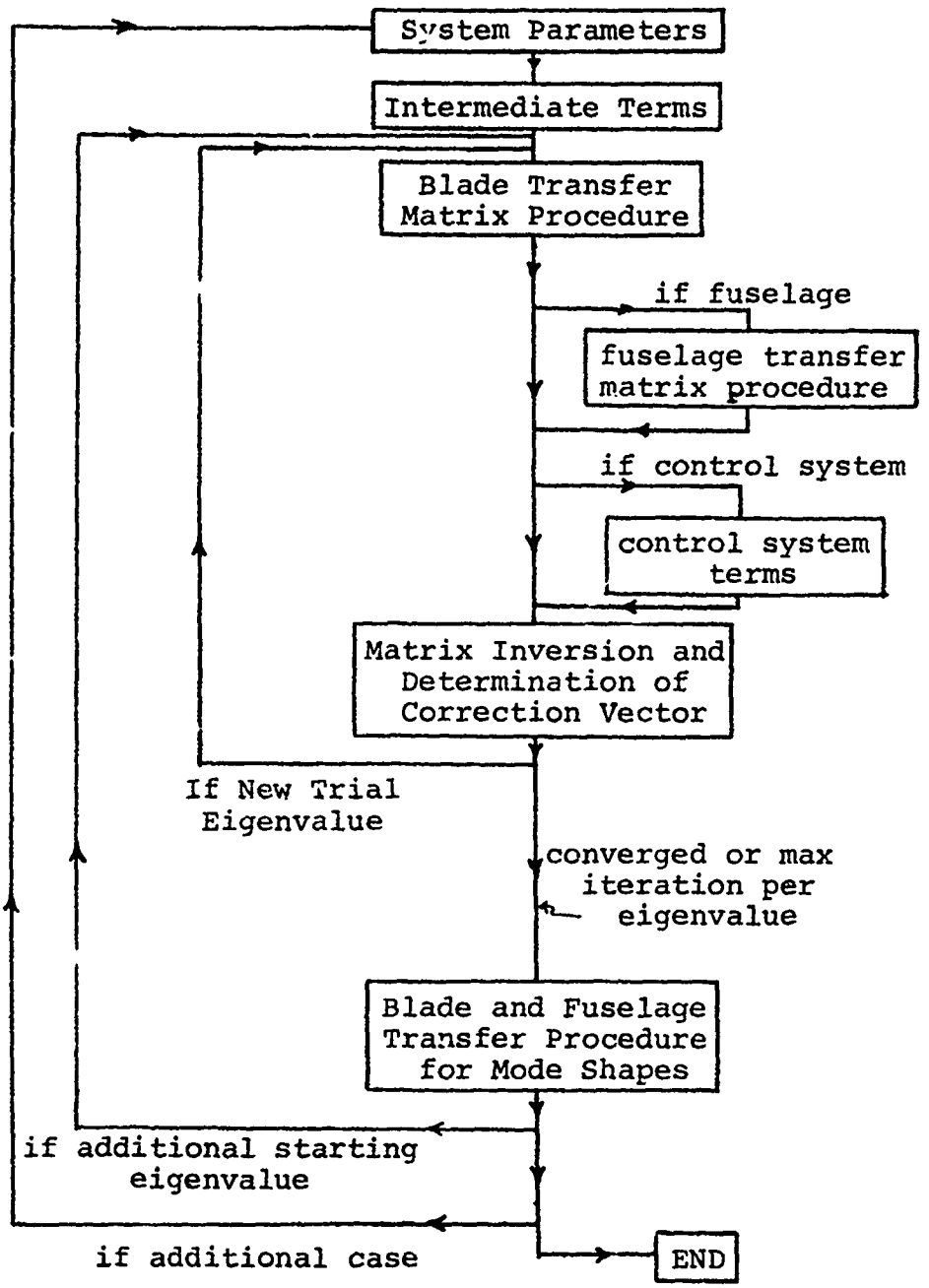

Figure 10. Overall Iterative System Flow.

blade azimuthal position-related arrays, and the arrays associated with the solution of the final matrix. The second set of dimensional restrictions resulted from the reduction of the size of the arrays associated with the final matrix solution to that required on the assumption of blade phasing, which allows the consideration of a rotor consisting of an arbitrary number of identical blades equally spaced azimuthally. This latter set was implemented since most tail rotor systems do consist of equally spaced identical blades, for which the assumption of blade phasing provides an adequate representation of the air resonance behavior without the penalty of higher core requirements and running time. If this restriction is not acceptable for a specific helicopter/tail rotor configuration which has identical blades but unequal spacing, only the dimensions need to be modified for the computer program to be applicable.

High core requirements result due to the necessity of employing double precision real and complex variables in the computer program to achieve convergence and accurate solution eigenvalues, eigenvectors, and mode shapes on an IBM 360 system. The accuracy problems are primarily associated with the mode shapes, since slight inaccuracies in the eigenvalue and eigenvector are further distorted as the transfer matrix procedure is applied on the final pass for the mode shapes; that is, as the procedure progresses along the structure of interest, the mode shapes become more inaccurate. Thus, in order to achieve accurate mode shapes, double precision is required. To reduce core requirements, an overlay structure was incorporated into the program; with the result that for smaller final governing matrices, the combination of the main program and the blade transfer procedure subroutines set the core requirement - as in the case of NF = 1 and blade phasing. However, with NF = 1 and without blade phasing for more than one blade, the final governing matrix manipulation portion for obtaining the determinant and eigenvector correction array and the main program determine the core requirements. Also, the larger the final matrix, the longer the running time. Matrix multiplication subroutines have been utilized in assembly language form to reduce matrix multiplication time.

GENERAL APPLICATION OF PREDICTIVE PROGRAM TO A FULL-SCALE HELICOPTER

In order to investigate the effects of various system parameters on the air resonance frequencies, mode shapes, and stability characteristics of a full-scale helicopter tail rotor system and its supporting structure, and to establish the ability of the resultant predictive program, an overall full-scale helicopter model was employed which is representative of a UTTAS helicopter configuration. This system configuration has a tail rotor consisting of four identical and equally spaced blades of the flexstrap type whose collective pitch is controlled by a swashplate control system. The tail rotor drive shaft is attached to a tail rotor gearbox which is mounted to the fin in such a manner that the mounting flexibility can be represented by mutually orthogonal spring-damper units of the torsional type. The remaining portion of the overall model consists of the fuselage-tailboom-fin structure.

The basic analytical representation models for various components of the overall helicopter system employed in the parametric sensitivity analysis were based upon the form required by the analysis developed and coded into a computer program which has been discussed previously. Thus, the basic flexstrap blade model representation (including pitch horn) consisted of a lumped parameter model representation of the structural characteristics of the full-scale tail rotor flexstrap blade configuration. The blade collective pitch, coning, and uniform induced velocity values corresponding to the desired thrust values were obtained by use of the simplified mathematical representation of helicopter rotor behavior presented in Reference 12. In the determination of these thrust related values, an equivalent flap hinge was assumed, and the contributions of the built-in linear twist included. The blade pitch radial distributions were obtained by proper superposition of the resultant collective pitch values and the built-in linear twist. The prelag was assumed to be the built-in geometric sweep of the blade configuration.

The basic fuselage-tailboom-fin structure model representation consisted of a lumped parameter model representation of the full-scale fuselage-tailboom-fin structure configuration without inclusion of stabilizer fin surface. The basic swashplate control system was represented by the definition of the parameters required in the swashplate related analysis, such as stiffnesses and geometric parameters. For the tail rotor of interest, only collective flexibility of the swashplate was necessary. This was represented by the collective

support spring. The basic control rods were represented with the necessary values for orientation and length corresponding to that representative of the UTTAS configuration. A slight axial flexibility of the control rods was allowed. The value for the drive shaft torsional flexibility was taken such that the frequency of torsional oscillation of the tail rotor inertia was approximately 20 radians/second. The basic tail rotor gearbox flexibility in two orthogonal directions was taken such that the rocking motion in the two directions due to hub mass and inertia was approximately 106 radians/second (i.e., the gearbox was isotropically supported).

The various system parameters whose effect on the air resonance modal behavior of the tail rotor system and/or fuselage-tailboom-fin structure was investigated may be separated into flight parameter and structural support parameter groups. The former group consists of parameters such as tail rotor rotational speed, advance ratio, collective pitch, coning, and induced velocity field. The latter group consists of the various structure parameters such as drive shaft torsional flexibility, gearbox support flexibility, swashplate control system flexibility, and fuselage-tailboom-fin structure flexibility. The parametric investigations for hover to varying degrees were concerned with:

1. The effect of rotational speed and aerodynamic thrust (thereby collective pitch, induced velocity, and coning values) on the cantilevered blade behavior.

2. The effect of the above parameters with nominal (basic) drive shaft torsional flexibility included (reference configurations) on blade behavior.

3. The effect of the addition of tail rotor gearbox support flexibilities, nominal (basic) and others, to some of the reference configurations in regard to blade behavior.

4. The effect of the addition of swashplate control system collective flexibilities, nominal (basic) and other, to some of the reference configurations in regard to blade behavior.

5. The effect of both the addition of tail rotor gearbox support flexibility and swashplate control system collective flexibility to some of the reference configurations in regard to blade behavior.

6. The modal behavior of the nominal (basic) and a

softer fuselage-tailboom-fin structure and the effect of the addition of these fuselage-tailboom-fin structure configurations to some of the reference configurations in regard to fuselage-tailboom-fin structure and blade behavior.

7. The effect of inclusion of a flexible fuselage-tailboom-fin structure, swashplate control system collective flexibility, and tail rotor gearbox flexibility on a reference configuration (total system) in regard to both fuselage-tailboom-fin structure and blade behavior.

The parametric investigations for forward flight (advance ratios greater than zero) to varying degrees were concerned with:

1. The effect of advance ratio, rotational speed, drive shaft torsional flexibility, and thrust (thereby collective pitch, inducity and coning values) on the cantilevered blade behavior.

2. The effect of the above parameters in combination with the effect of the addition of swashplate control system collective flexibility and tail rotor gearbox support flexibility on the blade behavior (complete forward flight configurations).

3. The effect of the parameters involved in the complete forward flight configurations in combination with the effect of the addition of fuselage-tailboom-fin structure flexibility on the blade and fuselage-tailboom-fin structure behavior.

In the investigation of the effects of advance ratio on the modal behavior of the various tail rotor configurations, two different approaches were taken in regard to the thrust related parameters. The first was to consider the addition of forward flight velocity to hover configurations without altering the thrust related parameters such that the changes in modal behavior of the tail rotor system would be due only to changes in advance ratio. The second approach was to not only consider the addition of forward flight velocity to hover configurations but also to reduce the thrust acting on the tail rotor, since the thrust required from a tail rotor in actual flight decreases as the advance ratio increases. A more realistic thrust for the tail rotor in forward flight was used with the mathematical representation provided by Reference 12 to obtain a modified set of thrust related parameters (collective pitch, coning, and induced velocity values) for

this apprcach. The use of both of these approaches allows the determination of the effect of forward flight velocity, by itself and in combination with a thrust reduction, on the modal behavior of the tail rotor systems of interest.

DISCUSSION OF RESULTS

The setup of the computer program on a computer system and its subsequent execution to carry out a parametric sensitivity analysis regarding the modal behavior of a helicopter configuration provided several results. These results were not only of a numerical nature such as frequencies, stability characteristics, and mode shapes but also provided information pertaining to the computer program operational behavior, limitations and possible future capabilities. These various types of results obtained from use of the computer program will be discussed.

PROGRAM OPERATIONAL RESULTS

Perhaps one of the most relevant results of the program operation was the ease with which personnel at the Fort Eustis computer facility, who were unfamiliar with the computer program and its development, were able to obtain and execute the computer program object module for their specific IBM-360 digital computer system. The object module is constructed as a compiled and link-edited version of the source program which consists of a main program and several subroutines in FORTRAN IV language and matrix multiplication subroutines in assembler language placed in an overlay structure. This overlay structure in its final form minimized core requirements to 250 K for the dimensions utilized. In fact, incompatibilities in program coding capabilities between that required on the computer utilized for developmental purposes and that required for the Fort Eustis computer system did not occur, such that debugging of the computer program on the Fort Eustis computer system was not required. It is believed that the resultant computer program can be put up on other existing IBM-360 computer systems with the same ease. For CDC 6600 computer systems, modifications to the program prior to compiling would be necessary since double precision variables are not required and the overlay structure is defined in a different manner for this type of computer system. These changes are not likely to be difficult.

During program operation, the time required per iteration for various runs was found to be primarily dependent on the degree of interharmonic coupling (controlled by the program variable equivalent to Nf) allowed in the system configuration being investigated. On the Fort Eustis computer system, runs for Nf = 0 (no harmonic coupling) required between 4 to 5 seconds CPU per iteration (calculations involving a trial eigenvalue) such that if convergence is obtained in seven iterations, 28 to 35 seconds CPU time would be required to obtain a solution

eigenvalue, eigenvector and corresponding mode shapes. For Nf = 1 (+ and -1/rev harmonic coupling allowed), runs required approximately 35 seconds CPU time per iteration; such that if convergence is obtained in seven iterations, 175 seconds - or, roughly, 3 minutes - of CPU time would be required to obtain a solution eigenvalue, eigenvector and corresponding mode shapes. These CPU estimates were obtained by dividing the time required for various program runs consisting of several starting eigenvalues by the respective total number of iterations involved in the program run, thus smearing out the CPU time required for determination of the intermediate terms and mode shapes. It should also be noted that these time estimates are based on runs employing the assumption of blade phasing in which the relative motion of the blades is specified.

Based on the degree of inclusion of fuselage representation in various runs, the major portion of the CPU time required for a run is not due to the transfer matrix operations, but rather to the operations involving the solution of the final matrix for its determinant and correction eigenvectors. The transfer matrix operations are fast due to the use of assembler language subroutines for transfer matrix multiplications. The inclusion or exclusion of aerodynamic considerations would not result in a significant difference in running time, since the Fourier analysis involved is done at the program level of generation of intermediate terms which are used directly in the construction of the aerodynamic transfer matrices. The running time is for the most part related to the number of terms involved in the final matrix; such that for Nf = 1, nine times as many terms (nine times as many $\left[\bar{T}_{k,n}\right]$ arrays) are involved as in the Nf = 0 case where, depending on type of mode, the running time is increased by a factor of seven to nine. On a similar basis for four blades without the assumption of blade phasing, the CPU times required for Nf = 0 and Nf = 1 runs would be increased by a factor of seven to nine compared to those mentioned previously, since each array denoted by $\left[\bar{T}_{k,n}\right]$ would increase in size by a factor of nine due to inclusion of arrays associated with the additional blades, as can be noted in Equation (37).

As noted above, the use of the assumption of blade phasing requires significantly less program running time to obtain a solution eigenvalue than when this assumption is not used. The reduction of computer program dimensions allowed by the use of the assumption of blade phasing results in a computer

program requiring significantly less core storage than is required by a program with independent blade representation. In addition to these advantages of the use of the assumption of blade phasing, other advantages were apparent during the execution of the parametric sensitivity analysis. One advantage is associated with the fact that the use of the blade phasing assumption reduces the size of the final matrix and removes from consideration the solution eigenvalues for types of blade modes other than that specified by the assumed blade phasing relationship. For example, if reactionless blade behavior is assumed, the solution eigenvalues for the umbrella, forward cyclic, and backward cyclic modes cannot be obtained unless they are identical to the solution eigenvalue for the reactionless modes. This blade phasing assumption characteristic allows the solution eigenvalues for different types of blade modes occurring in a narrow range of eigenvalues to be determined with less difficulty than would be encountered without use of the assumption of blade phasing.

An additional advantage is that with faster running time on use of the assumption of blade phasing, the air resonance behavior can be obtained for simpler system configurations to provide starting trial eigenvalues for slightly more complex configurations. These solution eigenvalues can then be used as starting values for even more complex configurations. This procedure can be continued until the air resonance behavior of the most complex system of interest which the program is capable of representing is obtained. This procedure, with the use of blade phasing, reduces the amount of engineering judgment required for starting eigenvalues of complex systems such that the likelihood of successful convergence of a run is significantly enhanced.

Air resonance mode shapes resulting from program execution consist of real and imaginary parts, as discussed previously. These complex number mode shapes not only are damped by the $e^{\sigma t}$ term but also are such that the phasing $\beta_p^{(i)}$ associated with the motions at radial stations on the blade differs from station to station. This motion may be described as similar to flutter motion, with phasing of blade motion varying radially, instead of the type of motion obtained from free vibration analyses in which the motions at all radial stations of the blade are in phase. Of course, the analysis developed for this computer program will provide free vibration results if aerodynamics and damping are not involved in the model.

PRESENTATION OF SELECTED NUMERICAL RESULTS

In order to ascertain the effects of various tail rotor and

support structure parameters on the air resonance modal behavior of a four-bladed flexstrap tail rotor system, the resultant computer program was used to determine the air resonance modal behavior of many tail rotor system configurations with varying degrees of complexity. This computational exercise was undertaken to determine the capability of the resultant computer program as a design tool for the development of new, or the modification of existing tail rotor systems by providing adequate prediction of the air resonance modal behavior of these systems.

In the analyses that were conducted, the various system parameters were varied independently or in combination with other system parameters. The general context of the parametric sensitivity investigation was outlined previously. Due to the numerous representational configurations of interest and the number of air resonance modes of reactionless, umbrella, forward cyclic, and backward cyclic types possible for each configuration, the computational effort for the most part was restricted to the first flapwise, first edgewise, and first torsion blade modes and the lowest six fuselage modes. Even though this restriction was employed, an extremely large amount of results were obtained. For the purposes of the report, only the results which show general trends of significant interest will be presented.

Effect of Thrust on Basic Blade Modes

For the basic flexstrap tail rotor configuration in hover, cantilevered to a rigidly supported hub and having a rigid control system, the reactionless, umbrella, forward cyclic, and backward cyclic blade air resonance modes would have identical eigenvalues - with the only difference being due to the relative phasing of the blade mode shapes. The basic (reactionless) first flapwise, first chordwise, and first torsion air resonance modes for three different thrust values and for two rotor speeds are presented in Table 1. The nominal tail rotor thrust and rotor speed were taken as $\sim$ 1300 pounds and $\sim$ 140 radians per second, respectively. The thrust values are not directly used by the program, but rather the associated coning, collective pitch, and uniform induced velocity theoretically related to the thrust value and rotational speed.

The real part of the eigenvalue represents the stability or damping of the blade motion where a negative value denotes a stable blade motion and a positive value denotes an unstable motion. The imaginary part corresponds to the frequency of the blade motion. At each thrust value the real and imaginary parts of the eigenvalues for the first torsion air resonance

TABLE 1
BASIC (REACTIONLESS) AIR RESONANCE MODES

Predominate Mode Type	Theoretical Thrust		
	75% nominal	nominal	126% nominal
first flapwise Ω = nominal	-28.82+201.8i	-28.51+199.2i	-26.28+193.9i
first flapwise Ω = 90% nominal	-25.09+177.4i	-25.06+175.0i	-28.08+173.0i
first chordwise Ω = nominal	3.59+213.3i	4.25+209.3i	5.08+204.3i
first chordwise Ω = 90% nominal	3.07+203.7i	3.64+197.7i	6.22+190.9i
first torsion Ω = nominal	-24.27+329.7i	-25.13+331.9i	-28.09+346.6i

mode decrease with a reduction in rotor speed. The variations of these three types of modes with change in rotor speed provide changes in frequency consistent with the behavior of rotor natural frequency fan plots of most rotor systems, with the exception that mode switching between the first chordwise and first flapwise modes may occur at a higher rotor speed than was investigated. With the inclusion of a better representation of the flexstrap mean orientation, which would provide more coupling of blade motion, this phenomenon may occur at a lower rotor speed and, possibly, in the normal operating rotor speed range.

All three types of blade motion modes (first flapwise, first chordwise, and first torsion) exhibit strong flapwise-chordwise coupling, with the first torsion mode exhibiting strong torsion-flapwise and torsion-chordwise coupling also. This strong coupling is the result of the elastic coupling in the flexstrap blade retention. In general, an increase in thrust increases the coupling noted above for the first flapwise and first chordwise modes, with the greatest effect noted for the lower rotor speed. For the first torsion mode the torsion-flapwise coupling decreased with increasing thrust, whereas the torsion-chordwise coupling increased.

Effect of the Addition of Drive Shaft Torsional Flexibility

The inclusion of drive shaft torsional flexibility in the tail rotor system configuration resulted in a modification of the previous umbrella modes which were coincident with the

basic reactionless modes. The greatest effect of the drive shaft torsional flexibility was on the first chordwise mode. With the nominal drive shaft torsional flexibility defined as that necessary for a shaft torsional frequency of $\sim$ 20 radians per second, based on the hub and rotor inertia, the first chordwise umbrella mode dropped in frequency from that of the basic system first chordwise umbrella mode frequency (same as reactionless) to a value in the neighborhood of 20 radians per second. Since the second chordwise umbrella mode frequency would be expected to increase in value slightly due to the addition of drive shaft torsional flexibility, there would not be a chordwise umbrella mode in the neighborhood of the first basic (reactionless) chordwise frequency. The eigenvalue results obtained for the nominal drive shaft torsional flexibility and the thrust and rotor speed values utilized in the previous section are given in Table 2.

TABLE 2
UMBRELLA AIR RESONANCE MODES WITH INCLUSION OF NOMINAL DRIVE SHAFT TORSIONAL FLEXIBILITY

Predominate Mode Type	Theoretical Thrust		
	75% nominal	nominal	126% nominal
first flapwise Ω = nominal	-25.18+203.7i	-25.02+203.3i	-21.13+197.9i
first flapwise $\Omega \approx$ 90% nominal	-21.64+177.4i	-20.10+175.4i	-20.30+175.4i
first chordwise Ω = nominal	-0.39 +20.8i	-0.50 +19.3i	-0.61 +17.1i
first chordwise $\Omega \approx$ 90% nominal	-0.43 +21.7i	-0.59 +19.8i	-0.82 +15.9i
first torsion Ω = nominal	-22.55+319.0i	-22.90+317.7i	-25.25+328.1i
first torsion $\Omega \approx$ 90% nominal	-20.24+303.0i	-21.28+306.1i	-21.44+302.4i

The effect of an increase in thrust related parameters and rotor speed on the first flapwise, first chordwise, and first torsion air resonance modes can be seen in Table 2. On comparison of these results with those of the reactionless air resonance modes of the basic tail rotor system, the primary effect of the inclusion of drive shaft torsional flexibility is on the first chordwise air resonance umbrella modes. In particular, the frequencies corresponding to this type of

blade mode are reduced to values close to that on which the nominal drive shaft torsional flexibility was based; and the associated stability values are altered such that these modes are slightly stable instead of unstable, as they were for the basic tail rotor system. The effects of the nominal drive shaft torsional flexibility on the first flapwise and first chordwise umbrella air resonance mode eigenvalues were of less significance. However, as a result of the reduction of the first chordwise air resonance mode frequencies, the degree of coupling of chordwise blade motions with flapwise blade motions and torsional blade motions in the first flapwise, first chordwise, and first torsion umbrella air resonance modes was significantly reduced. The results shown in Table 2 are as would be expected on inclusion of the nominal drive shaft torsional flexibility.

Effect of Control System Collective Stiffness

The inclusion of a finite control system collective stiffness, in addition to the drive shaft torsional flexibility, modified the umbrella air resonance modes that were discussed in the previous section. The forward cyclic and backward cyclic air resonance modes are not affected by a variation in the control system collective stiffness because these modes are not coupled to collective control system motion, but are coupled to cyclic control system motion. It should be noted, however, that for an anisotropically supported control system, which is not the case for most tail rotor systems, the cyclic air resonance modes would be affected due to the cyclic variation of control system stiffness. The eigenvalues obtained for the first flapwise, first chordwise, and first torsion umbrella air resonance modes are presented in Table 3 for three values of control system collective stiffness and a set of conditions for which results were presented in the previous sectic .

The effect of a finite control system collective stiffness and rotor speed on the first flapwise, first chordwise, and first torsion umbrella air resonance mode eigenvalue can be ascertained from Table 3. On comparison of the above results with those of Table 2 corresponding to 75% thrust, the most significant effect of the control system collective stiffness is on the first flapwise umbrella air resonance eigenvalues, which are significantly changed. An important result of this comparison is the lack of a significant change in the first torsion umbrella air resonance frequency. This behavior is different from that common to articulated rotor systems. This modal behavior is reasonable for flexstrap blades on consideration of the elastic coupling effects which occur with this type of blade retention. In particular, for a rigid control system, the point of control rod attachment to the pitch horn is not

TABLE 3
UMBRELLA AIR RESONANCE MODES WITH INCLUSION OF DRIVE SHAFT TORSIONAL FLEXIBILITY AND CONTROL SYSTEM COLLECTIVE STIFFNESS

Predominate Mode Type	Control System Collective Stiffness		
	115% nominal	nominal	85% nominal
first flapwise Ω = nominal	-18.07+174.7i	-17.30+170.9i	-16.39+166.1i
first flapwise $\Omega \approx$ 90% nominal	-16.88+157.6i	-16.30+154.9i	-15.60+151.5i
first chordwise Ω = nominal	-0.43 +19.1i	-0.44 +18.8i	-0.49 +18.0i
first chordwise $\Omega \approx$ 90% nominal	-0.51 +20.0i	-0.51 +20.0i	0.52 +19.7i
first torsion Ω = nominal	-35.55+323.8i	-39.21+322.7i	-43.00+319.8i
first torsion $\Omega \approx$ 90% nominal	-28.19+306.2i	-31.07+305.9i	-34.75+303.7i

allowed to move. Thus, a flapwise motion of the blade requires the blade to also rotate against the flexstrap torsional stiffness such that the flapwise stiffness is strongly coupled to the flexstrap torsional stiffness. For a control system having finite collective stiffness, the control rod attachment point is allowed to move in a flapwise direction. In this case, the flapwise stiffness is less dependent on the flexstrap torsional stiffness and decreases in value such that a lower flapwise umbrella frequency results. The torsional stiffness of the flexstrap and the stiffness of the control system combine in a manner such that the apparent effect of control system stiffness on the effective torsional stiffness is minor for the control stiffnesses used. Thus, the first torsion umbrella frequency changes only slightly as the collective control system stiffness decreases. The variation of the umbrella mode eigenvalues depicted in Table 3 as the control system collective stiffness decreases would normally be expected for a flexstrap rotor.

The allowance of control system collective stiffness, besides modifying existing modes, also allows additional umbrella modes resulting from the control representation. For the nominal control system collective stiffness, control system umbrella modes were obtained having eigenvalues of

(-4.69+358.1i) and (-6.01+341.6i) for the nominal rotor speed and 90% nominal rotor speed, respectively. The effect of control system collective stiffness on the coupling of blade motion for the three types of blade modes was minor. In addition, as the control system collective stiffness decreased the amplitude of control system deflection increased for all three types of blade modes investigated, as would be expected.

Effect of Gearbox Support Stiffness

A tail rotor system attached to a gearbox, which in turn is attached to the ground through springs, will affect the cyclic air resonance modes of the tail rotor system. Since the addition of finite tail rotor gearbox support stiffness can only provide cyclic motion to the tail rotor hub via the rocking motion of the tail rotor shaft, the reactionless and umbrella air resonance modal behavior will not be affected.

Prior to presenting the results obtained for the cyclic air resonance modes, a discussion of gearbox-blade coupling behavior for cyclic modes is advantageous. Since the blade motion associated with a blade cyclic frequency occurs in a rotating reference frame and the gearbox and tail rotor shaft motion in a fixed reference frame, the blade motion for a given cyclic blade frequency will not couple with a gearbox motion at the same frequency. Instead, blade motions for a backward cyclic mode will couple with gearbox rocking motion occurring at a frequency 1/rev below that of the corresponding backward cyclic blade mode. Thus, if the gearbox basic rocking frequency is close to 1/rev below that of a backward cyclic blade mode, strong coupling of gearbox and blade motion will occur and cause a significant alteration of the modal behavior of the blades. On the other hand, the blade motions for a forward cyclic mode will couple with gearbox rocking motion occurring at a frequency 1/rev above that of the forward cyclic blade mode.

Some of the forward and backward cyclic blade air resonance eigenvalue results obtained for the basic tail rotor system attached to a tail rotor gearbox using the rotor speeds and thrust of the previous section, the hub mass and inertias corresponding to the full-scale helicopter model, and three isotropic gearbox support stiffnesses are presented in Table 4. Also presented in this table are results for cyclic blade modes which correspond to gearbox rocking frequencies 1/rev above or below that of the blade motion, depending on the type of cyclic mode involved (denoted as gearbox modes). These latter results were obtained during program runs to determine flapwise and chordwise cyclic modes of the blade.

TABLE 4
CYCLIC MODE AIR RESONANCE EIGENVALUES
FOR THE BASIC TAIL ROTOR SYSTEM
WITH ISOTROPICALLY SUPPORTED GEARBOX

Predominate Mode Type	Isotropic Gearbox Support Stiffness		
	infinite	9 X nominal	nominal
Backward Cyclic			
first chordwise Ω = nominal	3.59+213.3i	3.31+211.7i	-8.58+205.7i
first chordwise Ω = 90% nominal	3.07+203.7i	2.80+202.1i	-9.37+193.0i
first torsion Ω = nominal	-24.37+329.7i	-25.41+331.3i	-24.66+328.7i
first torsion Ω = 90% nominal	-21.81+317.8i	-21.56+319.0i	-22.32+317.6i
gearbox mode Ω = nominal	none	NO*	0.00+246.5i
gearbox mode Ω = 90% nominal	none	NO	0.00+232.1i
Forward Cyclic			
first flapwise Ω = nominal	-28.82+201.8i	-17.48+205.4i	-17.48+205.4i
first flapwise Ω = 90% nominal	-25.09+177.4i	-16.57+180.6i	-16.56+180.6i
first torsion Ω = nominal	-24.37+329.7i	-24.86+330.4i	-24.86+330.4i
first torsion Ω = 90% nominal	-21.81+317.8i	-22.72+318.7i	-22.73+318.7i
gearbox mode Ω = nominal	none	0.00+179.6i	NO
gearbox mode Ω = 90% nominal	none	0.00+193.9i	NO

* Not obtained during parametric investigation.

The effect of finite gearbox support stiffness on the forward and backward cyclic blade air resonance eigenvalues can be noted in Table 4. The results are as generally would be

expected, considering the gearbox rocking motion-blade motion coupling that occurs for the various mode types and gearbox support stiffnesses that are presented. Unfortunately, the basic gearbox rocking frequencies corresponding to the nine times nominal and nominal gearbox stiffness do not couple strongly with the first flapwise, first chordwise, and first torsion cyclic air resonance modes. Thus, the results depicted show minor effects of the gearbox support stiffness except for the first chordwise backward cyclic air resonance mode for the nominal gearbox support stiffness, which does have enough coupling for some effect to be noted. For this air resonance cyclic mode, the frequency was reduced and the mode became stable as a result of the slight coupling of the blade motions to the gearbox rocking motion which provides aerodynamic damping. The frequencies provided in Table 4 for gearbox modes correspond to that of the blade motions such that the basic gearbox rocking frequency is 1/rev below the frequency provided for the backward cyclic modes and 1/rev above the frequency provided for the forward cyclic modes. Also, because of the flexibility in the blades, the blade motion for the gearbox modes included elastic motion in addition to motion resulting from translation and rotation of the rotor hub due to the rocking of the gearbox.

The effect of anisotropic gearbox support stiffness was investigated briefly for the nominal rotor speed, 75% nominal thrust, and for the average of the gearbox support stiffness in the two mutually orthogonal directions being equivalent to the nominal isotropic gearbox support stiffness values. With the use of anisotropic gearbox support stiffness, the stability of the backward cyclic gearbox mode became much more stable without the frequency changing significantly. Because of the minor degree of coupling of gearbox motion and blade motion as a result of the gearbox support stiffness utilized, the forward cyclic blade modes (first flapwise, first chordwise, and first torsion) were essentially unaffected by anisotropy of the gearbox support stiffness. Similarly, the effect of gearbox support stiffness anisotropy on the backward cyclic blade air resonance modes was insignificant except for the first chordwise backward cyclic mode for which the frequency decreased slightly and became less stable as the anisotropy of the gearbox support was increased.

Modal Behavior of Tail Rotor System with All Allowed Flexibilities

The modal behavior of a tail rotor system consisting of the basic tail system with finite gearbox support stiffness, finite collective control system stiffness, and drive shaft torsional flexibility can be ascertained on the basis of

knowledge of the four types of air resonance modes based on consideration of the system parameters which affect these various modes. For example, the cyclic air resonance modes are only dependent upon the gearbox support stiffness parameters. Thus, for a tail rotor system configuration which includes the various stiffness parameters for which the eigenvalues of the affected types of air resonance modes have been determined, the eigenvalues corresponding to the four types of air resonance modes can be obtained from Tables 1 through 4. However, if a tail rotor system is to include an anisotropically supported control system, the control system representation will then affect the cyclic blade modes such that for correct cyclic modal behavior determination, both the control system and the tail rotor gearbox representation must be considered simultaneously.

Effect of Advance Ratio on the Basic Tail Rotor Attached to a Flexible Drive Shaft

The dynamic characteristics of the basic tail rotor system with drive shaft flexibility operating at an advance ratio other than zero will be modified from the hover results due to the aerodynamic blade interharmonic coupling that is present. Due to this coupling, cyclic air resonance mode eigenvalues will be altered such that they will not be coincident with the reactionless air resonance modes of the system. In investigating the effects of advance ratio on the modal behavior of this tail rotor system for the nominal drive shaft flexibility and different rotor speeds, modified and unmodified thrust related parameters were used. The unmodified thrust parameters, used in hover configurations, correspond to 75% nominal thrust. The modified thrust related parameters correspond to 12% nominal thrust, which is more realistic for a tail rotor in forward flight than the tail rotor thrust required in hover. The reactionless air resonance eigenvalues obtained for the nominal rotor speed for both unmodified thrust related parameters and modified thrust related parameters are presented in Table 5.

The umbrella and cyclic air resonance mode results obtained are not presented above since they exhibit the same general trends as the reactionless air resonance modes above, except for the first chordwise umbrella air resonance mode. This mode, only slightly stable for hover, at an advance ratio of 0.3 was almost neutrally stable for unmodified thrust related parameters and was slightly unstable for modified thrust related parameters. The effect of advance ratio on the frequency of this mode was insignificant, but the effect of using the modified thrust parameters resulted in an increase of the frequency from 20.8 radians per second to 25 radians per

TABLE 5
EFFECT OF ADVANCE RATIO ON REACTIONLESS MODES OF BASIC TAIL ROTOR SYSTEM WITH DRIVE TORSIONAL FLEXIBILITY AND NOMINAL ROTOR SPEED*

Predominate Mode Type	Advance Ratio		
	0.0	0.1	0.3
first flapwise	-28.82+201.8i	-29.95+201.8i -26.88+204.5i	-30.37+208.3i -29.53+209.2i
first chordwise	3.59+213.3i	3.74+213.3i 0.44+221.8i	3.06+213.1i 0.29+223.2i
first torsion	-24.37+329.7i	-23.28+330.0i -21.59+322.9i	-21.28+330.5i -16.73+321.7i

*The upper row of eigenvalues opposite mode type corresponds to values obtained for 75% nominal thrust without modification of thrust related parameters, and the subsequent row corresponds to values obtained for thrust related parameters associated with a 12% nominal thrust at each advance ratio.

second. In general, the frequencies associated with the four types of first flapwise air resonance modes increased as the advance ratio was increased independent of the set of thrust related parameters utilized, whereas the effects on the stability of these modes were minimal. For the first chordwise reactionless and cyclic air resonance modes, the greatest change in eigenvalues resulted due to the change in thrust related parameters rather than advance ratio. For these modes, the use of the modified thrust related parameters increased the frequencies and significantly reduced the degree of instability. For the four types of first torsion air resonance modes, the greatest effect was also due to the use of the modified thrust related parameters which reduced both the frequency and stability of these modes.

Effect of Advance Ratio on the Eigenvalues of a Tail Rotor System with Control System, Gearbox, and Drive Shaft Flexibilities

In this part of the parametric sensitivity analysis, the effect of advance ratio was investigated by considering only changes in flight velocity to occur while maintaining the thrust related parameters corresponding to 75% thrust for three advance ratios and by considering the thrust related parameters corresponding to 12% thrust at an advance ratio of 0.3 The rotor speed, control system collective stiffness,

gearbox support stiffness and drive shaft torsional flexibility used correspond to those which have been referred to in previous sections as the nominal values. Some of the eigenvalue results obtained for the umbrella, forward cyclic, and backward cyclic air resonance modes for the advance ratios of the previous section are presented in Table 6.

TABLE 6
EFFECT OF ADVANCE RATIO ON THE EIGENVALUES OF A TAIL ROTOR SYSTEM WITH DRIVE SHAFT TORSIONAL, CONTROL SYSTEM, AND GEARBOX SUPPORT FLEXIBILITIES

Predominate Mode Type*	Advance Ratio		
	0.0	0.1	0.3
Umbrella			
first flapwise	-17.30+170.9i	-17.26+171.6i	-14.94+169.7i -13.83+173.4i
first chordwise	-0.44 +18.8i	-0.33 +18.5i	0.41 +17.1i 0.18 +24.7i
first torsion	-39.21+322.7i	-37.92+322.9i	-32.09+326.7i -24.69+320.4i
Backward Cyclic			
first chordwise	-8.58 205.8i	-8.73+205.3i	-7.29+201.2i -6.92+219.3i
gearbox	0.00+246.5i	0.00+246.5i	0.00+246.5i 0.00+246.5i
first torsion	-24.66+328.7i	-24.63+328.3i	-15.08+310.0i -25.09+326.0i
Forward Cyclic			
first flapwise	-17.48+205.4i	-17.90+205.7i	-20.31+202.8i -30.75+212.0i
first torsion	-24.86+330.4i	-23.80+330.7i	-21.29+330.7i -16.57+321.7i

*The same convention for placing of eigenvalues corresponding to thrust related parameters as used for the previous table was also employed for this table.

As can be noted in Table 6, the stability and frequency characteristics of the umbrella, forward cyclic, and backward cyclic air resonance modes do not change significantly as the advance ratio increases from zero to 0.1. However, except for the gearbox modes, significant changes in stability and frequency values do occur as the advance ratio is increased from 0.1 to 0.3. These changes result from the interharmonic blade coupling which is a function of the forward velocity and the interharmonic coupling provided by the additional degrees of freedom of the gearbox and control system support configurations. Not only are the stability and frequency characteristics affected significantly by the increase in advance ratio to 0.3 but also the coupling of blade motions corresponding to the eigenvalues is altered significantly. It should be noted that at an advance ratio of 0.3 the first chordwise umbrella air resonance mode becomes unstable regardless of whether or not the modified thrust related parameters are utilized. This result is reasonable since the first chordwise umbrella modes of the basic tail rotor system with drive shaft torsional flexibility were only very slightly stable at an advance ratio of 0.3. A slight destabilizing effect on these modes due to addition of finite control system stiffness is sufficient to make the modes unstable.

Fuselage-Tailboom-Fin Structure Modal Behavior

The nominal fuselage-tailboom-fin structure lumped parameter model was based upon a full-scale UTTAS configuration. A softer than nominal fuselage-tailboom-fin structure, in which the section stiffnesses in three directions were reduced by a factor of two, was also investigated. Whereas all previous results presented were obtained by assuming the tail rotor hub, or gearbox supports (if gearbox included) to be essentially cantilevered to ground, the calculations for configurations involving the fuselage-tailboom-fin structure were based on the assumption of a free-free system (nose to tail). The first six free-free fuselage-tailboom-fin structure eigenvalues for the nominal and soft configurations are presented in Table 7.

All of these modes except the first and second vertical bending modes exhibit a high degree of vertical-lateral-torsion coupling. The eigenvalues presented in Table 7 for the nominal fuselage-tailboom-fin stiffness configuration compare favorably with those obtained for this configuration by the developer of the UTTAS configuration, based on a beam analysis and NASTRAN. As would be expected, all of the frequencies obtained for the softer fuselage-tailboom-fin structure are approximately 30% lower than those obtained for the nominal fuselage-tailboom-fin structure.

TABLE 7
FUSELAGE-TAILBOOM-FIN STRUCTURE
EIGENVALUES

Predominate Mode Type	Fuselage-Tailboom-Fin Stiffness	
	nominal	soft
lateral bending	0.00 +41.9i	0.00 +29.4i
vertical bending	0.00 +46.4i	0.00 +32.8i
coupled bending-torsion	0.00 +96.3i	0.00 +68.0i
coupled bending-torsion	0.00+104.2i	0.00 +73.2i
coupled bending-torsion	0.00+148.7i	0.00+105.1i
vertical bending	0.00+227.7i	0.00+161.0i

Modal Behavior of Fuselage-Tailboom-Fin Structure with Basic Tail Rotor System Plus Drive Shaft Flexibility

The effect of the attachment of the basic tail rotor configuration with drive shaft torsional flexibility to the nominal and soft fuselage configurations on the coupled modes of the complete system was investigated for the two rotor speeds used previously. With the coupling of the blade modes to those of the fuselage, coupled modes of the system are obtained that are related to the various types of blade modes that exist. Thus, there are sets of coupled rotor-fuselage modes that are related to the umbrella, forward cyclic, and backward cyclic types of blade motion. The reactionless type of blade modes do not alter the fuselage-tailboom-fin modes, since no forces or moments are transmitted to the fuselage by the blades.

The eigenvalues obtained for the fuselage-tailboom-fin structure modes for the various types of blade motion are presented in Table 8 for the nominal rotor speed, nominal fuselage-tailboom-fin structure stiffness configuration, and 75% nominal thrust for an advance ratio of 0.0. Results for the lower rotor speed were essentially the same as for the nominal rotor speed, which means that the rotor speed has little, if any,

TABLE 8
EFFECT OF THE ADDITION OF THE BASIC TAIL ROTOR WITH DRIVE SHAFT TORSIONAL FLEXIBILITY ON THE FUSELAGE-TAILBOOM-FIN MODES

Type of Blade Motion			
Reactionless	Umbrella	Forward Cyclic	Backward Cyclic
0.00 +41.9i	-0.84 +42.8i	0.00 +45.0i	0.00 +45.0i
0.00 +46.4i	-0.00 +49.7i	0.00 +49.8i	0.00 +49.8i
0.00 +96.3i	-0.12+105.3i	0.00+105.9i	0.00+105.9i
0.00+104.2i	-0.04+109.8i	0.00+110.0i	0.00+110.0i
0.00+148.7i	-0.37+168.6i	0.00+169.6i	0.00+169.6i
0.00+227.7i	-0.03+232.2i	0.00+232.2i	0.00+232.2i

effect on the fuselage-tailboom-fin structure modes. The results obtained for the softer fuselage-tailboom-fin structure are very similar to those obtained for the nominal stiffness configuration.

On the basis of the results presented in Table 8, it can be seen that the fuselage-tailboom-fin modes coupled with the umbrella, forward cyclic, and backward cyclic modes of the blade have a higher frequency than the corresponding modes with reactionless blade behavior and are either neutrally stable or slightly damped. The fuselage modes corresponding to backward and forward cyclic blade motion were found to be identical. Although these cyclic blade modes have frequencies very close to those of the umbrella blade modes, the degree of coupling between blade motion and fuselage-tailboom-fin motion is much less than that observed for the umbrella blade modes. Due to the significant differences in frequency and fuselage-tailboom-fin mode shape observed between the fifth fuselage-tailboom-fin mode coupled with reactionless blade behavior and those listed as the fifth fuselage-tailboom-fin modes coupled with umbrella, forward cyclic, and backward cyclic blade behavior, it is believed that the latter modes correspond to an additional basic mode not obtained for reactionless blade behavior.

Effect of Advance Ratio on the Modal Behavior of the Fuselage-Tailboom-Fin Structure when Coupled with Total Tail Rotor System

The modal behavior of the fuselage-tailboom-fin structure with a tail rotor system attached which includes the effects of flexibilities allowed by finite gearbox support stiffness, finite control collective stiffness, and drive shaft torsional flexibility will also be dependent upon the type of blade motion. Although the effects of rotor rotational speed and fuselage stiffness were considered in the investigation of the effects of advance ratio, only the results obtained for the nominal rotor speed and fuselage configuration will be presented, as no significantly different effect was noted for these different configurations. The eigenvalues obtained for the fuselage-tailboom-fin structure modes for the various types of blade motion are presented in Table 9 for the rotor speed and fuselage stiffness configuration specified above.

TABLE 9
EFFECT OF ADVANCE RATIO ON THE FUSELAGE-TAILBOOM-FIN MODES OF THE COMPLETE HELICOPTER SYSTEM

μ	Type of Assumed Blade Motion			
	Reactionless	Umbrella	Forward Cyclic	Backward Cyclic
0.0	0.00 +41.9i	-0.87 +42.2i	0.00 +44.9i	0.00 +44.9i
0.3	0.83 +45.3i	-2.62 +44.3i	0.00 +45.4i	0.00 +45.3i
0.0	0.00 +46.4i	-0.50 +49.2i	0.00 +49.2i	0.00 +49.2i
0.3	-0.04 +49.2i	0.48 +48.2i	0.78 +48.7i	0.78 +48.7i
0.0	0.00 +96.3i	-0.01 +96.7i	0.00 +96.8i	0.00 +94.4i
0.3	-0.13 +96.8i	-0.05 +94.4i	0.00 +94.4i	0.27 +96.6i
0.0	0.00+104.2i	NO	NO	NO
0.0	NO	-0.23+120.3i	0.00+124.6i	-0.35+121.2i
0.3	-0.11+124.6i	0.49+121.4i	0.88+12[illegible].0i	-1.05+122.4i
0.0	0.00+148.7i	NO	NO	NO
0.0	NO	NO	0.36+168.3i	0.00+169.0i
0.3	NO	0.01+169.0i	0.40+168.2i	0.01+169.0i
0.0	0.00+227.7i	0.00+234.4i	0.00+234.0i	0.47+234.0i
0.3	NO	0.48+231.8i	0.48+231.8i	NO

This table presents results at two advance ratios for each type of fuselage-tailboom-fin mode except the fourth and fifth modes at an advance ratio of 0.0, where an extra row has been added. This has been done since it is believed, on the basis of frequency and fuselage mode shape differences, that two additional basic fuselage-tailboom-fin modes exist in the area of these two original basic fuselage modes presented in Table 9. A comparison of the results presented in Table 9 with those presented in Table 8 would yield the conclusion that the advance ratio has very little effect on the modal behavior of the coupled system. However, even though the frequencies appear unaffected by advance ratio, the fuselage-tailboom-fin mode shapes, except for those corresponding to the first fuselage-tailboom-fin mode types, are drastically altered by an increase in advance ratio. For example, the umbrella blade motion fuselage-tailboom-fin mode (-0.50+49.2i) at an advance ratio of 0.0 is very predominantly vertical fuselage-tailboom-fin motion, whereas the mode (0.48+48.2i) at an advance ratio of 0.3 is very predominately lateral fuselage-tailboom-fin motion. Thus, although the effect of advance ratio on the umbrella, reactionless, forward cyclic, and backward cyclic blade modes was noted to be insignificant, the effect of advance ratio on the tail rotor system behavior when coupled to a fuselage-tailboom-fin structure causes significant alteration in the coupling characteristics. This alteration in coupling characteristics significantly modifies the motions of the fuselage-tailboom-fin structure without significantly modifying the related frequencies.

Another significant effect of advance ratio on the coupled system modes is the apparent destabilization that occurs. While the fuselage damping effect is undoubtedly always positive, the aerodynamic damping forces generated by the tail rotor system tend to dominate since the effective disc area of the tail rotor is significantly larger than the effective area of the fin and fuselage. Thus, if the tail rotor tended to be unstable, the entire fuselage-tail rotor system would probably be unstable. While this result might be surprising, it is not without precedence for rotor systems mounted to flexible structures. Therefore, the effect of advance ratio on the coupled air resonance modes consists of two primary effects: (1) a significant change in the components of the modal functions, and (2) a reduction in the stability of the modes.

Effect of Advance Ratio on the Blade Modal Behavior of Total Tail Rotor System Attached to Fuselage Structure

For the blade modes, there is a significant effect of rotor speed on the first flapwise and first torsion air resonance modes. Since the results obtained for both rotor speeds had

basically the same trend with advance ratio, only the results for the nominal rotor speed will be presented. The results obtained for tne umbrella and cyclic blade modes of the full system are presented in Table 10 for advance ratios of 0.1 and 0.3.

TABLE 10
BLADE MODE EIGENVALUES OF
COMPLETE TAIL ROTOR SYSTEM-FUSELAGE STRUCTURE
AT TWO ADVANCE RATIOS

Predominate Mode Type	Advance Ratio	
	0.1	0.3
Umbrella		
first flapwise	-14.76+183.5i	-12.87+180.6i
first chordwise	-0.34 +18.6i	0.14 +18.2i
first torsion	-36.24+317.7i	-32.85+320.0i
Backward Cyclic		
first flapwise	-3.90+186.6i	-3.53+187.5i
first chordwise	NO	-18.22+226.8i
first torsion	-25.00+326.9i	-22.70+318.6i
Forward Cyclic		
first flapwise	-3.30+186.6i	-3.31+186.6i
first torsion	-24.40+331.0i	-21.70+330.7i

When the results given in Table 10 are compared with the results of Table 6, several conclusions are apparent regarding the effects of advance ratio and the inclusion of the flexible fuselage-tailboom-fin structure. As would be expected, the effect of the flexible fuselage-tailboom-fin structure on the blade air resonance modes is much more pronounced than the effect of the blade flexibilities on the modes of the flexible fuselage. In particular, the results obtained for the first

flapwise umbrella and cyclic modes and the first chordwise cyclic mode showed significant effects of the inclusion of the fuselage flexibility on the frequencies and stabilities of these modes. In addition, fuselage flexibility significantly increased the frequency of the first flapwise umbrella mode and first chordwise cyclic modes and decreased the frequencies of the first flapwise cyclic modes. The fuselage flexibility slightly reduced the damping associated with the first flapwise umbrella mode, reduced very significantly the damping associated with the flapwise cyclic air resonance modes, and significantly increased the stability of the first chordwise backward cyclic modes. The trends observable with respect to advance ratio are essentially similar to those presented in Table 6, with the exception that the fuselage-tailboom-fin structure at an advance ratio of 0.3 provides an additional stabilizing effect on the first chordwise umbrella mode and an additional destabilizing effect on the first flapwise forward cyclic mode.

OVERALL CAPABILITIES OF PRESENT PROGRAM

The results obtained for the complete fuselage-tail rotor system, with all allowed flexibilities included, have substantiated the significance of the effect of the tail rotor system on the basic fuselage-related modes and the effect of the fuselage-tailboom-fin structure on the blade-related air resonance modes. These have not been shown by previously existing analyses.

The computer program used for the parametric sensitivity analyses is capable of predicting the air resonance behavior of complex tail rotor/fuselage systems. Although the predicted results obtained suggest modal behavior that may be expected, the validity of these results - other than on a theoretical basis - cannot be established until the program is utilized to obtain predicted results for direct comparison with experimental results for a specific helicopter system.

The only basic limitations of the computer program result from restrictions utilized during its construction and requirements related to the computer system employed. The only limitation in the nature of coding of the program was the assumption of identical blades on the tail rotor, which was reasonable for the intent of general application of the computer program. This restriction can be easily removed from the present program by modifying the program to the form necessary for the consideration of nonidentical blades. An additional restriction of the computer program resulted from the dimensioning of large storage arrays such that only the blade phasing assumption for which the rotor blades must be equally spaced

azimuthally can be employed for more than one blade. This restriction is removable by increasing the dimensions of the involved arrays. This, of course, will increase significantly the core requirements, which are presently 250K octal with an overlay structure. The computer program, as developed, is compatible with existing IBM 360 computer systems. With minor format changes, it would also be compatible with the CDC 6600 computer system.

The computer program developed can be used in its present form to aid in the development of new, and the modification of existing helicopter tail rotor/fuselage systems with improved dynamic characteristics. This program is capable of extension to the representation for main rotor/fuselage or main rotor-tail rotor/fuselage modal behavior or dynamic forced response characteristics. It is also modifiable to an analysis which can investigate rotor systems with unequally spaced blades or systems consisting of blades of different properties.

CONCLUSIONS

It is concluded that:

1. The computer program in its present form can be easily installed on an IBM computer system and executed, as was demonstrated by Ft. Eustis Computer Facility personnel not familiar with the program.

2. The use of the eigenvalue scanning technique provides an efficient means of obtaining solution eigenvalues within a range of stability and frequency parameters if there is no prior knowledge regarding the location of possible eigenvalues.

3. The effect of system parameters on either the umbrella, the reactionless, the forward cyclic, or the backward cyclic blade/fuselage air resonance modes can be efficiently determined with the use of blade phasing relationships.

4. The results obtained through the use of the computer program (i.e., the system air resonance frequencies, damping, and mode shapes) have provided a much better understanding of the dynamic modal coupling of complex flexstrap tail rotor systems.

5. The effect of drive shaft torsional flexibility results in a significant alteration of the chordwise umbrella blade modes.

6. Due to the complex coupling of flapwise and torsional motions of a flexstrap retention system, the effect of control system collective flexibility of a flexstrap tail rotor configuration results in a significant drop in the first flapwise umbrella frequency, but only a slight alteration of the first torsion frequency of this type of rotor.

7. The effect of tail rotor gearbox support stiffness can significantly alter the forward and backward cyclic modes of the tail rotor system.

8. The effect of advance ratio on the umbrella, reactionless, forward cyclic, and backward cyclic blade modes of a flexstrap tail rotor system was found to be limited for the tail rotor thrust values considered.

9. The effect of advance ratio on the coupled tail rotor/fuselage-tailboom-fin structure air resonance modes related to the fuselage appears to cause a significant change in the relative importance of the various components of the modal shapes (in some cases, it causes a reduction in the modal stability).

10. The primary effect of advance ratio on the coupled tail rotor/fuselage-tailboom-fin structure air resonance modes related to the blades was to change the stability characteristics.

RECOMMENDATIONS

The following recommendations are made:

1. The computer program should be extended to predict the mean and dynamic forced response characteristics of tail rotors in steady state forward flight.

2. The accuracy of the stability and forced response versions of the computer program should be verified by comparing predicted results with well-documented experimental data.

3. The stability and forced response versions of the computer program should be utilized to determine means of improving significantly the dynamic characteristics associated with a tail rotor of an existing inventory aircraft.

4. The stability and forced response versions of the computer program should be extended to include the dynamic characteristics of the main rotor, its control system, and the supporting gearbox transmission system so that the interactive dynamic characteristics of the main rotor-fuselage-tail rotor can be adequately investigated.

REFERENCES

1. Balke, R. W., Bennett, R. L., Ph.D., Gaffey, T.M., Lynn, R. R., TAIL ROTOR DESIGN Part II - Structural Dynamics, Presented at the 25th Annual National Forum Proceedings, Washington, D. C., May 14, 15, 16, 1969. Bell Helicopter Company, Fort Worth, Texas.

2. Sadler, S. G., MAIN ROTOR FREE WAKE GEOMETRY EFFECTS ON BLADE AIR LOADS AND RESPONSE FOR HELICOPTERS IN STEADY MANEUVERS, NASA CR-2110, National Aeronautics and Space Administration, September 1972.

3. Piarulli, V.J., THE EFFECTS OF NONUNIFORM SWASH-PLATE STIFFNESS ON COUPLED BLADE-CONTROL SYSTEM DYNAMICS AND STABILITY, NASA CR-1817, National Aeronautics and Space Administration, September 1971.

4. Brandt, David E., THE EXPERIMENTAL DETERMINATION OF THE AEROELASTIC STABILITY CHARACTERISTICS OF A HINGELESS COMPOSITE (FLEX STRAP) TAIL ROTOR,presented at Aerospace Flutter and Dynamics Council Meeting, Atlanta, Georgia, November 8 and 9, 1973 (Proprietary).

5. Lynn, R. R., Robinson, F. S., Batra, N. N., Duhon, J.M., Bell Helicopter Company, Fort Worth, Texas. TAIL ROTOR DESIGN Part I - Aerodynamics. Presented at the 25th Annual National Forum Proceedings, Washington, D. C., May 14, 15, 16, 1969.

6. Wylie, C. R., Jr., ADVANCED ENGINEERING MATHEMATICS, 2nd Edition, New York, New York, McGraw Hill, 1960.

7. THE INTERNATIONAL DICTIONARY OF APPLIED MATHEMATICS, Princeton, New Jersey, D. Van Nostrand Company, Inc., 1967.

8. Hildebrand, Francis B., ADVANCED CALCULUS FOR APPLICATIONS, Englewood Cliffs, New Jersey, Prentice-Hall, Inc., 1965.

9. Pestel, Dr.-Ing. Eduard, C., Leckie, Frederick A., PH.D., MATRIX METHODS IN ELASTO MECHANICS, New York, New York, McGraw-Hill, 1963.

10. Coleman, Robert P., and Feingold, Arnold M., THEORY OF SELF-EXCITED MECHANICAL OSCILLATIONS OF HELICOPTER ROTORS WITH HINGED BLADES, NACA TR-1351, CHAPTER III, National Advisory Committee for Aeronautics, 1958.

11. Sutton, Lawrence R., and Rinehart, Stephen A., DEVELOPMENT OF AN ANALYSIS FOR T"E DETERMINATION OF COUPLED HELICOPTER ROTOR CONTROL SYSTEM DYNAMIC RESPONSE PART I, NASA CR-2452, National Aeronautics and Space Administration , January 1975.

12. Gessow, Alfred, and Myers, Garry C., Jr., AERO-DYNAMICS OF THE HELICOPTER, New York, The Mac Millan Company, 1952.

APPENDIX A
SIMPLIFIED EXAMPLE OF CONSTRUCTION OF FINAL GOVERNING MATRIX EQUATION

The application of Laplace transforms and truncation procedures to a simple problem is presented to provide some insight into the method of development of the final governing matrix equation.

To provide a background for the simple example, the general nature of real-time equations involved in the analysis for representing the behavior of a coupled tail rotor system will be briefly presented. The real-time equations for the state variables at the inboard end of a mass, aerodynamic, or torsional spring section characteristic, in terms of the state variables at the outboard end, may involve time-derivative operators. For example, the consideration of a lumped mass and inertia results in real-time equations for the forces and moments involving d^2/dt^2 operators (acceleration terms) and d/dt operators (velocity terms) applied to slope and displacement variables. The consideration of an aerodynamic characteristic results in real-time equations for forces and moments involving d/dt operators and $e^{in\Omega t}$ terms where n can be a positive or negative integer. Thus, application of the real-time equations consecutively from the blade tip inboard results in increasingly higher order time differential equations for the state variables at each further inboard section. Similarly, the same type time differential behavior occurs for the fuselage-tailboom-fin structure. Thus, applying boundary conditions at the hub-tail rotor shaft interface, the resulting boundary condition equations are high order differential equations including terms involving $e^{in\Omega t}$. Discontinuity equations, since they involve blade variables at specific points on the blade, are also high order differential equations with $e^{in\Omega t}$ terms. The swashplate governing equation, without baseplate motion, is a time differential equation involving d^2/dt^2 and d/dt operators and $e^{in\Omega t}$ terms.

Thus, the governing equations for a coupled tail rotor system can be represented as a set of high order time differential equations which must be solved. Although the actual analysis developed for the representation of coupled helicopter/tail rotor systems makes use of the application of Laplace transforms prior to the obtaining of final governing equations, the resultant Laplace transformed equations of the developed analysis represent equations which are a function of time differential operators and $e^{in\Omega t}$ type terms. The manner in

which the time differential equations can be put in a final matrix form can be shown by considering a simple example where the equations of motion can be defined by the two second order time differential equations,

$$b_1 d^2 f_1(t)/dt^2 + b_2 f_2(t)\sin\Omega t = 0$$

$$b_3 d^2 f_2(t)/dt^2 + b_4 f_2(t) + b_5 f_1(t)\sin\Omega t = 0$$

where b_i are constants and $f_1(t)$ and $f_2(t)$ are two functions of time. These equations can also be expressed in the form

$$b_1 d^2 f_1(t)/dt^2 - ib_2 f_2(t) e^{i\Omega t}/2 + ib_2 f_2(t) e^{-i\Omega t}/2 = 0$$

$$b_3 d^2 f_2(t)/dt^2 + b_4 f_2(t) - ib_5 f_1(t) e^{i\Omega t}/2 + ib_5 f_1(t) e^{-i\Omega t}/2 = 0$$

where the expression $\sin\Omega t = -ie^{i\Omega t}/2 + ie^{-i\Omega t}/2$ has been substituted.

Application of the Laplace transforms, assuming quiescent initial conditions, to these two equations provides the Laplace transformed equations

$$b_1 s^2 \bar{f}_1(s) - ib_2 \bar{f}_2(s-i\Omega)/2 + ib_2 \bar{f}_2(s+i\Omega)/2 = 0$$

$$(b_3 s^2 + b_4)\bar{f}_2(s) - ib_5 \bar{f}_1(s-i\Omega)/2 + ib_5 \bar{f}_1(s+i\Omega)/2 = 0$$

in which it can be noted that the nonshifted Laplace transformed variables are dependent on the shifted Laplace transformed variables. Relationships for the shifted Laplace transformed variables are obtained by frequency shifting the Laplace transform variables in the last two expressions by $-ik\Omega$ such that

$$b_1(s^2 - 2ik\Omega s - k^2\Omega^2)\bar{f}_1(s-ik\Omega) - ib_2 \bar{f}_2(s-ik\Omega-i\Omega)/2 + ib_2 \bar{f}_2(s-ik\Omega+i\Omega)/2 = 0$$

$$\left[b_3(s^2-2ik\Omega s-k^2\Omega^2) + b_4\right]\bar{f}_2(s-ik\Omega) - ib_5\bar{f}_1(s-ik\Omega-i\Omega)/2 + ib_5\bar{f}_1(s-ik\Omega+i\Omega)/2 = 0$$

Substitution of k = -1, 0 and +1 corresponding to inclusion of coupling effects one per rev above and below the main frequency equation for which k = 0 provides a set of six equations which can be written with truncation of terms applied for k = -1 and +1 in the matrix form

$$\begin{bmatrix} \bar{A}_{-1,-1} & 0 & 0 & \bar{B}_{-1,0} & 0 & 0 \\ 0 & \bar{D}_{-1,-1} & \bar{C}_{-1,0} & 0 & 0 & 0 \\ 0 & \bar{B}_{0,-1} & \bar{A}_{0,0} & 0 & 0 & \bar{B}_{0,1} \\ \bar{C}_{0,-1} & 0 & 0 & \bar{D}_{0,0} & \bar{C}_{0,1} & 0 \\ 0 & 0 & 0 & \bar{B}_{1,0} & \bar{A}_{1,1} & 0 \\ 0 & 0 & \bar{C}_{1,0} & 0 & 0 & \bar{D}_{1,1} \end{bmatrix} \begin{Bmatrix} \bar{f}_1(s+i\Omega) \\ \bar{f}_2(s+i\Omega) \\ \bar{f}_1(s) \\ \bar{f}_2(s) \\ \bar{f}_1(s-i\Omega) \\ \bar{f}_2(s-i\Omega) \end{Bmatrix} = 0$$

where the subscripts represent integer values for k and n and

$$\bar{A}_{k,n} = b_1(s^2-2ik\Omega s-k^2\Omega^2)\ \delta^0_{n-k}$$

$$\bar{B}_{k,n} = -(n-k)ib_2(\delta^1_{n-k} + \delta^{-1}_{n-k})$$

$$\bar{C}_{k,n} = -(n-k)ib_5(\delta^1_{n-k} + \delta^{-1}_{n-k})$$

$$\bar{D}_{k,n} = \left[b_3(s^2-2ik\Omega s-k^2\Omega^2) + b_4\right]\delta^0_{n-k}$$

This matrix equation is identical in concept to that of Equation (38) and can be represented in the same manner with

$$\left[\bar{T}_{k,n}\right] = \begin{bmatrix} \bar{A}_{k,n} & \bar{B}_{k,n} \\ \bar{C}_{k,n} & \bar{D}_{k,n} \end{bmatrix}$$

Additional harmonic coupling can be represented by expanding the number of values of k used in constructing the final matrix governing equation to a higher number which is equivalent to increasing the value of Nf.

LIST OF SYMBOLS*

a	general variable used in defining other variables
$\left[\bar{A}_{ij}\right]$	final governing matrix
$\left[A'_{ij}\right]$	modified final governing matrix obtained by removal of row and column from final governing matrix
$\left[\bar{A}_k\right]_m^i$	k frequency shifted Laplace transform version of the transfer matrix representing the lumped mass and inertia of the ith section of the mth blade
$\bar{A}_{k,n}$	variable defined for use in simplified example of analysis
a_m	effective length of pitch horn, positive if control rod is attached aft of blade shear center, ft
a_{max}	highest harmonic coefficient obtainable by basing Fourier analysis or values of the function of interest at uniformly spaced azimuthal steps for one rotor revolution
A_n, a_n	general Fourier harmonic coefficients
b_i	coefficients of the two equations used for simplified example of analysis
b_j	offset of the jth linear spring attachment point from neutral axis of swashplate ring, positive inward, ft

*All units given in English units but equivalent SI units may be used if applied to all definitions of program variables.

$\left\{\bar{b}_k\right\}$ general k frequency shifted discontinuity column matrix for inclusion of effects of the first discontinuity term on the blade state variables

$\bar{B}_{k,n}$ variable defined for use in simplified example of analysis

$\left[\bar{B}_{k,n}\right]^j$ associated transfer matrix specifying contribution of n frequency shifted blade tip variables to the k frequency shifted blade state variables at the inboard end of the jth lumped parameter characteristic

$\left[\bar{B}_{k,n}\right]^i_m$ associated transfer matrix specifying contribution of n frequency shifted blade tip unknowns of the mth blade to the k frequency shifted state variables of the mth blade at the inboard end of the ith blade section

$\left\{\bar{E}_{k,n}\right\}^j$ column matrix specifying contribution of the n frequency shifted first discontinuity term to the k frequency shifted blade state variables at the inboard end of the jth lumped parameter characteristic

$\left\{\bar{b}_{k,n}\right\}^i_m$ column matrix specifying contribution of the n frequency shifted first discontinuity term to the k frequency shifted mth blade state variables at the inboard end of the ith blade section

$\left[B0\right]^{m-1}_m$ matrix used in specifying contribution of the (m-1)th blade tip and discontinuity unknowns to the mth blade related slope and deflection boundary condition equations

$\left[B1\right]_m$ matrix used in specifying contribution of the mth blade tip and discontinuity unknowns to the mth blade related slope and deflection boundary condition equations

$\left[B2\right]_m^{m+1}$ matrix used in specifying contribution of the (m+1)th blade tip and discontinuity unknowns to the mth blade related slope and deflection boundary condition equations

$\left[\overline{BB}_{k,n}\right]_m^j$ matrix specifying contribution of the jth blade n frequency shifted tip and discontinuity unknowns to the mth blade related k frequency shifted slope and deflection boundary condition equations and discontinuity equations

$\left[\overline{BBB}_{k,n}\right]_m$ matrix specifying contribution of the mth blade n frequency shifted tip unknowns to its related k frequency shifted slope and deflection boundary condition equations

$\left[\overline{BBC}_{k,n}\right]_m$ matrix specifying contribution of the mth blade n frequency shifted tip unknowns to its related k frequency shifted discontinuity equations

$\left[\overline{BBD}_{k,n}\right]_m$ matrix specifying contribution of the mth blade n frequency shifted discontinuity unknowns to its related k frequency shifted discontinuity equations

$\left[\overline{BBJ1}_{k,n}\right]_m^j$ matrix specifying contribution of the jth blade n frequency shifted tip unknowns to the mth blade related k frequency shifted slope and deflection boundary condition equations

$\left[\overline{BBJ2}_{k,n}\right]_m^j$ matrix specifying contribution of the jth blade n frequency shifted discontinuity unknowns to the mth blade related k frequency shifted slope and deflection boundary condition equations

$\left[\overline{BBR}_{k,n}\right]_m$ matrix specifying contribution of the mth blade n frequency shifted discontinuity unknowns to its related k frequency shifted slope and deflection boundary condition equation

$\left[\overline{BE}\right]_m^i$	transfer matrix representing a lumped geometric bend in shear center axis of the ith section of the mth blade
$\left[\overline{BF}_{k,n}\right]_m$	matrix specifying contribution of the n frequency shifted fuselage nose unknowns to the mth blade related k frequency shifted slope and deflection boundary condition equations and discontinuity equations
$\left[\overline{BS}_k\right]_m$	matrix specifying contribution of the k frequency shifted swashplate displacement unknowns to the mth blade related k frequency shifted slope and deflection boundary condition equations and discontinuity equations
C	damping coefficient of control system collective base plate spring-damper support, lb-sec/ft
$\left[\overline{C}_0\right]_s^i$	matrix specifying contribution of aerodynamic damping to the aerodynamic transfer matrix of the ith fuselage section
$C_{i,m}$	influence coefficients of the restraint transfer matrix of the mth blade
c_j	damping coefficient of the jth control system spring-damper unit, lb-sec/ft
$\left\{\overline{c}_k\right\}$	general k frequency shifted discontinuity column matrix for inclusion of the effects of the second discontinuity term on blade state variables
$\overline{C}_{k,n}$	variable defined for use in simplified example of analysis
$\left\{\overline{c}_{k,n}\right\}^j$	column matrix specifying contribution of frequency shifted second discontinuity term to k frequency shifted blade state variables at the inboard end of the jth lumped parameter characteristic

$\left\{\overline{c}_{k,n}\right\}_m^i$ column matrix specifying contribution of the n frequency shifted second discontinuity term to the k frequency shifted mth blade state variables at the inboard end of the ith section

$\left[\overline{C}_{.-k}\right]_m^i$ matrix specifying contribution of aerodynamic damping to the aerodynamic transfer matrix relating k frequency shifted blade state variables inboard of the aerodynamic application point of the ith section of the mth blade to the n frequency shifted state variables outboard of the same point

$\left(\overline{CN}_{k,n}\right)_m$, $\left(\overline{CVy}_{k,n}\right)_m$, $\left(\overline{CVz}_{k,n}\right)_m$ row vectors specifying contribution of blade tip unknowns to the forces acting on the mth blade control rod at the pitch horn attachment point in the same orientation as the rotating shaft coordinate system x, y, and z axes of the mth blade, respectively

$c\theta_j$ torsional damping coefficient of the jth torsional spring-damper unit counteracting local lateral rotation of control system ring, ft-lb-sec/rad

$c\tau_{c,m}$ damping coefficient of mth control rod for flexstrap rotor, sec

$c\phi_j$ torsional damping coefficient of the jth torsional spring-damper unit counteracting local longitudinal rotation of the control system ring, ft-lb-sec/rad

$\left[\overline{C}_k\right]_s^i$ k frequency shifted aerodynamic transfer matrix of the ith section of fuselage structure

$\left[\overline{C}_{n-k,n}\right]_m^i$ blade aerodynamic transfer matrix relating k frequency shifted blade state variables inboard of the aerodynamic application point of the ith section of the mth blade to the n frequency shifted state variables outboard of the same point

$\left\{\bar{D}_0\right\}_s^i$	matrix specifying nondamping contribution to the aerodynamic transfer matrix of the ith fuselage section
$\left[D_I\right]_m$	matrix utilized in defining contribution of fuselage hub variables to the mth blade related slope and deflection boundary conditions
$\left\{\bar{d}_k\right\}$	general k frequency shifted discontinuity column matrix for inclusion of the effects of the third discontinuity term on blade state variables
$\bar{D}_{k,n}$	variable defined for use in simplified example of analysis
$\left\{\bar{d}_{k,n}\right\}^j$	column matrix specifying contribution of n frequency shifted third discontinuity term to k frequency shifted blade state variables at the inboard end of the jth lumped parameter characteristic
$\left\{\bar{d}_{k,n}\right\}_m^i$	column matrix specifying contribution of the n frequency shifted third discontinuity term to the k frequency shifted mth blade state variables at the inboard end of the ith section
d_m	rigid offset of the mth control rod attachment point from the neutral axis of the ring, positive outward, ft
$\left[\bar{D}_{n-k}\right]_m^i$	matrix specifying nondamping contribution to the aerodynamic transfer matrix relating k frequency shifted blade state variables inboard of the aerodynamics of application point of the ith section of the mth blade to the n frequency shifted state variables outboard of the same point
$d(\theta,t)$, $d(\chi_j,t)$	definitions involving control system displacements to reduce length of equations

$\left[DB\right]_M$	row matrix specifying a contribution of mth blade k frequency shifted state variables at restraint to the third restraint discontinuity equation of the mth blade
$\left[\overline{DX}_{k,n}\right]_m, \left[\overline{DY}_{k,n}\right]_m,$ $\left[\overline{DZ}_{k,n}\right]_m$	row matrices specifying contribution of n frequency shifted mth blade related tip unknowns to the first, second, and third restraint discontinuity equations, respectively, of the mth blade
$DX1_m, DX2_m, DX3_m$	terms specifying contribution of the first, second, and third k frequency shifted mth blade related restraint discontinuities, respectively, to the first restraint discontinuity equation of the mth blade
$DY1_m, DY2_m, DY3_m$	terms specifying contribution of the first, second, and third k frequency shifted mth blade related restraint discontinuities, respectively, to the second restraint discontinuity equation of the mth blade
$DZ1_{k,m}, DZ2_{k,m},$ $DZ3_{k,m}$	terms specifying contribution of the first, second, and third k frequency shifted mth blade related restraint discontinuities, respectively, to the third restraint discontinuity equation of the mth blade
e^x	general exponential variable
$\left[E\right]_m^i$	transfer matrix representing the elastic characteristics of the ith section of the mth blade
$e_{I,m}$	variable defined for convenience in boundary condition equation representation
EI	bending stiffness of control system ring, $lb\text{-}ft^2$
$\left\{\overline{F}_j\right\}, \left\{\overline{F}'_j\right\}$	full and modified forcing function column vectors, respectively, used to determine correction vectors

$\bar{f}_1(s), \bar{f}_2(s)$	Laplace transformed functions involved in simplified example of analysis
$f_1(t), f_2(t)$	time dependent functions used in simplified example of analysis
$f_m(t)$	function of time for the mth blade defined by exponential Fourier analysis representation
$f_n(t)$	form used to represent the nth function of time
$F(a)$	variable defined to reduce length of control system equations
$\bar{F}(s)$	Laplace transform of f(t)
$\bar{F}(s-a)$	shifted Laplace transform of f(t)
$f(t)$	general function of time
$f(t)^{(i)}$	general state variable associated with ith section
$f(\psi_j)$	general function of ψ_j
$\left[\overline{FB}_{k,n}\right]_m$	matrix specifying contribution of the mth blade n frequency shifted tip and discontinuity unknowns to the fuselage related k frequency shifted moment and shear boundary condition equations
$\left[\overline{FBB}_{k,n}\right]_m$	matrix specifying contribution of the mth blade n frequency shifted tip unknowns to the fuselage related k frequency shifted moment and shear boundary condition equations
$\left\{\overline{FBb}_{k,n}\right\}_{m'}$ $\left\{\overline{FBc}_{k,n}\right\}_{m'}$ $\left\{\overline{FBd}_{k,n}\right\}_m$	column matrices specifying contribution of the mth blade n frequency shifted first, second, and third discontinuities, respectively, to the fuselage related k frequency shifted moment and shear boundary condition equations

$\left[FU_k\right]$	matrix specifying contribution of the k frequency shifted fuselage unknowns to the fuselage related k frequency shifted boundary condition equations
$\overline{FX2}_{k,m}, \overline{FY2}_{k,m}, \overline{FZ2}_{k,m}$	forces acting in the control rod local coordinate system x, y and z axes, respectively
$\left[G\right]$	general real-time transfer matrix
$\left[\bar{G}_k\right]$	general k frequency shifted Laplace transformed transfer matrix
$\left[\bar{G}(s)\right]$	general Laplace transformed transfer matrix
GJ	torsional stiffness of control system ring, lb-ft^2
$\left[\bar{G}_k\right]_s^i$	k frequency shifted aerodynamic transfer matrix of the ith section of fuselage structure
$\left[\bar{G}_{k,n}\right]^j$	Laplace transformed transfer matrix specifying the contribution of the n frequency shifted state variables outboard of an aerodynamic load point at j to the k frequency shifted state variable just inboard of the load point
$\left[\bar{G}_n\right]$	Laplace transformed transfer matrix specifying the contribution of the n frequency shifted state variables to the zero frequency shifted state variables due to aerodynamic considerations at an aerodynamic load point
i	imaginary number, $\sqrt{-1}$
$\bar{i}, \bar{j}, \bar{k}$	general orthogonal unit vectors of a coordinate system

$\bar{i}_{bm}, \bar{j}_{bm}, \bar{k}_{bm}$	orthogonal unit vectors of the mth blade (rotating) coordinate systems which vary from section to section
$\bar{i}_{f}, \bar{j}_{f}, \bar{k}_{f}$	orthogonal unit vectors of fixed shaft coordinate system
$\bar{i}_{fc}, \bar{j}_{fc}, \bar{k}_{fc}$	orthogonal unit vectors of fixed control system coordinate system
$\bar{i}_{fs}, \bar{j}_{fs}, \bar{k}_{fs}$	orthogonal unit vectors of the fixed fuselage coordinate system
$\bar{i}_{rc}, \bar{j}_{rc}, \bar{k}_{rc}$	orthogonal unit vectors of the rotating control system coordinate systems, one corresponding to each blade
$\bar{i}_{rm}, \bar{j}_{rm}, \bar{k}_{rm}$	orthogonal unit vectors of rotating shaft coordinate system of mth blade
$\bar{i}_{s}, \bar{j}_{s}, \bar{k}_{s}$	orthogonal unit vectors of the local fuselage coordinate systems which vary from section to section
IBC	integer controlling type of rotor system
K	stiffness of collective spring-damper unit supporting control system base plate, lb/ft
$K_{c,m}$	linear stiffness of the control rod of the mth blade of a flexstrap rotor system, lb/ft
kd	drive shaft torsional flexibility, ft-lb/rad
k_j	linear stiffness of the jth spring-damper support unit, lb/ft
k_m	linear stiffness of the control rod of the mth blade, lb/ft
$\overline{KI}^{a}_{b,c}$	variable defined to reduce length of control system equations

$\overline{K2}^{a}_{b,c}$	variable defined to reduce length of control system equations
$\overline{K3}^{a}$	variable defined to reduce length of control system equations
$\overline{K4}^{a}_{b}$	variable defined to reduce length of control system equations
$\overline{KC}_{a}$	variable defined to reduce length of control system equations
$\overline{KC\theta}_{a}$	variable defined to reduce length of control system equations
$\overline{KC\phi}_{a}$	variable defined to reduce length of control system equations
$k\theta_{j}$	torsional stiffness of the jth torsional spring-damper unit counteracting local lateral rotation, ft-lb/rad
$k\phi_{j}$	torsional stiffness of the jth torsional spring-damper unit counteracting local longitudinal rotation, ft-lb/rad
$\left[\overline{L}\right]^{i}_{m}$	transfer matrix representing the elastic restraint at section i of the mth blade, only allowed once on the blade
$Ll2_{m}$	distance from center of rotor hub to the mth control rod attachment point to the control system ring, ft
M	mass of control system ring, slugs
$\left[M_{I}\right]_{m}$	matrix utilized in defining contribution of blade hub variables to the fuselage related moment and shear boundary conditions
$\overline{M}_{m}$	blade root moment vector for the mth blade defined relative to the rotating coordinate system of the mth blade, ft-lb

$\bar{M}_s$	fuselage structure hub moment vector defined relative to the fixed shaft coordinate system, ft-lb
max	maximum number of harmonics obtainable by Fourier analysis based on values of the function of interest at uniformly spaced azimuthal steps for one rotor revolution
Mct	integer control parameter for inclusion of control torque discontinuity
Mer	integer control parameter specifying degree of convergence required by user
Mfea	integer control parameter for inclusion of feathering bearing discontinuity
Mflap	integer control parameter for inclusion of flap hinge discontinuity
Mr	integer control parameter for inclusion of flexstrap restraint discontinuities
My,Mz,T	flapwise bending, chordwise bending, and pitching moments, respectively, ft-lb
$\bar{My},\bar{Mz},\bar{T}$	Laplace transformed flapwise bending, chordwise bending and pitching moments, respectively, ft-lb
$(\bar{My}_k)^i_m, (\bar{Mz}_k)^i_m$ $(\bar{T}_k)^i_m$	k frequency shifted Laplace transformed flapwise bending, chordwise bending, and pitching moments, respectively, at the inboard end of the ith section of mth blade, ft-lb
$(\bar{My}_m)^i_k, (Mz_m)^i_k,$ $(\bar{Tm})^i_k$	k frequency shifted Laplace transformed flapwise bending, chordwise bending, and pitching moments, respectively, at the inboard end of the ith section of mth blade, ft-lb
My_m, Mz_m, T_m	blade root flapwise bending, chordwise bending, and pitching moments, respectively, of the mth blade in its rotating shaft coordinate system, ft-lb

$(\bar{My}_m)_k, (\bar{Mz}_m)_k, (\bar{T}_m)_k$	k frequency shifted Laplace transformed blade root flapwise bending, chordwise bending, and pitching moments, respectively, of the mth blade in its rotating shaft coordinate system, ft-lb
My_s, Mz_s, T_s	fuselage flapwise bending, chordwise bending, and pitching moments, respectively, in the local fuselage coordinate system at tail rotor hub, ft-lb
$\bar{My}^*_s, \bar{Mz}^*_s, \bar{T}^*_s$	Laplace transformed fuselage flapwise bending, chordwise bending, and pitching moments, respectively, in the fixed fuselage coordinate system at the nose of helicopter, ft-lb
$(\bar{My}_s)_k, (\bar{Mz}_s)_k, (\bar{T}_s)_k$	k frequency shifted Laplace transformed fuselage flapwise bending, chordwise bending, and pitching moments, respectively, in the local fuselage coordinate system at tail rotor hub, ft-lb
$Mz(\theta,t)$	local bending moment acting on the control system ring, ft-lb
N, Vy, Vz	radial, chordwise shear, and flapwise shear forces, respectively, lb
$\bar{N}, \bar{Vy}, \bar{Vz}$	Laplace transformed radial, chordwise shear, and flapwise shear forces, respectively, lb
$(\bar{N}_m)_k, (\bar{Vy}_m)_k, (\bar{Vz}_m)_k$	k frequency shifted Laplace transformed blade root radial, chordwise shear, and flapwise shear forces, respectively, of the mth blade in its rotating shaft coordinate system, lb
$\bar{N}^*_s, \bar{Vy}^*_s, \bar{Vz}^*_s$	Laplace transformed fuselage axial, chordwise shear, and flapwise shear forces, respectively, in the fixed fuselage coordinate system at the nose of helicopter, lb

$(\bar{N}_s)_k, (\bar{V}y_s)_k,$ $(\bar{V}z_s)_k$	k frequency shifted Laplace transformed fuselage axial, chordwise shear, and flapwise shear forces, respectively, in the local fuselage coordinate system at tail rotor hub, lb
$(\overline{N2}_k)_m, (\overline{Vy2}_k)_m,$ $(\overline{Vz2}_k)_m$	k frequency shifted Laplace transformed forces acting on the control rod of the mth blade at its attachment to the pitch horn in the x, y, and z direction, respectively, of the mth blade rotating shaft coordinate system, lb
NAS	number of uniformly spaced azimuthal steps in one revolution used to determine harmonic coefficients of aerodynamic functions
Nb	number of rotor blades
Nct	blade section immediately inboard of which the control torque is applied
Nf	maximum number of harmonics included for interharmonic coupling
Nfea	blade section immediately inboard of which the feathering bearing occurs
Nflap	blade section immediately inboard of which the flap hinge occurs
Nmax	highest azimuthal harmonic of control system ring displacement to be included
Nps	integer denoting type of relative blade motion assumed with blade phasing
Nr	blade section at which the flexstrap restraint representation is to be considered
Ns	number of elastic spring-damper units supporting control system ring
NS	number of blade sections
NSF	number of fuselage-tailboom-fin sections
NSP	integer control parameter specifying inclusion of control system representation

$(\overline{P}_k)_m$	k frequency shifted force acting on the control system ring due to the mth control rod, lb
$P_m(t), \overline{P}_m(s)$	real-time and Laplace transformed force, respectively, acting on the control system ring in the negative z_{fc} axis direction due to the mth control rod, lb
$\left\{\overline{P}_n\right\}_m$	column matrix containing the n frequency shifted tip variable and discontinuity unknowns of the mth blade
PFC	pitch-flap coupling factor
PLC	pitch-lag coupling factor
$Q_\ell(t)$	ℓth Fourier harmonic of the $Q(\theta,t)$ loading function, lb/ft
$\left\{\overline{q}_n\right\}^*$	n frequency shifted unknown column matrix containing control system displacement, fuselage related, and blade related unknowns
$Q(\theta,t)$	applied force per unit length acting on the control system ring in the negative z_{fc} axis direction, lb/ft
R	radius of control system ,, ft
$\left[\overline{R}\right]_m^i$	transfer matrix representing rigid offset characteristics of the ith section of the mth blade
$\left\{r_i\right\}$	twelve-element row matrix with the ith element equal unity and all others equal zero
$\left\{\overline{r}_n\right\}$	column matrix containing n frequency shifted control system unknowns
$R_p^{(i)}$	p/rev amplitude of a state variable at the inboard end of the ith section

$\left[r_{PFC}\right]$	twelve-element row matrix with fourth element equal PFC and eleventh element equal unity with all others zero
$\left[r_{PLC}\right]$	twelve-element row matrix with fourth element equal unity and seventh element equal PLC with all others zero
s	Laplace transform variable
S_a	variable defined to reduce length of control system equations
s_{CU}	eigenvalue for iteration just completed during program iteration procedure
$\left\{\bar{S}_k\right\}^i$	k frequency shifted Laplace transformed blade state variable vector at the inboard end of ith section
$\left\{\bar{S}_k\right\}^{j-}, \left\{\bar{S}_k\right\}^{j+}$	k frequency shifted Laplace transformed blade state variable vector at the inboard and outboard ends, respectively, of the jth lumped parameter characteristic
$\left\{\bar{S}_k\right\}_s^i$	k frequency shifted Laplace transformed fuselage structure state variable vector after ith section has been crossed
$\left[\bar{S}_k\right]_s^i$	k frequency shifted associated fuselage structure transfer matrix relating fuselage structure state variables after ith section has been crossed to the fuselage structure unknowns
$\left\{\bar{S}_k\right\}_s^*$	k frequency shifted fuselage structure variable unknowns at nose of helicopter
s_{LA}	eigenvalue of iteration prior to the iteration just completed during program iteration procedure
$S_{m,\ell}$	variable defined to reduce length of control system equations

$\left\{\bar{S}_n\right\}^*$	n frequency shifted Laplace transformed blade tip state variable slope and deflection unknowns
s_{NE}	next trial eigenvalue based on previous two eigenvalues
$\left\{S(t)\right\}^-, \left\{S(t)\right\}^+$	general state variable vector inboard and outboard of a blade section, respectively
$\left\{\bar{S}(s)\right\}^-, \left\{\bar{S}(s)\right\}^+$	Laplace transformed general state variable vector inboard and outboard of a blade section, respectively
$\left[\overline{SB}_{k,n}\right]$	matrix specifying contribution of n frequency shifted blade tip and discontinuity unknowns to the k frequency shifted control system related equations
$\left[\overline{SF}_{k,n}\right]$	matrix specifying contribution of n frequency shifted fuselage structure nose unknowns to the k frequency shifted control system related equations
$\left[\overline{SK}_k\right]_m^i$	k frequency shifted Laplace transformed version of transfer matrix representing the torsional spring-damper characteristics of the ith section of the mth blade
$\left[\overline{SW}_{k,n}\right]$	matrix specifying contribution of n frequency shifted control system unknowns to the k frequency shifted control system equations
t	time, sec
$\left[\bar{T}_{k,n}\right]$	matrix specifying contribution of all n frequency shifted unknowns to all k frequency shifted governing equations
$T(\theta,t)$	local torque acting on the control system ring, ft-lb

$u_0(t), \bar{u}_0(s)$	real-time and Laplace transformed version of the displacement of the collective base plate of control system relative to ground, respectively, ft
$\bar{u}_m$	blade root deflection vector for the mth blade defined relative to the rotating coordinate system of the mth blade
$\bar{U}_n^q$	influence coefficient matrix denoting contribution of n frequency shifted hub motion to q related control system equations
$\bar{u}_s$	fuselage structure hub deflection vector defined relative to the fixed shaft coordinate system, ft
ux, uy, uz	real-time axial, chordwise, and flapwise deflections of a section, respectively, ft
$\overline{ux}, \overline{uy}, \overline{uz}$	Laplace transformed axial, chordwise, and flapwise deflections of a section, respectively, ft
$\overline{ux}^*, \overline{uy}^*, \overline{uz}^*$	Laplace transformed axial, chordwise, and flapwise blade tip deflections, respectively, ft
ux_m, uy_m, uz_m	blade root radial, chordwise, and lapwise deflections, respectively, of the mth blade in its rotating shaft coordinate system, ft
$(\overline{ux}_m)_k, (\overline{uy}_m)_k, (\overline{uz}_m)_k$	k frequency shifted Laplace transformed blade root radial, chordwise, and flapwise deflections, respectively, of the mth blade in its rotating shaft coordinate system, ft
$\overline{ux}_r, \overline{uy}_r, \overline{uz}_r$	discontinuity deflection variables for a flexstrap blade at the control rod attachment to pitch horn in the control rod coordinate system x, y, and z axis directions, respectively, ft

ux_s, uy_s, uz_s	fuselage radial, chordwise, and flapwise deflections, respectively, in the local fuselage coordinate system at tail rotor hub, ft
$(\overline{ux}_s)_k, (\overline{uy}_s)_k,$ $(\overline{uz}_s)_k$	k frequency shifted Laplace transformed fuselage radial, chordwise, and flapwise deflections, respectively, in the local fuselage coordinate system at the tail rotor hub, ft
$(\overline{uxa}_k)_m, (\overline{uya}_k)_m$ $(uza_k)_m$	k frequency shifted deflections of the mth control rod attachment point to the pitch horn, oriented in the x, y, and z axis directions of the mth blade rotating coordinate system, respectively, ft
$(\overline{uxp}_k)_m, (\overline{uyp}_k)_m$ $(\overline{uzp}_k)_m$	k frequency shifted deflections of the mth control rod attachment point to the control system ring oriented in the x, y, and z axis directions of the mth blade rotating coordinate system, respectively, ft
$v_\ell(t)$	azimuthal harmonic of $v(\theta,t)$
$\overline{V}_m$	blade root force vector for the mth blade defined relative to the rotating coordinate system of the mth blade
$\overline{V}_s$	fuselage structure hub force vector defined relative to the fixed shaft coordinate system
$v(\theta,t)$	displacement of the control system ring in negative z_{fc} direction as a function of θ and t, ft
$v(\chi_j,t)$	control system displacement in the negative z_{fc} direction dependent on χ_j and t, ft
$Vy(\theta,t)$	local shear force acting on control system ring, lb

$w_\ell(t), \bar{w}_\ell(s)$	azimuthal harmonic of $w(\phi,t)$ in real-time and Laplace transformed form, respectively, ft
$w(\phi,t)$	displacement of the control system ring relative to the rotating reference coordinate system, ft
x,y,z	general rectangular Cartesian coordinate system axes
x_{bm}, y_{bm}, z_{bm}	blade local rotating rectangular Cartesian coordinate system axes
$x_{e,m}$	linear extension of mth control rod, ft
x_f, y_f, z_f	shaft fixed (nonrotating) rectangular Cartesian coordinate system axes
x_{fc}, y_{fc}, z_{fc}	control system fixed rectangular Cartesian coordinate system axes
x_{fs}, y_{fs}, z_{fs}	fuselage fixed rectangular Cartesian coordinate system axes
$\left\{\bar{X}_j\right\}, \bar{X}_j$	final column matrix of all system unknowns and an element of this matrix
$\bar{\bar{X}}^{k,n}_{q,\ell}$	control system impedances associated with asymmetry of support configuration
$X_{\ell,p}$	real part of the ℓth spatial harmonic of control system ring displacement in the rotating control system coordinate system at a frequency $p\Omega$ above the main frequency, ft
$X_p^{(i)}$	real part of a general state variable with frequency p/rev above the main frequency at the inboard end of the ith section, ft
x_{rc}, y_{rc}, z_{rc}	control system rotating rectangular Cartesian coordinate system axes

x_{rm}, y_{rm}, z_{rm}	shaft rotating rectangular Cartesian coordinate system axes associated with the mth blade
x_s, y_s, z_s	local fuselage rectangular Cartesian coordinate system axes
$\bar{Y}_{k,m}$	variable introduced to reduce length of control system equations
$Y_p^{(i)}$	imaginary part of a general state variable with frequency p/rev above the main frequency at the inboard end of the ith section, ft
$Y_{\ell,p}$	imaginary part of the ℓth spatial harmonic of control system displacement in rotating control system coordinate system at a frequency pΩ above the main frequency, ft
$\bar{Z}_n^{\ell}$	control system impedances associated with symmetric properties of control system and its support configuration
$[\alpha]$	boundary condition operational array for obtaining blade root displacements and slopes
α_l	pitch-lag coupling angle
$\alpha_{i,m}$	quantities representing sine and cosine terms involving control rod orientation angles of the mth control rod when flexstrap blades are used
$[\alpha G]_m$	matrix operator specifying contribution of the mth blade root state variables to the mth blade related deflection and slope boundary condition equation for a gimballed rotor

$\left[\alpha G'\right]_{m+1}$	matrix operator specifying contribution of the (m+1)th blade root state variables to the mth blade related deflection and slope boundary condition equation for a gimballed rotor
$\left[\alpha R\right]$	matrix operator specifying contribution of the mth blade root state variables to the mth blade related boundary condition equations for an articulated, rigid, or flexstrap rotor
$\left[\alpha T'\right]_{m+1}$	matrix operator specifying contribution of the second blade root state variables to the first blade related boundary condition equations for a teetering rotor
$\left[\alpha T''\right]_{m-1}$	matrix operator specifying contribution of the first blade root state variables to the second blade related boundary condition equations for a teetering rotor
$\left[\alpha T1\right]_{m}$	matrix operator specifying contribution of the first blade root state variables to the first blade related boundary condition equations for a teetering rotor
$\left[\alpha T2\right]_{m}$	matrix operator specifying contribution of the second blade root state variables to the second blade related boundary condition equations for a teetering rotor
$\beta_{\ell}(t)$	Fourier harmonic of $\beta(\theta,t)$, ft-lb/ft
$\beta_{p}^{(i)}$	phase angle associated with a general state variable inboard of the ith section having a frequency of p/rev above that of the main frequency, rad
$\beta(\theta,t)$	applied torque per unit length acting on control system ring, ft-lb/ft
$\left[\beta G_I\right]_{m}$	matrix operator specifying contribution of fuselage hub state variables to the mth blade related boundary condition equations for a gimballed rotor

$\left[\beta R_I\right]_m$	matrix operator specifying contribution of fuselage hub state variables to the mth blade related boundary condition equations for an articulated, rigid, or flexstrap rotor
$\left[\beta T_I\right]_m$	matrix operator specifying contribution of fuselage hub state variables to the mth blade related boundary condition equations for a teetering rotor
$\left[\gamma\right]$	matrix operator specifying contribution of fuselage structure hub state variables to fuselage structure related moment and force boundary condition equations
δ_3	pitch-flap coupling angle, degrees
δ_a^b	Kronecker's delta which equals unity if a is equal to b and otherwise is zero
$\delta(\theta-\theta_0)$	Dirac delta function which is unity if θ is greater than or equal to θ_0 and otherwise is zero
$\overline{\Delta 1}_n, \overline{\Delta 2}_n, \overline{\Delta 3}_n$	n frequency shifted blade discontinuity variables which correspond to $\overline{ux}_r$, $\overline{uy}_r$, and $\overline{uz}_r$ variables, respectively, for a flexstrap rotor and control torque, feathering and flap angle discontinuity variables, respectively, for an articulated rotor
$(\overline{\Delta 1}_n)_m, (\overline{\Delta 2}_n)_m$ $(\overline{\Delta 3}_n)_m$	n frequency shifted blade discontinuity variables, as defined above, for the mth blade
$\overline{\Delta}_{cu}$	complex variable value of the iteration just completed during solution iteration procedure
Δ_{j-m}	function equal to unity if (j-m) equals 1 or if (j-m) equals (1-Nb) for a gimballed rotor and otherwise is zero

$\overline{\Delta}_{IA}$	complex variable value of the iteration just prior to the iteration just completed during solution iteration procedure
$\left[\Delta G_I\right]_m$	matrix operator specifying contribution of blade root variables to fuselage related moment and force boundary condition equations for a gimballed rotor
$\left[\Delta R_I\right]_m$	matrix operator specifying contribution of blade root variables to fuselage related moment and force boundary condition equations for an articulated, rigid, or flexstrap rotor
$\left[\Delta T_I\right]_m$	matrix operator specifying contribution of blade root variables to fuselage of blade root variables to fuselage related moment and force boundary condition equations for a teetering rotor
$(\overline{\Delta T}_k)_m, (\overline{\Delta\phi x}_k)_m$ $(\overline{\Delta\phi y}_k)_m$	k frequency shifted blade torque, torsional deflection, and flap angle discontinuities of the mth blade
$\Delta T_m, (\Delta T)_m$	real-time torque applied to the mth blade by its associated control rod, in-lb
$\left\{\overline{\varepsilon}_j\right\}, \overline{\varepsilon}_j, \left\{\overline{\varepsilon}_j'\right\}$	eigenvector correction column matrix, element of eigenvector correction column matrix, and reduced eigenvector column matrix, respectively
θ	azimuthal independent coordinate for control system variable referred to fixed control system coordinate system, rad
$\Theta(\theta,t)$	local bending slope of control system ring, rad
$\Theta(\chi_j,t)$	local bending slope at χ_j as a function of time, rad
$\kappa_{k,m}$	k frequency shifted linear stiffness and damping related to the mth control rod, lb/ft

$\left\{\bar{\chi}_j\right\}, \chi_j$	trial eigenvector column matrix and an element of the matrix
μ	mass per unit length of control system ring, slugs/ft
π	pi, 3.1415927
σ	real part of eigenvalue specifying blade motion damping of the form $e^{\sigma t}$, 1/sec
$\sigma_\ell(t)$	Fourier harmonic of $\sigma(\theta,t)$, ft-lb/ft
$\sigma(\theta,t)$	applied moment per unit length acting on control system ring, ft-lb/ft
Σ	summation symbol
τ_m	damping retardation time of mth control rod spring-damper unit for rotor type other than flexstrap, sec
ϕ	azimuthal independent coordinate for control system variables referred to the control system rotating coordinate system corresponding to the first blade, rad
Φ,Θ,Ψ	finite angles defining orientation of blade local coordinate system where Φ corresponds to forward sweep, Θ corresponds to downward coning, and Ψ corresponds to nose up twist and/or collective angle of attack, rad
ϕ_m	phase angle of mth blade relative first blade, rad
$\bar{\phi}_m$	blade root slope vector for the mth blade defined relative to the rotating coordinate system of the mth blade, rad
$\bar{\phi}_s$	fuselage structure hub slope vector defined relative to the fixed shaft coordinate system, rad

$\Phi(\theta,t)$	local twist angle of control system ring, rad
$\Phi(\chi_j,t)$	local twist angle at χ_j as a function of time, rad
$\phi x, \phi y, \phi z$	torsional, flapwise, and chordwise bending slopes, respectively, rad
$\overline{\phi x}, \overline{\phi y}, \overline{\phi z}$	Laplace transformed torsional, flapwise, and chordwise bending slopes, respectively, rad
$\overline{\phi x}^*, \overline{\phi y}^*, \overline{\phi z}^*$	Laplace transformed torsional flapwise, and chordwise bending slopes, respectively, at the blade tip, rad
$\phi x_m, \phi y_m, \phi z_m$	blade root torsional, flapwise, and chordwise bending slopes, respectively, of the mth blade in its rotating shaft coordinate system, rad
$(\phi x_m)_k, (\phi y_m)_k, (\phi z_m)_k$	k frequency shifted Laplace transformed blade root torsional, flapwise, and chordwise bending slopes, respectively, of the mth blade in its rotating shaft coordinate system, rad
$(\overline{\phi x}_m^i)_k, (\overline{\phi y}_m^i)_k, (\overline{\phi z}_m^i)_k$	k frequency shifted Laplace transformed torsional, flapwise, and chordwise bending slopes, respectively, at the inboard end of the ith section of mth blade, rad
$\phi x_s, \phi y_s, \phi z_s$	fuselage structure torsional, flapwise, and chordwise bending slopes, respectively, in the local fuselage coordinate system at tail rotor hub, rad
χ_j	azimuthal angle of jth spring-damper unit supporting control system ring, rad
ψ_j	azimuthal location of jth point used for Fourier analysis of $F(\psi_j)$, rad

ω	imaginary part of eigenvalue corresponding to main frequency of tail rotor system, rad/sec
Ω	rotor speed, rad/sec
$\{\ \}$	denotes row matrix
$[\ ]$	denotes rectangular matrix
$\{\ \}$	denotes column matrix